2013

Development of Modeling Tools for Predicting Smoke Dispersion from Low-Intensity Fires

Warren E. Heilman
USDA Forest Service, wheilman@fs.fed.us

Shiyuan Zhong
Michigan State University, zhongs@msu.edu

John L. Hom Dr.
jhom@fs.fed.us

Joseph J. Charney
USDA Forest Service, jcharney@fs.fed.us

Development of Modeling Tools for Predicting Smoke Dispersion from Low-Intensity Fires

Project Title: Development of Modeling Tools for Predicting Smoke Dispersion from Low-Intensity Fires

Final Report: JFSP Project Number 09-1-04-1
Project Website: http://www.geo.msu.edu/firesmoke/index.html

Principal Investigator:

Dr. Warren E. Heilman, Research Meteorologist, USDA Forest Service, Northern Research Station, 1407 S. Harrison Road, Room 220, East Lansing, MI 48823; Phone: 517-355-7740 x110; Fax: 517-355-5121; Email: wheilman@fs.fed.us

Co-Principal Investigators:

Dr. Shiyuan Zhong, Professor, Department of Geography, 208 Geography Building, Michigan State University, East Lansing, MI 48824; Phone: 517-432-4743; Fax: 517-432-1671; Email: zhongs@msu.edu

Dr. John L. Hom, Biological Scientist, USDA Forest Service, Northern Research Station, 11 Campus Blvd., Suite 200, Newtown Square, PA 19073; Phone: 610-557-4097; Fax: 610-557-4095; Email: jhom@fs.fed.us

Dr. Joseph J. Charney, Research Meteorologist, USDA Forest Service, Northern Research Station, 1407 S. Harrison Road, Room 220, East Lansing, MI 48823; Phone: 517-355-7740 x105; Fax: 517-355-5121; Email: jcharney@fs.fed.us

Collaborators:

Dr. Michael T. Kiefer, Michigan State University, East Lansing, MI
Dr. Kenneth L. Clark, USDA Forest Service, Northern Research Station, New Lisbon, NJ
Dr. Nicholas Skowronski, USDA Forest Service, Northern Research Station, Morgantown, WV
Dr. Gil Bohrer, Ohio State University, Columbus, OH
Dr. Wei Lu, Michigan State University, East Lansing, MI
Dr. Yonqiang Liu, USDA Forest Service, Southern Research Station, Athens, GA
Dr. Robert Kremens, Rochester Institute of Technology, Rochester, NY
Mr. Xindi Bian, USDA Forest Service, Northern Research Station, East Lansing, MI
Mr. Michael Gallagher, USDA Forest Service, Northern Research Station, New Lisbon, NJ
Mr. Matthew Patterson, USDA Forest Service, Northern Research Station, Newtown Square, PA
Ms. Jovanka Nikolic, Michigan State University, East Lansing, MI
Ms. Thalia Chatziefstratiou, Ohio State University, Columbus, OH
Ms. Christie Stegall, USDA Forest Service, Southern Research Station, Athens, GA
Mr. Ken Forbus, USDA Forest Service, Southern Research Station, Athens, GA

This research was sponsored in part by the Joint Fire Science Program. For further information, go to www.firescience.gov

Table of Contents

I. Abstract

Of particular concern to fire and air-quality management communities throughout the U.S. are the behavior and air-quality impacts of low-intensity prescribed fires for fuels management. For example, smoke from prescribed fires, which often occur in wildland-urban interface (WUI) areas and in areas where forest vegetation has a significant impact on the local meteorology, can linger for relatively long periods of time and have an adverse effect on human health. Smoke from wildland fires can also reduce visibility over roads and highways in the vicinity of and downwind of these fires, reducing the safety of our transportation system. The planning for and tactical management of low-intensity prescribed fires can be enhanced with models and decision support tools developed with a fundamental understanding of how the atmosphere interacts with these types of fires and the smoke they generate.

This particular study focused on (1) an evaluation of several existing coupled meteorological and atmospheric dispersion modeling systems for their potential use as tools to predict the local meteorological and air-quality impacts of low-intensity wildland fires in forested environments, (2) the further development of those modeling systems deemed most appropriate for low-intensity wildland fire applications to enhance their local meteorological and air-quality predictive capabilities within forested environments, and (3) the development and analysis of new observational data sets that can be used to evaluate current and future modeling systems and to improve our understanding of fundamental fire-fuel-atmosphere interactions.

II. Background and Purpose

The use of prescribed fires is a viable and well-utilized tool for forest ecology and fuels management in many regions of the U.S. From 1998-2011, more than 184,000 prescribed fires were carried out in the U.S. by Federal, State, and other agencies/groups, resulting in a burned area of more than 30 million acres (National Interagency Fire Center 2012). In addition to their use by land managers for fuel reduction, prescribed fires are also used by farming communities for burning agricultural debris (Hays et al. 2005, McCarty et al. 2006). Unlike major wildfires that are more intense, spread rapidly, and may pose significant threats to resources, property, and even life, prescribed fires are typically low intensity and carefully managed so that they are confined to a small area and do not spread into surrounding communities. However, smoke from low-intensity prescribed fires can degrade local air quality in the vicinity of those fires and also be transported to surrounding areas where it can cause health concerns. This is particularly relevant for prescribed fires occurring in wildland-urban-interface zones (Winter et al. 2002). Smoke from low-intensity prescribed fires can also create travel hazards on surrounding roads and highways (Spainhour et al. 2005, Charney et al. 2006).

Given the potential health and safety concerns associated with smoke generated from low-intensity prescribed fires, operational predictions of the impacts of prescribed burning on local air-quality could provide fire and air-quality managers with an additional tool for the planning and management of prescribed fires. There are a variety of predictive air-quality models and systems currently available to the operational fire and air quality management communities for prescribed fire planning, as summarized in Goodrick et al. (2012). These include box models (e.g. Atmospheric Dispersion Index (Lavdas 1986), Ventilation Index (Ferguson et al. 2003)); Gaussian plume models (e.g. VSMOKE (Lavdas 1996), SASEM (Sestak and Riebau 1988));

puff models (e.g. CALPUFF (Scire 2000), HYSPLIT (Draxler and Rolph 2003)); particle models (e.g. FLEXPART (Stohl et al. 2005), DaySmoke (Achtemeier et al. 2011), PB-Piedmont (Achtemeier 2005)); Eulerian grid models (e.g. CMAQ (Byun and Ching 1999), AERO-RAMS (Wang et al. 2006), WRF-Chem (Skamarock et al. 2005)); and smoke modeling frameworks (e.g. BlueSky (Larkin et al. 2009)). All of these models and systems have enhanced the effectiveness of fire management activities in the U.S. and many have contributed to an increased understanding of smoke dispersion processes. However, all of the aforementioned models and systems are limited in their ability to simulate/predict local air-quality conditions in the immediate vicinity of wildland fires in forested environments, where small-scale fire-forest-atmosphere interactions play a crucial role in the local behavior of smoke plumes. There is a need for new air-quality related predictive tools that can account for the effects of forest vegetation and fire-forest-atmosphere interactions on local smoke dispersion.

The development and adaptation of new and existing predictive tools for assessing the air-quality impacts of low-intensity prescribed fires in forested environments also requires extensive meteorological and air-quality related observational data sets for evaluating the effectiveness of the predictive tools. While there have been numerous wildland fire studies to date that have included measurements of atmospheric conditions in the vicinity of wildland fires, few studies have focused on *in situ* monitoring of the atmospheric mean and turbulent conditions and fire-atmosphere feedbacks that play a major role in fire spread and smoke dispersion processes. Well-known examples of past *in situ* monitoring type studies during wildland fire events include the International Crown Fire Modeling Experiment (ICFME) (Alexander 1998, Stocks et al. 2004, Taylor et al. 2004), the FireFlux grassland experiment (Clements et al. 2007; Clements 2010), and the Prescribed Fire Combustion and Atmospheric Dynamics Research Experiment (RxCADRE) (Hiers et al. 2009). The paucity of available comprehensive data sets for examining fire-vegetation-atmosphere interactions and smoke dispersion during wildland fire events, and particularly during low-intensity prescribed fires, has hampered the scientific community in its effort to better understand local wildland fire dynamics and local smoke transport and diffusion processes in forested environments, which in turn has hampered efforts to evaluate the effectiveness of new and existing predictive tools.

In recognition of the current needs for new air-quality predictive tools and observational data sets for low-intensity prescribed fires, this study was put together to (1) determine the feasibility of adapting one or more existing modeling systems for predicting local smoke transport and diffusion from low-intensity wildland fires occurring in forested environments, (2) carry out the necessary revisions to the most appropriate modeling systems so that they could potentially be used for predicting the meteorological and air quality conditions in the vicinity of actual low-intensity prescribed fires where forest overstory vegetation is present, and (3) develop and analyze new observational datasets that can be used to evaluate current and future modeling systems and improve our understanding of fundamental fire-fuel-atmosphere interactions.

III. Study Description and Location

This project involved both a model development/adaptation component and a field monitoring component for the purpose of collecting relevant observational data to aid in model evaluation. Descriptions of both components are described in the sections below.

A. Model Development/Adaptation

Simulating local smoke transport and diffusion from low-intensity wildland fires is particularly challenging because local atmospheric transport and diffusion processes are very sensitive to near-surface meteorological conditions. Local terrain variations, land-water variations, and surface variations in vegetation cover can all influence smoke-plume behavior and resulting local air quality. Of particular concern for low-intensity wildland fires occurring in forested environments is the effect of local fire-vegetation-atmosphere interactions on the transport and dispersal of smoke beneath forest canopies, and the potential for smoke to linger in an area for an extended period of time - a human health and safety issue. In recognition of the limitations in current operational- and research-based meteorological and smoke modeling systems in their ability to adequately resolve small-scale fire-vegetation-atmosphere interactions, which is critical for predicting low-intensity wildland fire effects on local air quality, our research team examined the feasibility of adapting several state-of-the-art meteorological and atmospheric dispersion modeling systems for low-intensity wildland fire applications. The modeling systems considered in our assessment included (1) the operational version of the Atmosphere-to-Computational Fluid Dynamics (A2C) system (Yamada 2004), (2) the Weather Research and Forecasting (WRF) model (Skamarock et al. 2005) coupled with the FLEXPART community Lagrangian particle dispersion model (Stohl et al. 2005), (3) the Advanced Regional Prediction System (ARPS) (Xue et al. 2000, 2001) coupled with FLEXPART, and (4) the Regional Atmospheric Modeling System-based Forest Large-Eddy-Simulation (RAFLES) system (Pielke et al. 1992; Bohrer 2007).

1) A2C

Developed by the Yamada Science and Art Corporation, the A2C model (Yamada 2004) is a next-generation atmospheric model designed as an operational meso-to-microscale forecasting system for air flow and dispersion of pollutants. A2C is comprised of a High Order Turbulence Model for Atmospheric Circulation (HOTMAC), a three-dimensional primitive equation model developed primarily to predict airflows over complex terrain and around buildings, and a Lagrangian-based Random Particle Transport and Diffusion (RAPTAD) model based on random walk theory for simulating the transport and dispersion of pollutants over complex terrain and around buildings. HOTMAC serves as the meteorological driver for RAPTAD.

2) WRF/FLEXPART

The WRF model (Skamarock et al. 2005) has become one of the standard models for operational mesoscale weather forecasting and meso- and fine-scale research applications. The Lagrangian particle dispersion model FLEXPART is a comprehensive tool currently being used operationally and for research applications to predict and analyze the transport/diffusion of atmospheric pollutants (Stohl et al. 2005). Fast and Easter (2006) successfully coupled WRF with FLEXPART, and the coupled WRF/FLEXPART system has since been used to simulate pollutant dispersion events from local to regional scales (e.g. Doran et al. 2008; Massoli et al. 2009; de Foy et al. 2009; Lu et al. 2012). WRF/FLEXPART can be used for both operational and research applications.

3) ARPS/FLEXPART

ARPS is a three-dimensional multiscale atmospheric model developed by the Center for Analysis and Prediction of Storms (CAPS) at the University of Oklahoma (Xue et al. 2000, 2001) for simulating microscale through regional scale flows. This modeling system has been validated extensively over the last two decades and used to investigate a variety of meteorological/air-quality events and atmospheric processes (e.g. Collischonn et al. 2005; Cheng et al. 2007; Weverberg et al. 2008; Mott and Lehning 2010). Similar to the coupling of WRF with FLEXPART, output from the ARPS model can be used to drive the FLEXPART particle dispersion model to create a coupled ARPS/FLEXPART system. ARPS/FLEXPART can be used for both operational and research applications.

4) RAFLES

The Regional Atmospheric Modeling System (RAMS), which has been employed in both regional and operational forecasting and research applications (Pielke et al. 1992, Cotton et al. 2003), has undergone further modifications to operate as a research-based, high resolution, large-eddy-simulation (LES) model capable of simulating circulations within three-dimensional heterogeneous vegetation layers. This new adaptation, known as RAFLES (Bohrer 2007), incorporates canopy characteristics from observational data or through a virtual canopy generator. RAFLES has been used to simulate biological dispersal in forest canopies (Bohrer et al. 2008) and is able to account for many of the small-scale vegetation-atmosphere interactions that impact the atmospheric environment within forests (Bohrer et al. 2009), including turbulent circulations that affect smoke dispersal. As an LES model with significant computational requirements, RAFLES is not an operational-type model.

B. Field Monitoring

1) Site Descriptions

In order to improve our understanding of fire-fuel-atmosphere interactions that occur during low-intensity wildland fires in forested environments and to develop new observational data sets that can be used to evaluate the meteorological and air quality predictive tools considered in this study, as well as other current and yet-to-be developed tools, two comprehensive low-intensity prescribed fire experiments were conducted. The experimental sites for this study were located in the New Jersey Pinelands National Reserve. The Pinelands are considered among the most volatile fire-cycle vegetation in the eastern U.S. Most of the upland forests in this area are dominated by highly flammable vegetation consisting of Pitch pine (Pinus rigida L.), dense scrub oaks and shrubs (Hom et al. 2013). The Pinelands region is surrounded by wildland-urban-interface (WUI) areas and by some of the densest population centers in the U.S., with Philadelphia and New York to the west and north, and Atlantic City and the New Jersey shore to the east and south. Parts of the region have been designated as non-attainment areas for particulate matter ($PM_{2.5}$) and ozone (O_3) by the U.S. Environmental Protection Agency (EPA). Smoke emissions and air quality in the Pinelands are of major concern to the NJ Forest Fire Service and other government agencies, including the U.S. Department of Defense - Joint Base

McGuire-Dix-Lakehurst and the Forsythe National Wildlife Refuge, in their efforts to use prescribed fires as a management tool to reduce fuel loads.

Fig. 1. Locations of the two prescribed fire experiments conducted in the NJ Pine Barrens on 20 March 2011 (Experiment E1) and 6 March 2012 (Experiment E2).

Figure 1 shows the two burn blocks within the NJ Pine Barrens that were utilized in this study. Both blocks were located within the Brendan T. Byrne State Forest. The first burn experiment (E1) was conducted on 20 March 2011 in a 107-ha (265-acre) burn block (center of block: 39.8726°N, 74.5013°W). Vegetation in the block consisted of Pitch pine and mixed oak overstory (~15-18 m height) with *Vaccinium* spp. and scrub oak understory. The second burn experiment (E2) was conducted on 6 March 2012 in a 97-ha (240-acre) burn block (center of block: 39.9141°N, 74.6033°W). Vegetation consisted of mixed oaks and scattered Pitch and Shortleaf pines in the overstory (~20-23 m height), and primarily *Vaccinium* spp. and *Gaylussacia* spp. in the understory. The overall plant area density in the E2 burn block was less than that in the E1 burn block. Both burn blocks were characterized by sandy soils and were relatively flat. Ground elevations above sea level varied from 37-48 m (42.58 ± 2.72 m) and 28-35 m (32.28 ± 1.51 m) in the E1 and E2 burn blocks, respectively.

2) Monitoring Networks

Fig. 2. Location of towers and surface monitoring stations in each burn block for the E1 (20 March 2011) and E2 (6 March 2012) prescribed fire experiments. 3 m towers: yellow circles; 10 m towers: blue circles; 20 m towers: purple circles; 30 m towers: red circles; 10 m control towers: green circles; $PM_{2.5}$ monitors: brown diamonds; ceilometer: blue star; remote helicopter: pink square.

For both prescribed fire experiments, a network of instrumented, guyed meteorological towers and surface monitoring sites was established within and in the vicinity of the burn blocks prior to the burn dates. Figure 2 shows the tower locations for the two burn experiments. For both burn blocks, a 10 m and 20 m tower were placed in the interior of the blocks, while a 30 m mobile tower was placed near the eastern perimeter of each block to capture downwind atmospheric conditions during each burn, assuming northwesterly to southwesterly ambient winds (the desired wind directions). Twelve 3-m towers were set up and distributed throughout both burn

Table 1. Summary of the instrumentation and monitoring protocols used at the 3 m, 10 m control, 10 m, 20 m, and 30 m towers for the E1 (20 March 2011) and E2 (6 March 2012) prescribed fire experiments.

Tower	Instrument	Variable	Measurement Height (m AGL)	Sampling Frequency
3 m	Thermocouples (Omega XC-24-K-12 @ 0 m) (Omega SSRTC-GG-K-36-36)	Temperature	0, 1, 3	0.5 Hz
	CO Sensors (Figaro TGS5042)	CO conc.	3	0.5 Hz
	Anemometers (E2 only) (Davis Instruments DV6410)	Mean wind speed and direction	3	0.5 Hz
	Temperature/RH probes (EME Systems SHT75PG)	Mean temperature and RH	2	0.5 Hz
10 m	3D sonic anemometers (R.M. Young 81000V)	u, v, w, t	3, 10	10 Hz
	Temperature/RH probes (Vaisala HMP50)	Mean temperature and RH	3, 10	10 HZ
	Thermocouples (Omega SSRTC-GG-K-36-36)	Temperature	0, 1, 2, 3, ... 10	10 Hz
	CO Sensors (Figaro TGS5042)	CO conc.	3, 10	10 Hz
	CO_2 Sensor (Vaisala GMM222E)	CO_2 conc.	5	10 Hz
	Radiative Heat Flux Sensor (Medtherm 64-20-20)	Radiative heat flux	4.5	10 Hz
	Barometer (Viasala PTB 110)	Pressure	7	10 Hz
	Soil thermocouples (Omega XC-24-K-12: Litter) (Omega KMQLX-032-6)	Temperature	Litter, -0.10, -0.20	10 Hz
20 m	3D sonic anemometers (R.M. Young 81000V)	u, v, w, t	3, 10, 20	10 Hz
	Temperature/RH probes (Vaisala HMP50)	Mean temperature and RH	3, 10, 20	10 HZ
	Thermocouples (Omega SSRTC-GG-K-36-36)	Temperature	0, 1, 2, 3, ... 10, 12.5, 15, 17.5, 20	10 Hz
	CO Sensors (Figaro TGS5042)	CO conc.	3, 10, 20	10 Hz
	CO_2 Sensor (Vaisala GMM222E)	CO_2 conc.	5	10 Hz
	Radiative Heat Flux Sensor (Medtherm 64-20-20)	Radiative heat flux	4.5	10 Hz
	Barometer (Vaisala PTB110)	Pressure	11	10 Hz
	Soil thermocouples (Omega XC-24-K-12: Litter) (Omega KMQLX-032-6)	Temperature	Litter, -0.10, -0.20	10 Hz
30 m	3D sonic anemometers (R.M. Young 81000V)	u, v, w, t	3, 10, 30	10 Hz
	Temperature/RH probes (Vaisala HMP50)	Mean temperature and RH	3, 10, 30	10 HZ
	Thermocouples (Omega SSC-TT-T-36-36)	Temperature	0, 1, 2, 3, ... 10, 12, 16, 20, 25, 30	10 Hz
	CO Sensors (Figaro TGS5042)	CO conc.	3, 10, 30	10 Hz
	CO_2 Sensor (LI-COR 820)	CO_2 conc.	5	10 Hz
	Net radiometer (Kipp and Zonen NR-Lite)	Net radiation	30	10 Hz
	Barometer (Vaisala PTB110)	Pressure	2.1	10 Hz
	Soil thermocouples (Omega KMQLX-032-6)	Temperature	-0.02, -0.20	10 Hz
10 m Control	3D sonic anemometers (R.M. Young 81000V)	u, v, w, t	3, 10	10 Hz
	Temperature/RH probes (Vaisala HMP50)	Mean temperature and RH	3, 10	10 HZ
	Thermocouples (Omega SSC-TT-T-36-36)	Temperature	0, 1, 2, 3, ... 10	10 Hz
	CO Sensors (Figaro TGS5042)	CO conc.	3, 10	10 Hz
	CO_2 Sensor (Li-Cor 820)	CO_2 conc.	5	10 Hz
	Net radiometer (Kipp and Zonen NR-Lite)	Net radiation	2	10 Hz
	Barometer (Viasala PTB110)	Pressure	1.5	10 Hz
	Soil thermocouples (Omega TMQSS-032U-6)	Temperature	-0.02, -0.20	10 Hz

blocks to provide enhanced spatial coverage of the near-surface atmospheric conditions as the prescribed fires spread through the burn blocks. Surface fuels under the 10, 20, and 30 m towers within the burn blocks were cleared to a distance of approximately 5-7 m from each tower base to minimize potential instrument loss as the fires burned through the tower locations. A 10 m control tower was also set up to the northwest and west of the E1 and E2 burn blocks, respectively, to collect expected upwind meteorological and air-quality data for characterizing the general ambient conditions within the vegetation layers.

Instrumentation mounted at multiple levels on each tower provided high frequency (0.5 or 10 Hz) measurements of component wind speeds, temperature, relative humidity, net radiation, atmospheric pressure, radiative heat fluxes, and carbon monoxide (CO) and carbon dioxide (CO_2) concentrations. The high-frequency (10 Hz) component wind-speed measurements at the 10 m, 20 m, and 30 m towers within the burn blocks were carried out using sonic anemometers oriented with their horizontal axes aligned in the east-west and north-south (true north) directions. This allowed for a characterization of the turbulence regimes before, during, and after the passage of the fire fronts through the tower locations. Soil temperatures outside the fuel-cleared areas surrounding the 10 m, 20 m, and 30 m towers and in close proximity to the 10 m control tower were also measured. Data collected from the

tower-based instrumentation were recorded using Campbell Scientific Inc. (CSI) dataloggers (CR-1000, CR-3000). Table 1 provides a summary of the tower instrumentation and monitoring strategies used in the E1 and E2 experiments.

The monitoring networks for the E1 and E2 burn experiments also included a number of non-tower based measurement platforms. They included phased array Doppler SODAR (Remtech PA0) measurements of upwind lower atmospheric boundary-layer (20 – 400 m AGL) wind speeds and directions (E2 only), measurements of near-surface $PM_{2.5}$ concentrations (Thermo Scientific Particulate Monitor – DataRAM 4; Met One EBAM), ceilometer measurements (Vaisala CL31) of downwind plume heights and boundary-layer $PM_{2.5}$ concentrations (E2 only), remotely operated helicopter measurements (MikroKopter - HexaKopter) of within-plume carbon monoxide concentrations at downwind locations from the burn blocks, aerial infrared (IR) camera imagery of the prescribed fires via the Wildfire Airborne Sensor Program instrument (WASP; 3 Indigo Phoenix Infrared imagers and a single Geospatial Systems KCM-11; Vodacek et al. 2005), and pre- and post-burn aerial LIDAR (Leica Airborne Laser Scanner 60) measurements of vegetation structure. The additional surface-based monitoring platforms are also shown in Fig. 2.

3) Fuel Loading and Fuel Moisture Measurements

Pre- and post-burn fuel loading and fuel moisture measurements were also carried out using vegetation samples obtained from sites near the 10 m and 20 m towers within the E1 and E2 burn blocks. Thirty 1-m^2 samples of understory vegetation and forest floor were destructively sampled pre- and post-burn by placing a 1-m^2 hoop on the forest floor at random locations within each burn block. All stems were clipped to the ground level, separated into foliage and live and dead 1-hr, 10-hr and 100-hr fuels. The forest floor was sampled to the top of the organic matter layer (O-horizon), and separated into 1-hr, 10-hr and 100-hr fuels. Previous research indicated that prescribed fires in the Pinelands rarely burn into the organic matter layer (Clark et al. 2010). All samples were dried at 70 ºC until dry and then weighed.

During each burn, the moisture contents of pine needles, 1-hr and 10-hr stems of shrubs, and 1-hr and 10-hr fuels on the forest floor were estimated from samples collected adjacent to the burn blocks at ca. 1100, 1300, and 1500 LT. Samples were collected in tared plastic bags, and returned to the laboratory and weighed immediately. Samples were then transferred to paper bags, dried at 70 ºC until dry, and then weighed again to compute moisture contents.

4) Vegetation Structure Measurements

High density airborne laser scanner (ALS) data were collected to quantify pre- and post-burn vegetation structure for the E1 burn block. An equipment malfunction limited the collection of E2 burn block vegetation structure to post-burn conditions only. These LiDAR data were processed using the Toolbox for LiDAR Data Filtering and Forest Studies (TiFFS; Chen 2007). The outputs of this processing include: 1 m horizontal resolution digital elevation models and canopy height models; and 25 m resolution LiDAR derived statistical parameters: mean height, decile heights of the distribution, standard deviation, and distribution shape characteristics of skewness and kurtosis. Additionally, the LiDAR data were processed to develop spatially

explicit estimates of vertical and horizontal vegetation structure following methodologies presented in Skowronski et al. (2011). This processing resulted in 25 m horizontal and 1 m vertical resolution rasters of LiDAR-derived canopy height profiles.

5) Aerial Infrared Imagery

Airborne thermal infrared data were collected at ~1 m horizontal resolution using the WASP sensor during both the E1 and E2 experiments. The WASP sensor consists of short, mid and long wavelength infrared cameras in addition to a high-resolution color infrared camera (VIS/NIR), resulting in 1 mrad resolution in the infrared. The burn extents were sampled at 3-5 minute intervals, the time for the aircraft to turn and return station over the fire ground, and resulted in 51 and 65 ortho-rectified frames for the E1 and E2 experiments, respectively. Frames were calibrated using absolutely calibrated infrared sensors at several locations on the ground to provide frame-by-frame calibration of flux for the airborne data, thus minimizing the effects of atmospheric transmission and instrument drift.

6) Prescribed Fire Ignition and Progression

The prescribed fires for this study were carried out and managed by the New Jersey Forest Fire Service (NJFFS). Using drip torches, personnel from the NJFFS initiated surface backing fires along the western and eastern perimeters of the E1 and E2 burn blocks, respectively. Initial ignitions occurred at 0955 EDT (E1: 20 March 2011) and 0930 EST (E2: 6 March 2012) near the southwestern (E1) and southeastern (E2) portions of the burn blocks and continued along the western (E1) and eastern (E2) burn block perimeters. Under light northeasterly to southeasterly ambient winds (generally less than 2.5 m s^{-1} at 10 m AGL) during the E1 experiment, the E1 fire line generally spread northeastward through the burn block throughout the day until reaching the northeastern portion of the burn block around 2100 EDT (Fig. 3). For the E2 experiment,

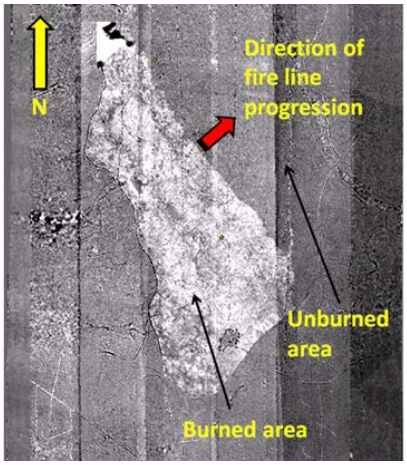

Fig. 3. Aerial LIDAR imagery of forest floor elevation differences between burned and unburned areas at 1715 EDT on 20 March 2011. Image shows the general backing fire line progression to the NE through the burn block, starting with an initial fire line ignition along the western border of the burn block (~0955 EDT).

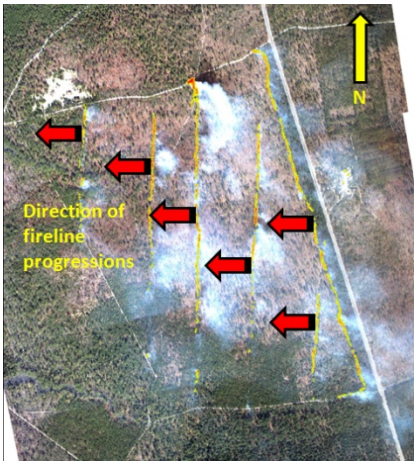

Fig. 4. Aerial visual and IR imagery of smoke and individual fire lines progressing to the west through the burn block at 1116 EST on 6 March 2012. Initial fire line was ignited along the eastern border of burn block between ~0930-1030 EST.

subsequent fire line ignitions along north-south oriented plow lines spaced ~200 m apart in the interior of the burn block following the initial fire line ignition along the eastern perimeter produced a more complicated burn pattern with multiple fire lines generally spreading westward through the burn block against light (< 3 m s^{-1}) northwesterly to southwesterly ambient winds. Active burning for the E2 experiment was completed by 1800 EDT (Fig. 4). Burning was confined to surface fuels for both experiments, except for brief and isolated episodes of crowning during the afternoon of the E1 experiment.

7) Data Processing

Following the collection of atmospheric- and soil-based data for the E1 and E2 experiments, computer programs for data quality assurance (QA) and quality control (QC) were developed. A despiking routine, the first step in the QA/QC process, was applied to all the data sets to remove obvious erroneous data values. The next QA/QC process involved further data filtering by removing data values exceeding 6 standard deviations from running one-hour means. The vertical wind speeds (W) obtained from the sonic anemometers were then tilt-corrected, following the methodology of Wilczak et al. (2001), to minimize errors in vertical wind speeds associated with sonic anemometers that were not mounted exactly level on the network towers. No horizontal coordinate rotations were performed on the sonic anemometer data in order to maintain the true east-west (U) and north-south (V) wind speed components for subsequent turbulent-kinetic-energy component analyses. The despiked and tilt-corrected 10 Hz sonic anemometer wind speed and temperature data were divided into one-hour block averaging periods over which perturbation velocities (u', v', w') and temperatures (t') at each 0.1 s were computed based on the mean component velocities and temperatures obtained for each one-hour period. One-hour averaging periods were adopted for this study based on the recommendation of Sun et al. (2006) for eddy flux measurements over forests. The computed perturbation velocities and temperatures formed the basis for the turbulent-kinetic-energy (TKE), turbulent heat flux, and turbulent momentum flux analyses carried out as part of this study.

The computation of perturbation velocities and temperatures during periods when the surface fires in the E1 and E2 experiments were strongly influencing the overall circulation and temperature fields in the vicinity of the tower-based sonic anemometers required special consideration. To alleviate the contamination of computed mean velocities and temperatures at the tower locations by the fire-induced circulations and temperatures, which were assumed to be completely turbulent, "fire periods" were delineated for each tower based on a subjective analysis of the temperature time series obtained from the tower sonic anemometer and thermocouple temperature measurements. The beginning and ending times for the "fire periods" for each tower were set according to when temperatures began to rise in response to the advancing fire lines and when temperatures returned to ambient values following the passage of the fire lines through the tower locations. As a first-order approximation, perturbation velocities and temperatures during these "fire periods" were computed by subtracting the measured 10 Hz "fire-period" velocities and temperatures from the mean velocities and temperatures associated with the one-hour period prior to the onset of the "fire period". Although this methodology can lead to errors in characterizing the turbulence regimes in fire environments, especially if ambient conditions are changing rapidly, this approach was preferred to the computation of velocity and temperature perturbations from a "fire-contaminated" mean state. During both the E1 and E2

experiments, the one-hour mean ambient winds and temperatures did not change rapidly from hour to hour, which helped to minimize potential errors.

IV. Key Findings

Feasibility Assessment of the A2C Modeling System: The A2C modeling system, currently available from Yamada Science and Art (http://ysasoft.com/), is only available for commercial, governmental, and educational institutions as an executable software package. The system has been marketed by Yamada Science and Art as an effective tool for simulating and visualizing airflow and dispersion of atmospheric pollutants in urban environments. It was designed to produce fast results and to be operated on a personal computer with a minimal amount of input information required. Despite these advantages, our feasibility assessment revealed significant limitations in the ability of A2C to simulate the atmospheric environment in the vicinity of wildland fires in forested and complex terrain environments.

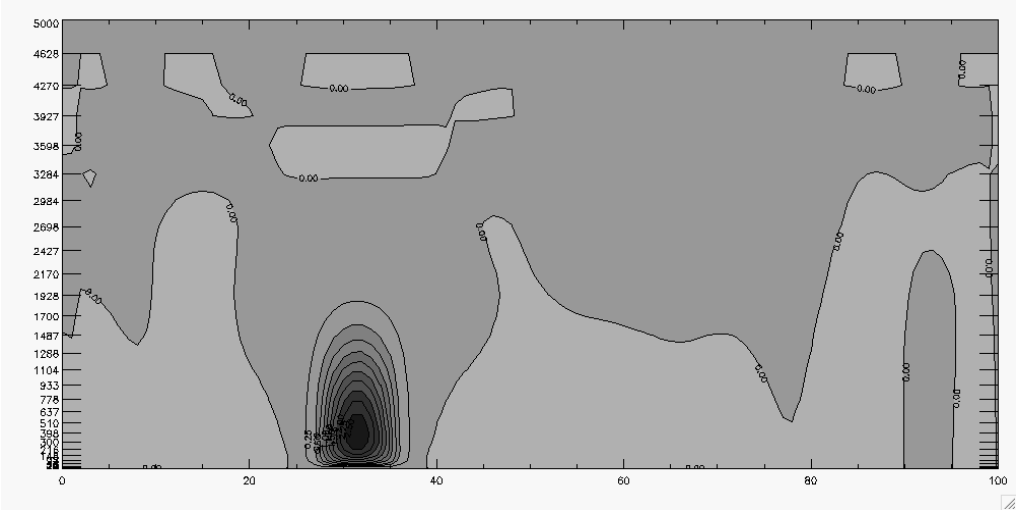

Fig. 5. Vertical cross-section showing example vertical velocities (after 1 hour) simulated with the A2C modeling system in a "synthetic" domain with an imposed surface heat flux of 9999 W m-2 at grid points 25-40 (horizontal axis), zero ambient wind speeds, and no overlying forest vegetation. Height in meters and number of grid points in the east-west direction are represented in the vertical and horizontal axes, respectively.

We found the most significant limitations to be the maximum surface heat flux allowed in any A2C simulation (9999 W m^2 - well-below the typical maximum surface heat flux values encountered during wildland fires) and the resulting unrealistic simulated vertical velocities generated by these areas of surface heating. A set of sensitivity simulations were performed to assess the model's ability to predict typical vertical velocities in the vicinity of an area of significant surface heating with and without an overlying forest vegetation layer. Figure 5 shows an example vertical cross-section of A2C-simulated vertical velocities resulting from an imposed surface heat flux of 9999 W m^2 with no overlying forest vegetation present. While simulated updrafts above the area of surface heating were prominent, the compensating downdrafts simulated by A2C were found to be unrealistic. Given these limitations, plus the unavailability of the A2C source code from Yamada Science and Art that would permit the introduction of the

required modifications (many of them substantial) to the model and make it more applicable for wildland fire applications, we deemed A2C to be inappropriate for further development in this project as a potential tool for predicting smoke transport and dispersion from low-intensity wildland fires.

Feasibility Assessment of the WRF/FLEXPART Modeling System: The WRF model is an atmospheric mesoscale modeling system that was developed as part of a massive collaborative effort involving scientists from the National Center for Atmospheric Research (NCAR), the National Oceanic and Atmospheric Administration (NOAA), the Department of Defense (DOD), the Center for Analysis and Prediction of Storms (CAPS) at the University of Oklahoma, the Federal Aviation Administration (FAA), and many universities (Skamarock et al. 2005). It is currently supported and maintained as a community model at NCAR, which provides a more formal and structured process for introducing modifications to the model and releasing new versions. The potential application of the coupled WRF/FLEXPART modeling system developed by Fast and Easter (2006) for simulating local meteorological conditions and local smoke transport/diffusion during low-intensity prescribed fires in forested environments requires the development of a version of WRF capable of resolving circulations and thermal fields within forest vegetation layers. Consultations with Dr. Fei Chen (Research Applications Laboratory – NCAR) indicated the development and implementation of a canopy sub-model within the WRF community model's computational framework that would allow WRF to resolve circulations and thermal fields within vegetation layers and fully account for the critical vegetation-atmosphere interactions important for local smoke dispersion would be a major undertaking and likely exceed the timelines established for this project. Such an effort would require substantial collaborations with the WRF developers and the WRF user community, further complicating the process for delivering a WRF-based predictive smoke dispersion tool in a timely fashion.

Given these issues, we concluded that further development of a coupled WRF/FLEXPART system suitable for predicting local air quality impacts of low-intensity prescribed fires in forested environments was not feasible within the context of this study. However, initial efforts are underway to deliver WRF/FLEXPART as a test product for simulating regional-scale smoke transport events via the Fire Consortia for Advanced Modeling of Meteorology and Smoke (FCAMMS) - Eastern Area Modeling Consortium (EAMC) web site (http://www.nrs.fs.fed.us/eamc). Additional/future research is needed to evaluate the overall effectiveness of a coupled WRF/FLEXPART system for predicting regional air quality impacts of wildland fires before it can be used as a stand-alone operational tool or an additional pathway within modeling frameworks such as the BlueSky smoke modeling framework (Larkin et al. 2009).

Feasibility Assessment of the ARPS/FLEXPART Modeling System: Within the framework of this project, the ARPS model (source code readily available for downloading from CAPS at the University of Oklahoma: http://www.caps.ou.edu/ARPS/) was viewed as the most viable atmospheric model for implementing a canopy sub-model capable of resolving many of the critical vegetation-atmosphere interactions that could potentially affect wildland fire smoke dispersion within forests. Fortuitous to this project, foundation work for building a canopy sub-model within the ARPS framework was previously carried out by Dupont and Brunet (2008). Although their modifications to ARPS were only applicable for simulating the effects of

vegetation on flow through a multi-layer canopy within a neutral atmospheric boundary layer, they demonstrated that implementing a canopy sub-model within ARPS is certainly feasible. Using ARPS meteorological output files as the driving meteorology for FLEXPART simulations, in a manner similar to the methodology of Fast and Easter (2006) for coupling WRF with FLEXPART, was found to be straightforward. Following this initial feasibility assessment, the actual development of a version of ARPS suitable for simulating circulations and thermal fields within vegetation layers during low-intensity wildland fires commenced. Key results in the development, application, and evaluation of this new version of ARPS, named ARPS-CANOPY, are described below.

Development and Evaluation of New Version of ARPS Capable of Simulating Canopy Flows (ARPS-CANOPY): Using the computational framework currently available in Version 5.2.12 of ARPS (Xue et al. 2000, 2003) along with the initial canopy parameterizations developed by Dupont and Brunet (2008) for ARPS, a new version of ARPS was developed (ARPS-CANOPY) that more fully accounts for the effects of vegetation elements on mean and turbulent atmospheric flows within vegetation layers. Specifically, (1) a drag term was added to the ARPS prognostic equations for the horizontal and vertical wind velocity components to account for pressure and viscous drag effects on circulations due to the presence of canopy elements, (2) a turbulence dissipation term was added to the prognostic sub-grid scale turbulent kinetic energy (TKE) equation in ARPS to account for the loss of TKE to both heat and very small wake-scale eddies around vegetation elements, (3) a turbulence production term was added to the sub-grid scale TKE equation to account for TKE production in the wakes of vegetation elements, and (4) a heating/cooling term due to the presence of vegetation elements and based on an exponential decay in net radiation from the canopy top to the surface was added to the ARPS prognostic potential temperature equation. A complete description of the modifications made to ARPS to create the new ARPS-CANOPY modeling system can be found in Kiefer et al. (2013a).

The ARPS-CANOPY modeling system was evaluated for its ability to simulate mean and turbulent circulations and thermal fields within a forested environment (no fire) using observational wind and temperature data collected during the 2007 Canopy Horizontal Array Turbulence Study (CHATS) (Patton et al. 2011). CHATS was conducted within a deciduous walnut orchard near Dixon, CA from 15 March to 12 June 2007, a period spanning pre leaf-out, transitional, and post leaf-out conditions for the orchard. ARPS-CANOPY simulations of mean and turbulent flow properties during the CHATS pre leaf-out and post leaf-out periods were carried out. The model was successful in reproducing the shapes of the vertical profiles of mean wind, temperature, and TKE observed during the CHATS experiment, with errors generally smaller in the afternoon and under stronger mean flow conditions (Figs. 6 and 7). The general success of ARPS-CANOPY in simulating the overall mean atmospheric conditions, and particularly the turbulence regimes which governed dispersion processes, within and above the vegetation layers for the CHATS experiment with no fires present was a key factor in moving forward with the subsequent testing of ARPS-CANOPY applied to low-intensity wildland fires in forested environments.

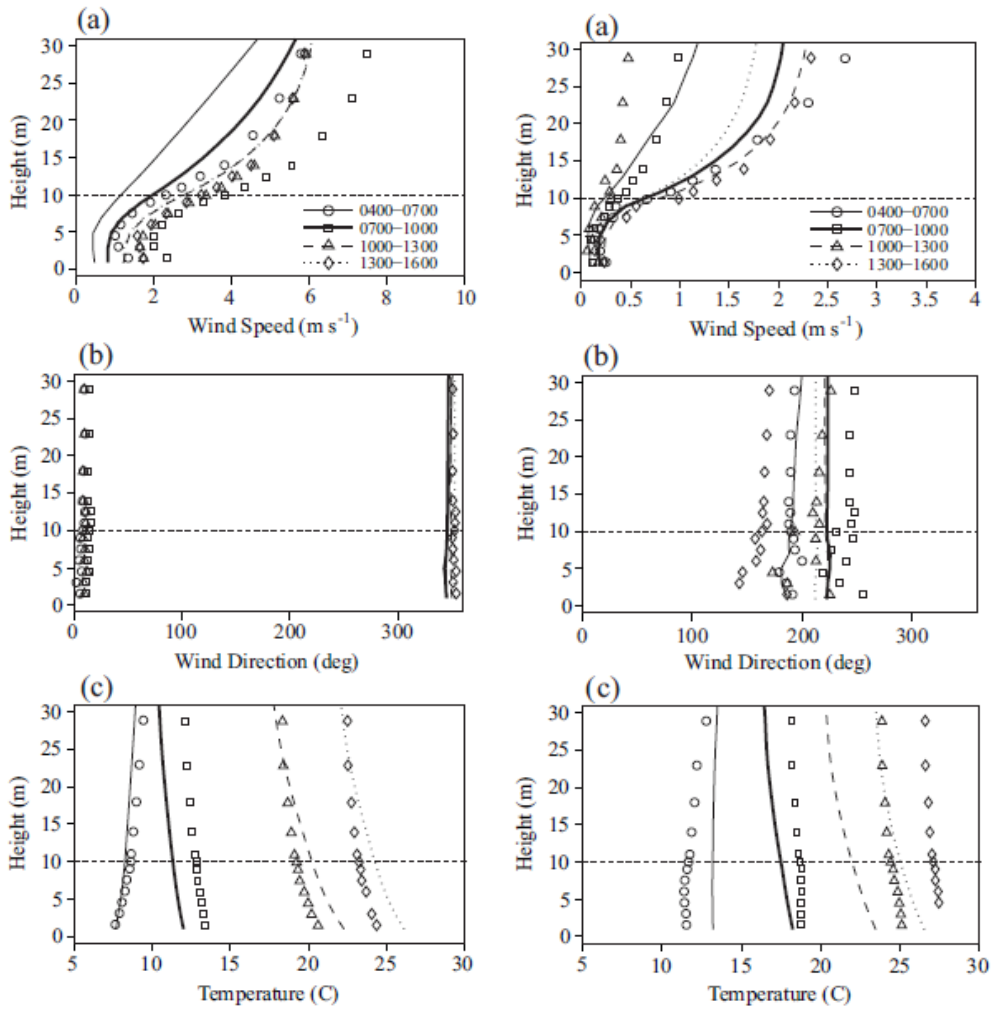

Fig. 6. Comparison of simulated pre leaf-out (29 March 2007: left column) and post leaf-out (20 May 2007: right column) (a) mean wind speeds, (b) mean wind directions, and (c) temperatures to values measured during the CHATS experiment. Line profiles are from the ARPS-CANOPY simulations and symbols denote the observed values. Legends in (a) apply to all panels. Both simulated and measured hourly wind speeds are averaged over four 3-hour windows. Times in legends are in Local Standard Time. Horizontal dashed line denotes the canopy top.

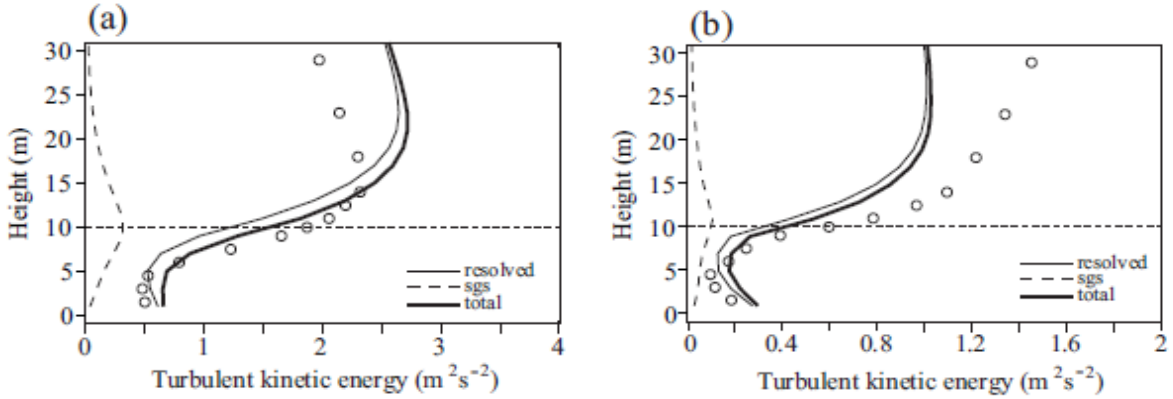

Fig. 7. Comparisons of ARPS-CANOPY simulated and observed 1300-1500 LT turbulent kinetic energy for the (a) pre leaf-out (29 March 2007) and the (b) post leaf-out (20 May 2007) CHATS case studies.. Horizontal dashed lines denote the canopy top. Profiles of resolved and sub-grid-scale (sgs) turbulent kinetic energy from the ARPS-CANOPY simulations are included.

Feasibility Assessment of the RAFLES Modeling System: Large-eddy-simulation (LES) models, while very computationally intensive and impractical for operational-type predictions of atmospheric phenomena, are able to resolve atmospheric circulations at horizontal and spatial scales on the order of a few meters and provide added insight into the small-scale turbulent circulations that govern the local dispersion of heat, moisture, and particulates/gases. One particular LES model that has already been developed to simulate the effects of heterogeneous forest vegetation on turbulent circulations within forest vegetation layers is the RAFLES modeling system (Bohrer 2007). RAFLES was specifically designed to handle the effects of the canopy on wind flow and turbulence and to increase the numerical stability at the typically high spatial and temporal resolutions of the simulations. It includes a multi-layer, three-dimensional heterogeneous canopy. It allows for the effects of leaves on drag and fluxes to the atmospheric surface layer in the canopy air space. Tree stems are represented in the atmospheric model as restrictions to the free-air volume. The typical grid-mesh spacing used in RAFLES (on the order of 1 m^3) allows for the simulation of many of the features that are generated by tree-crown structures. Its simulation domain, typically on the order of 1 km^3, is large enough to simulate a fully dynamic boundary layer. The canopy structure in the model can be prescribed based on remote sensing (Hardiman et al. 2011, Schlegel et al. 2012) data or constructed by the Virtual Canopy-Generator (V-CaGe) (Bohrer et al. 2007). V-CaGe generates canopies based on observed structure and randomly located structural features by combining remote sensing, ground observation and species-specific allometric relationships.

As part of the feasibility assessment of RAFLES, we examined the work of Bohrer et al. (2008, 2009) who used RAFLES along with remotely-sensed and ground observations of canopy structure to successfully simulate atmospheric turbulent flow and seed dispersal within and above the Duke Forest in North Carolina. Their simulations were particularly insightful in showing how tree-scale heterogeneities can affect the spatial variability and location of ejection-sweep cycles that lead to hot-spots of momentum and scalar ejection, which is relevant for smoke dispersion during wildland fires in forested environments (Fig. 8). Based on these initial RAFLES-based studies, further development of the RAFLES system as a research model to examine the effects of low-intensity wildland fires in forested environments on the small-scale turbulent circulations that govern heat and smoke dispersion was deemed appropriate. Key results in the development of a version of RAFLES that accounts for surface heating associated with low-intensity fires are described below.

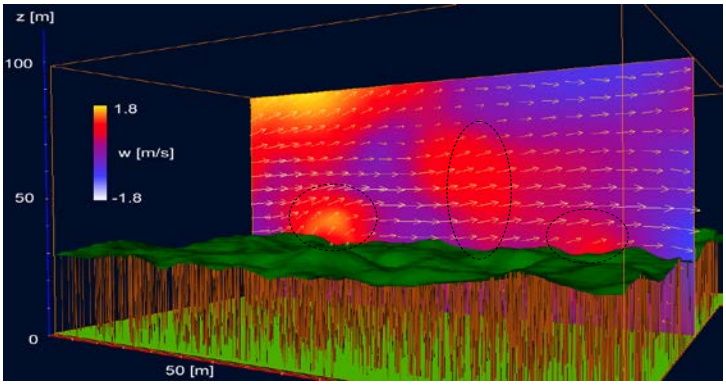

Fig. 8. Cross section (x–z) of wind velocities in a 200 × 200 × 100 m^3 sub-domain of a RAFLES simulation of the Duke Forest. Colors on the vertical plane indicate the vertical component of the wind, and arrows indicate the wind vector. Canopy-top contour is green and stems are brown. Three momentum ejections sites are highlighted with dashed contours. (From Bohrer et al. 2008)

Modification of RAFLES for Simulating Canopy Flows and Scalar Dispersion during Surface Fire Events: A number of modifications/enhancements were made to RAFLES to make it a more suitable research modeling system for simulating the atmospheric environment surrounding surface wildland fires and the dispersion of smoke from those fires. The original version of RAFLES developed by Bohrer (2007) did not include parameterizations to account for the presence of surface fires. A fire module was developed for RAFLES so that it is now able to simulate the movement of a fire line through the simulation domain, assuming a very simplistic down-wind accumulation of heat that drives the ignition from pixel to pixel (Bohrer et al. 2011). After ignition, the rate and direction of fire spread in RAFLES is driven by model-computed horizontal winds and a virtual heat accumulation function. Fire line intensity is calculated at each time step as a function of the remaining fuel level, which in turn is used to calculate a surface heat flux that can feed back on the wind field. A second option was also included in RAFLES to allow for an explicitly prescribed ignition pattern such as what might be encountered during a prescribed backing fire. The simple fire spread parameterizations incorporated into RAFLES were not intended to transform RAFLES into a "fire-behavior" prediction system. Rather, the new parameterizations allow the computationally intensive RAFLES system to now be used as a research tool to examine small-scale fire-atmosphere-vegetation interactions over relatively short time periods.

The numerical solver in RAFLES was also modified to account for stronger vertical flows as is typical from fire conditions. In the original version of RAFLES, the effects of canopy drag were explicitly added to the momentum equations in each direction. The three-dimensional solver in RAFLES includes a split-time scheme, according to which some terms in the momentum equations are solved explicitly and some of the vertical components are solved implicitly to add numerical stability. In this revision of RAFLES, the vertical effects of canopy drag and heat flux were added to the implicit solver. This modification provides numerical stability in cases of strong fire-driven updrafts and heat fluxes (Velissariou and Bohrer 2010).

Finally, a new post-processing tool called Hi-VACC (Kenny et al. 2012) was coupled to RAFLES to allow for faster computations of scalar (i.e. particle) dispersion. Hi-VACC uses the wind, sub-grid-scale turbulence, temperature, humidity, and pressure fields from RAFLES to calculate particle dispersion. With Hi-VACC, it is easy to run ensembles of sensitivity simulations with different scalar emission scenarios using the same atmospheric forcing and fire conditions. The coupling of Hi-VACC with RAFLES enhances RAFLES as a potential research tool for investigating smoke plume dynamics above forest vegetation layers.

Key Fuel, Meteorological, and Air-Quality Observations During the 20 March 2011 NJ Pine Barrens Prescribed Fire Experiment: The first low-intensity prescribed fire experiment (E1) was carried out on 20 March 2011 in the New Jersey Pine Barrens (see Figs. 1 and 2). Figure 9 shows the observed time series of ambient wind speeds, wind directions, temperatures, and relative humidity as measured on the 30 m tower located along the southeastern perimeter of the burn block. Ambient near-surface (3 m AGL) winds were relatively light (< 2 m s^{-1}) and varied from northerly to southeasterly during the burn. Temperatures reached a maximum of ~10° C in the afternoon, and relative humidity values dropped to ~30%. The average fire spread rate through the E1 burn block (generally toward the northeast) was estimated at 1.5 m min^{-1}. The following sub-sections provide a brief summary of the key fuel, meteorological, and air

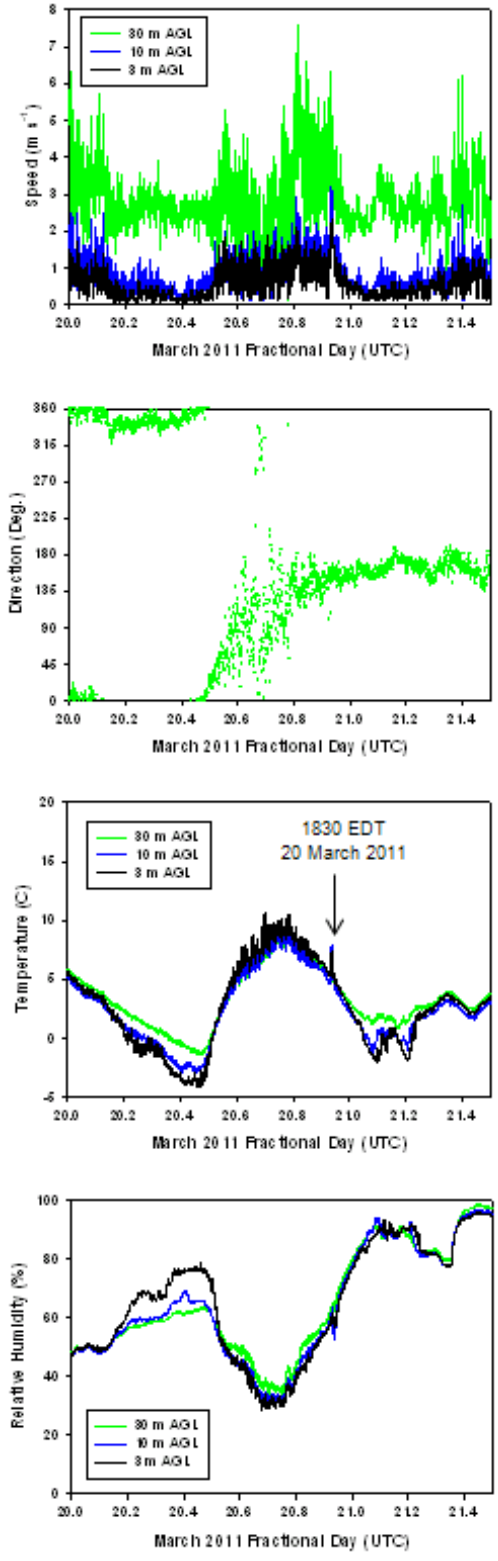

Fig. 9. Observed ambient wind speeds, wind directions (30 m AGL only), temperatures, and relative humidity on 20 March 2011 (E1 experiment) at 3 m, 10 m, and 30 m AGL at the 30 m tower location shown in Fig. 2. Time when the E1 fire line passed the 30 m tower is noted on the temperature time series figure.

quality observations for the E1 experiment. A comprehensive summary of the E1 observations can be found in Heilman et al. (2013).

1) Fuel Conditions

The average pre-burn fuel loading of understory vegetation and the forest floor for the E1 burn blocks totaled 1485 ± 388 g m^{-2}. About 43% (632.4 ± 288.8 g m^{-2}) of the total fuel loading was attributed to shrubs and about 57% (852.7 ± 252.3 g m^{-2}) attributed to forest floor fuels. Total fuel consumption during the E1 experiment was estimated at 696.2 g m^{-2}. This value represents about 47% of total fuel loading at the site. The observed fuel consumption was intermediate relative to other fuel consumption measurements made in the New Jersey Pinelands (Clark et al. 2009, 2010). Observed fuel moisture content was 22.6 ± 11.4% for the 1-hour forest floor fuels, 21.1 ± 8.2% for the 10-hour forest floor fuels, 53.4 ± 7.6% for the live 1-hour shrub stems, 120.5 ± 8.6% for the pine needles, and 92.6 ± 9.1% for the live 1-hour pine stems.

2) Thermal Fields

Based on temperature measurements made at multiple levels on the 20 m tower located well-within the E1 burn block perimeter, which was determined to be the most reliable tower for capturing atmospheric conditions during fire-front passage, the buoyancy induced by the low-intensity E1 fire line and the induced inflow into the fire behind the fire line (southwesterly flow) were still of sufficient strength to generate a convective plume tilted into the light ambient wind (easterly/southeasterly flow). Maximum one-minute averaged temperatures were observed at the 20 m level (47.3° C: 1517 EDT) three minutes before they were observed at the 3 m level at the time of fire front passage (60.5° C: 1520 EDT) (Fig. 10). About 4-5 minutes after the fire front passage through the 20 m tower location, thermocouple temperatures at numerous levels dropped below ambient temperatures (~10° C) due to downdrafts (see next section), with the largest drop occurring at the 20 m level where the one-minute averaged temperature reached 2.3° C. Following this drop, temperatures rebounded at all

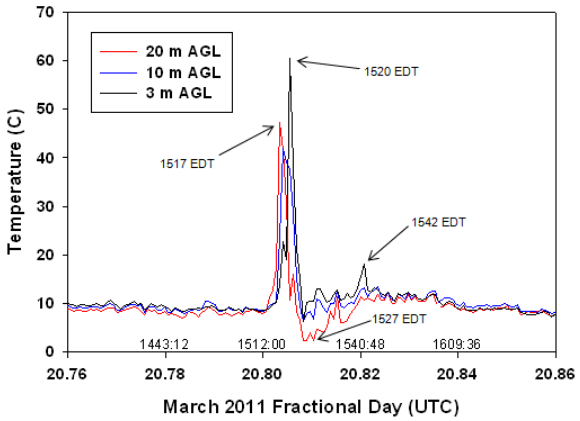

Fig. 10. Observed temperatures at 3 m, 10 m, and 20 m AGL on the 20 m tower (see Fig. 2) before, during, and after the E1 fire line passed the tower. Fire front passage occurred at 1520 EDT on 20 March 2011. Time stamps in EDT (hhmm:ss) are shown above the lower axis.

levels and rose above ambient temperatures until ~1542 EDT when they then gradually decreased to the ambient state. The E1 fire and the tilting of its convective plume produced thermally stable conditions throughout much of the 0-20 m layer immediately in front of the advancing fire line. This suggests near-surface turbulent mixing of heat and smoke due to buoyancy can be inhibited in the region immediately in front of an advancing, backing fire line that has a convective plume tilted into the prevailing winds.

3) Circulations

For the E1 fire, there was a clear shift in wind direction throughout the vertical extent of the vegetation layer from southeasterly winds well before fire front passage to southwesterly winds immediately before and during fire front passage at 1520 EDT (Figs 11a and 11b). The observed wind direction variations were consistent with the presence of a typical convergence zone at or in the immediate vicinity of the fire front. The southwesterly winds reached one-minute average maximum speeds of 4.8 m s^{-1}, 2.5 m s^{-1}, and 2.8 m s^{-1} at 20 m, 10 m, and 3 m AGL, respectively,

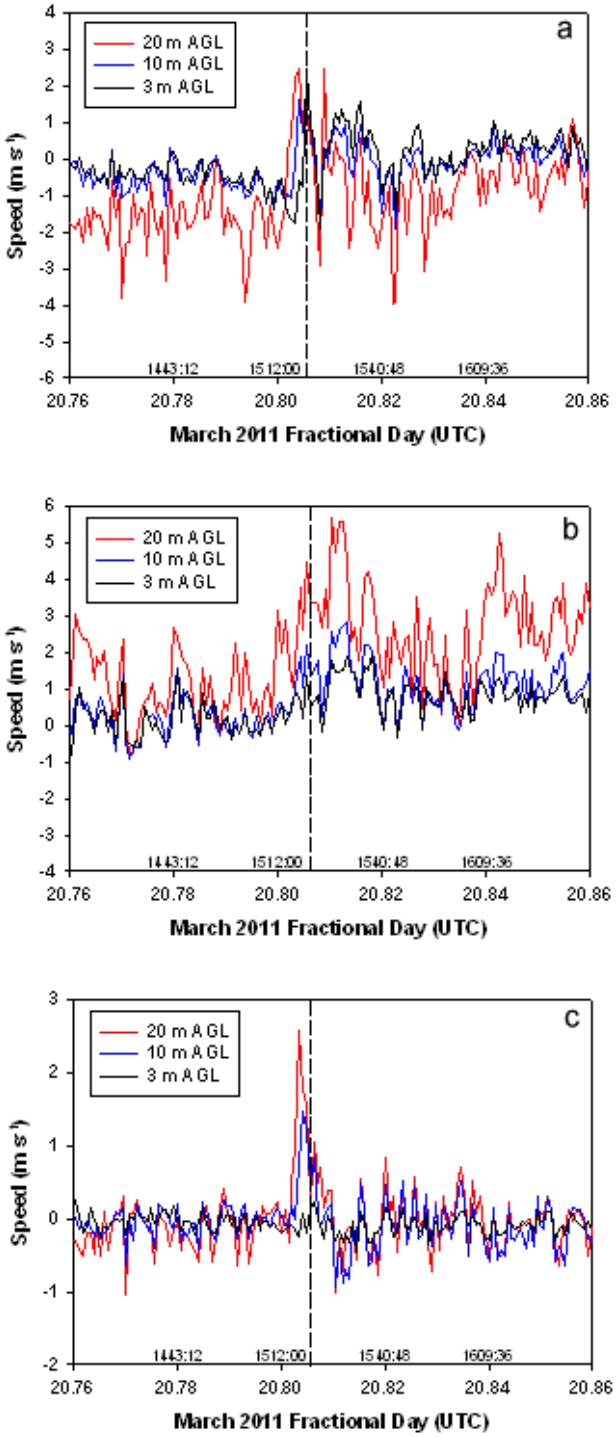

Fig. 11. Observed (a) east-west (U), (b) north-south (V), and (c) vertical (W) wind speeds at 3, 10, and 20 m AGL on the 20 m tower (see Fig. 2) before, during, and after the E1 fire line passed the tower. The vertical dashed lines indicate time of fire front passage (1520 EDT). Time stamps in EDT (hhmm:ss) are shown above the lower axes.

during this period. Following fire front passage at 1520 EDT, wind directions fluctuated back and forth between southwesterly and southeasterly, most prominently at the 20 m level, for a period of about 15 minutes before settling into a more persistent southeasterly direction consistent with the ambient wind direction. One-minute averaged vertical wind speeds reached maximum values of 2.6 m s^{-1} (1517 EDT), 1.5 m s^{-1} (1518 EDT), and 0.2 m s^{-1} (1521 EDT) at the 20 m, 10 m, and 3 m levels, respectively. At about seven minutes after fire front passage (1527 EDT), downdrafts were prominent, with one-minute averaged downdraft wind speeds reaching -1 m s^{-1} and -0.9 m s^{-1} at the 20 m and 10 m levels, respectively (Fig. 11c). This period of downdrafts was associated with the observed drop in temperatures below ambient conditions at numerous levels within the vegetation layer, as cooler air from above was transported into the vegetation layer behind the fire front. Downdrafts in this smoldering post fire-front-passage area suppressed the upward transport of smoke and kept smoke plumes closer to the surface.

4) Turbulence

For the E1 fire, atmospheric turbulence levels at the 20 m tower location (quantified by TKE per unit mass and equal to one-half of the sum of the horizontal and vertical velocity variances; Stull 1988) were consistently higher at 20 m (just above the canopy top) than at the 10 m and 3 m heights at all times (Fig. 12). During and immediately following fire front passage through the 20 m tower location, significant increases in TKE were measured, with the largest increases occurring at the 20 m level. At that height, one-minute averaged TKE values increased from < 5 m^2 s^{-2} well before fire front passage to about 20 m^2 s^{-2} three minutes prior to fire front passage, indicative of a highly turbulent canopy-atmosphere interface. TKE values then fluctuated wildly and generally diminished to < 5 m^2 s^{-2} by ~1610 EDT. At the 10 m and 3 m levels, TKE values reached maxima of ~8 m^2 s^{-2} (1517 EDT) and ~7 m^2 s^{-2} (1520 EDT), respectively, also indicative of highly turbulent conditions. Values then then diminished to < 2 m^2 s^{-2} by ~1541 EDT. These results suggest that the presence of forest overstory vegetation may affect the vertical distribution of turbulence above and in the vicinity of surface fires such that the most pronounced increases in TKE above a progressing fire line can potentially occur at or just above the canopy tops. Increased turbulence levels in the canopy-atmosphere interface region contribute to the enhanced mixing of heat, momentum, moisture, and smoke, and the enhanced entrainment of ambient air into the convective plume at that location.

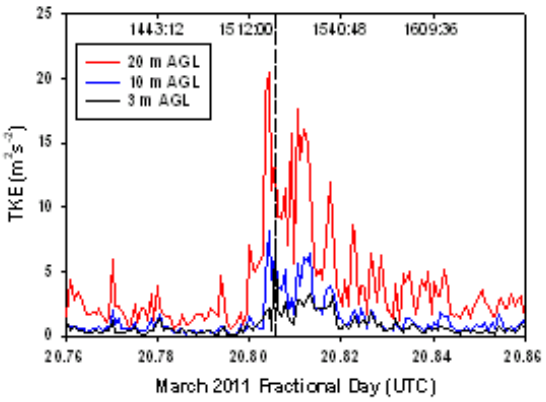

Fig. 12. Observed TKE at 3, 10, and 20 m AGL on the 20 m tower (see Fig. 2) before, during, and after the E1 fire line passed the tower. The vertical dashed line indicates time of fire front passage (1520 EDT). Time stamps in EDT (hhmm:ss) are shown below the upper axis.

The directional turbulent mixing of heat, moisture, and smoke during fire events depends on the distribution of energy among the horizontal and vertical components that comprise the total TKE field. To assess the relative contributions of these components to the total TKE field, a measure of turbulence anisotropy, values of $TKE_h = (u'^2+v'^2)/(2*TKE)$ and $TKE_w = w'^2/(2*TKE)$ were

computed. By definition, $TKE_h + TKE_w = 1$, with $TKE_w \approx 0.33$ and $TKE_h \approx 0.67$ under isotropic conditions. Computed TKE_h and TKE_w values during the E1 burn suggest that anisotropic turbulence was present at all levels within the vegetation layer before, during, and after fire front passage. The horizontal component of TKE usually comprised more than 80% of the total TKE on average. Furthermore, the presence of forest vegetation affected the degree of anisotropy in the turbulence field; anisotropy was stronger at the 3 m and 20 m levels than at the 10 m level, which is consistent with larger vertical wind shears expected at the 3 m and 20 m levels than at the mid-canopy 10 m level. The observed anisotropy in the turbulence regimes indicates horizontal mixing of heat, moisture, and smoke from low-intensity fires may very well dominate vertical mixing within and immediately above the vegetation layer.

5) Air Quality

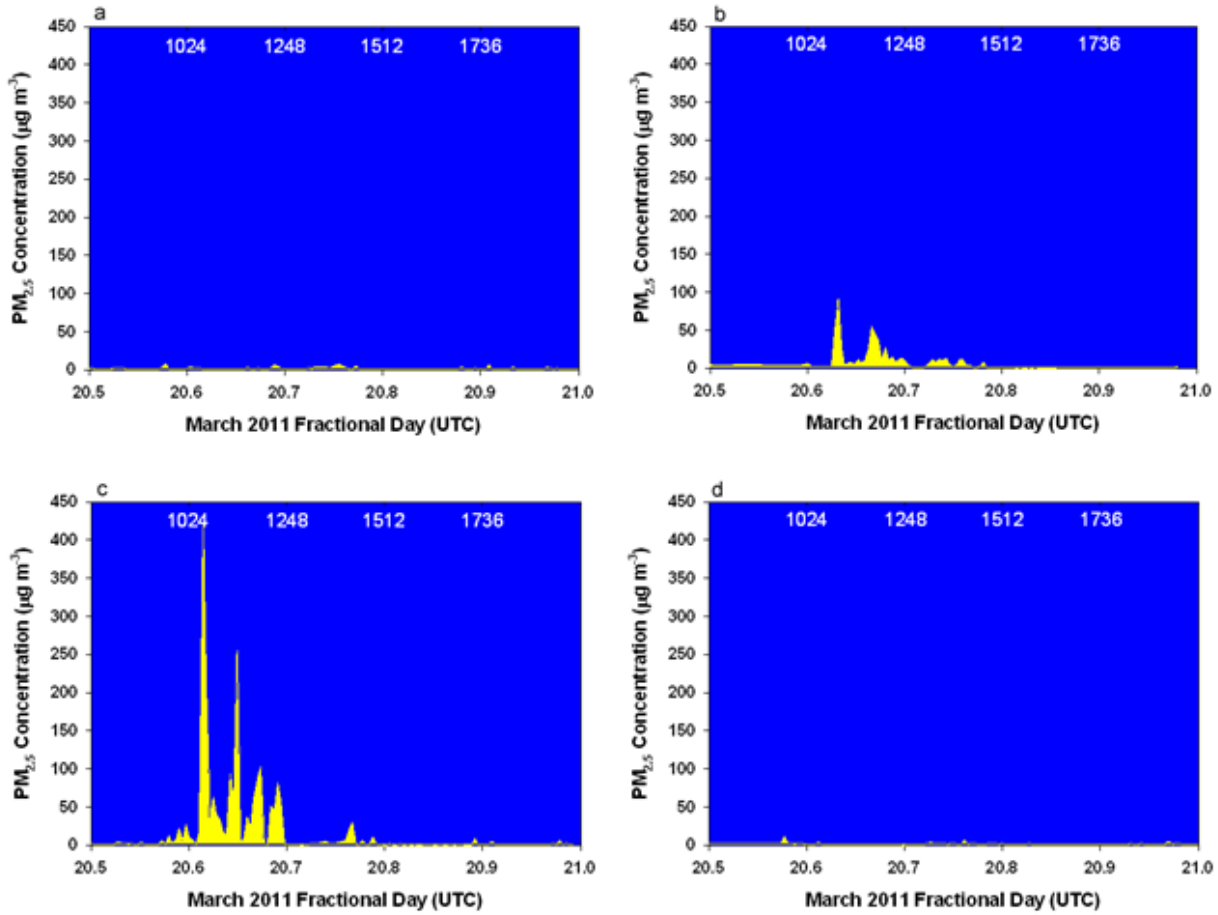

Fig. 13. Observed time series of near-surface $PM_{2.5}$ concentrations at the (a) PM1, (b) PM2, (c) PM3, and (d) PM4 Dataram monitors located downwind of the E1 burn block (see Fig. 2) for the E1 burn experiment. Time stamps in EDT (hhmm) are shown below the upper axis.

Near-surface concentrations of $PM_{2.5}$ measured downwind of the E1 burn block were highly variable (Fig. 13). A maximum concentration of 423 µg m^{-3} was observed at 1044 EDT at the PM3 Dataram monitor located along the southern perimeter of the burn block (see Fig. 2) about 49 minutes after the initial ignition time. The time series of $PM_{2.5}$ concentrations at that location

showed signs of periodicity over the 1044-1248 EDT time period, with relative maxima occurring at 1134 EDT, 1209 EDT, and 1234 EDT. After 1500 EDT, negligible concentrations of $PM_{2.5}$ at the PM3 monitor were observed. Elevated concentrations of $PM_{2.5}$ were also measured at the PM2 Dataram monitor located about 0.8 km west of the PM3 monitor. A maximum concentration of 91 μg m^{-3} at 1109 EDT was measured there. Similar to the PM3 monitor, concentrations at the PM2 monitor were negligible after 1500 EDT. The PM1 and PM4 monitors, located about 0.5 km and 1.0 km south of the PM3 monitor, respectively, did not record concentrations above 12 μg m^{-3} for the duration of the burn experiment. The veering ambient winds (northerly to southeasterly) on 20 March 2011 contributed to the low concentrations measured at the PM1 and PM4 monitors.

Within the E1 burn block, near-surface CO concentrations measured at the 3 m towers showed considerable spatial variation. Maximum CO concentrations ranged from 31 ppm (tower 9, Fig. 2) to 820 ppm (tower 4, Fig. 2) across the burn block, as measured at the 3 m towers, as the fire line progressed through the burn block (Fig. 14). The duration of elevated CO concentrations above 0 ppm at each 3 m tower was on the order of 30 minutes, with concentrations increasing rapidly as the fire line approached each tower and then decreasing to negligible levels more gradually during the post fire front passage period when smoldering was prevalent (see Fig. 15). The advancing fire line through the 3 m tower locations in the E1 burn block resulted in episodes of one-hour averaged CO concentrations exceeding the 35 ppm one-hour average National Ambient Air Quality Standard (NAAQS) only at tower 4 (47 ppm from 1844-1944 EDT). The measured CO concentrations suggest that CO emissions during the E1 burn experiment did not pose a substantial hazard from a NAAQS perspective.

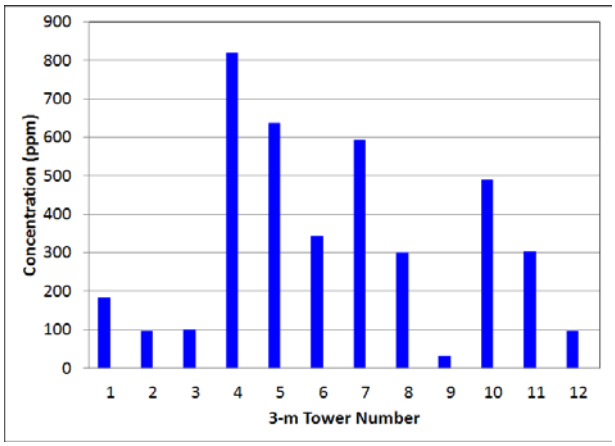

Fig. 14. Observed maximum CO concentrations at the twelve 3-m towers located within the E1 burn block (see Fig. 2) during the E1 burn experiment.

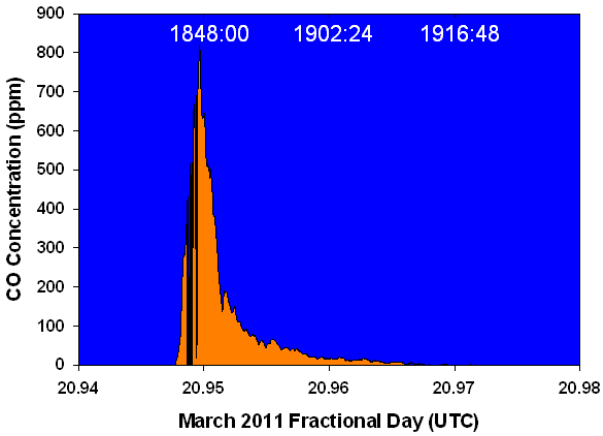

Fig. 15. Observed CO concentrations at tower #4 (see Fig. 2) located within the E1 burn block (see Fig. 2) during the E1 burn experiment. Time stamps in EDT (hhmm:ss) are shown below the upper axis.

Key Fuel, Meteorological and Air-Quality Observations During the 6 March 2012 NJ Pine Barrens Prescribed Fire Experiment: The second low-intensity prescribed fire experiment (E2) was carried out on 6 March 2012, also in the New Jersey Pine Barrens (see Figs. 1 and 2). The observed time series of ambient wind speeds, wind directions, temperatures, and relative

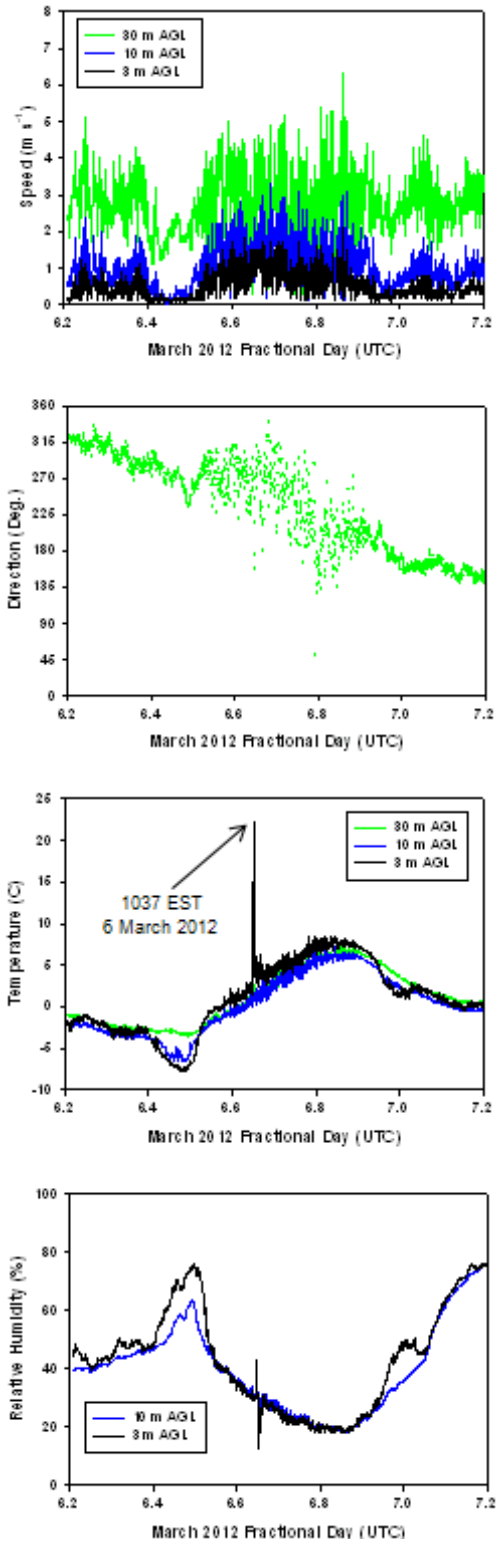

Fig. 16. Observed ambient wind speeds, wind directions (30 m AGL only), temperatures, and relative humidity on 6 March 2012 (E2 experiment) at 3 m, 10 m, and 30 m AGL at the 30 m tower location shown in Fig. 2. Time when the E2 fire line passed the 30 m tower is noted on the temperature time series figure.

humidity as measured on the 30 m tower located along the southeastern perimeter of the burn block are shown in Fig. 16. As with the E1 burn experiment, ambient near-surface (3 m AGL) winds were generally less than 2 m s^{-1}. The directions, however, varied from northwesterly to southerly during the burn. Temperatures reached a maximum of ~8° C in the afternoon, and relative humidity values dropped to ~20%. The estimated average westward fire spread rate for the individual fire lines established during the E2 burn experiment was 0.33 m min^{-1}. The following sub-sections provide a brief summary of the key fuel, meteorological, and air quality observations for the E2 experiment. A comprehensive summary of the E2 observations can also be found in Heilman et al. (2013).

1) Fuel Conditions

The average pre-burn fuel loading of understory vegetation and the forest floor for the E2 burn block totaled 1104 ± 246 g m^{-2}, about 26% less than the E1 burn block fuel loading. Only about 15% (169.6 ± 131.8 g m^{-2}) of the total fuel loading in the E2 burn block was attributed to shrubs, with the rest (~85%, 934.3 ± 192.4g m^{-2}) attributed to forest floor fuels. Burning during the E2 experiment resulted in an estimated total fuel consumption 507.3 g m^{-2}, which was 46% of total fuel loading at the site and ~27% less than the consumption during the E1 experiment. The pre-burn 1-hour and 10-hour forest floor fuel moisture was substantially higher for the E2 experiment than the E1 experiment, with values of 42.7 ± 13.4% and 56.3 ± 25.8%, respectively. Moisture contents were 53.2 ± 6.1%, 136.3 ± 8.3%, and 92.5 ± 8.0% for the live 1-hour shrub stems, pine needles, and live 1-hour pine stems, respectively. These latter values were similar to the corresponding fuel moisture contents for the E1 burn experiment.

2) Thermal Fields

Temperature measurements at the 10 m and 20 m towers located in the interior of the E2 burn block revealed that the intensity of the individual fire lines for the E2 experiment was much less than for the E1

fire line. Figure 17 shows the observed one-minute average temperature time series at 3 m, 10 m, and 20 m AGL on the 20 m tower for the time period during which the 20 m tower experienced a fire front passage. Maximum one-minute averaged air temperatures only reached ~18°C (9 m AGL) at the time of fire front passage at the 20 m tower in the E2 burn block. Unlike the E1 burn, tilting of the convective plume into the ambient wind within the vegetation layer was minimal; maximum one-minute averaged temperatures at the 3 m, 10 m, and 20 m levels on the 20 m tower were 14.4°C (1537 EST), 17.3°C (1539 EST), and 13.1°C (1538 EST), respectively. One-minute averaged temperatures immediately following the lower intensity E2 fire front passage through the 20 m tower location did not drop below ambient temperatures like they did for the higher intensity E1 burn. Instead, temperatures at all levels generally decayed to ambient values over a ~5-30 minute period, most rapidly at heights above 3 m. The E2 fire resulted in much smaller temporal variations in stability than what was observed for the E1 fire. Minimal tilting of the E2 convective plume led to a much less intense initial stable layer near the surface during the fire front passage period than for the E1 fire. This observed stability, although less than for the E1 fire, was due in part again to the clearing of surface fuels around the base of the tower for instrument protection. Instability within the 4-20 m layer following the E2 fire front passage was also much lower than that observed for the E1 fire.

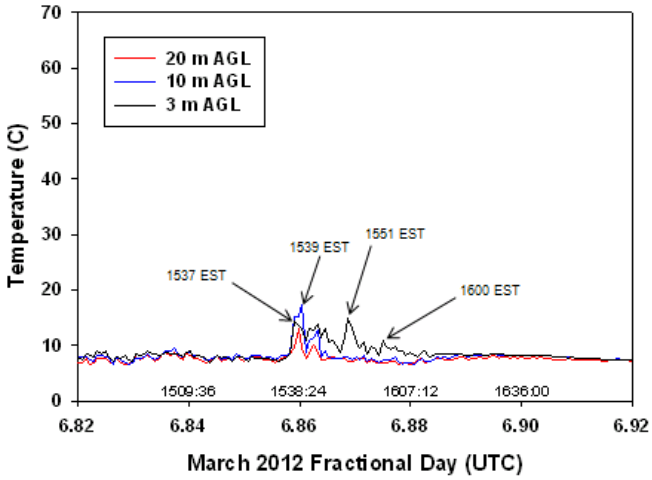

Fig. 17. Observed temperatures at 3 m, 10 m, and 20 m AGL on the 20 m tower (see Fig. 2) before, during, and after the E2 fire line passed the tower. Fire front passage occurred at 1537 EST on 6 March 2012. Time stamps in EST (hhmm:ss) are shown above the lower axis.

3) Circulations

The atmospheric circulation response to the lower intensity E2 fire was much less pronounced than for the E1 fire. Figure 18 indicates the horizontal (U and V) and vertical (W) wind speed component fluctuations at the 3 m, 10 m, and 20 m levels on the 20 m tower immediately before, during, and after fire front passage at 1537 EST were similar to the fluctuations characterizing the generally westerly and southwesterly ambient winds during the afternoon of 6 March 2012. The measured wind speeds did not pick up the presence of a significant convergence zone in the vicinity of the fire line that passed the 20 m tower. The fluctuating northwesterly to southwesterly winds during the fire front passage period yielded one-minute averaged maximum speeds of 3.4 m s^{-1}, 2.2 m s^{-1}, and 2.0 m s^{-1} at 20 m, 10 m, and 3 m AGL. The passage of the fire front through the 20 m tower location did not generate any substantial buoyancy driven updrafts or compensating downdrafts at that location. The fire's minimal impact on the overall circulation patterns and thermal fields within and immediately above the vegetation layer resulted in observed smoke plumes that did not exhibit significant local lofting (see Fig. 19). Rather, local smoke plume behavior was primarily influenced by mean and wind-shear driven

turbulent circulations resulting from typical canopy-atmosphere interactions that occur in an atmospheric boundary layer containing forest vegetation.

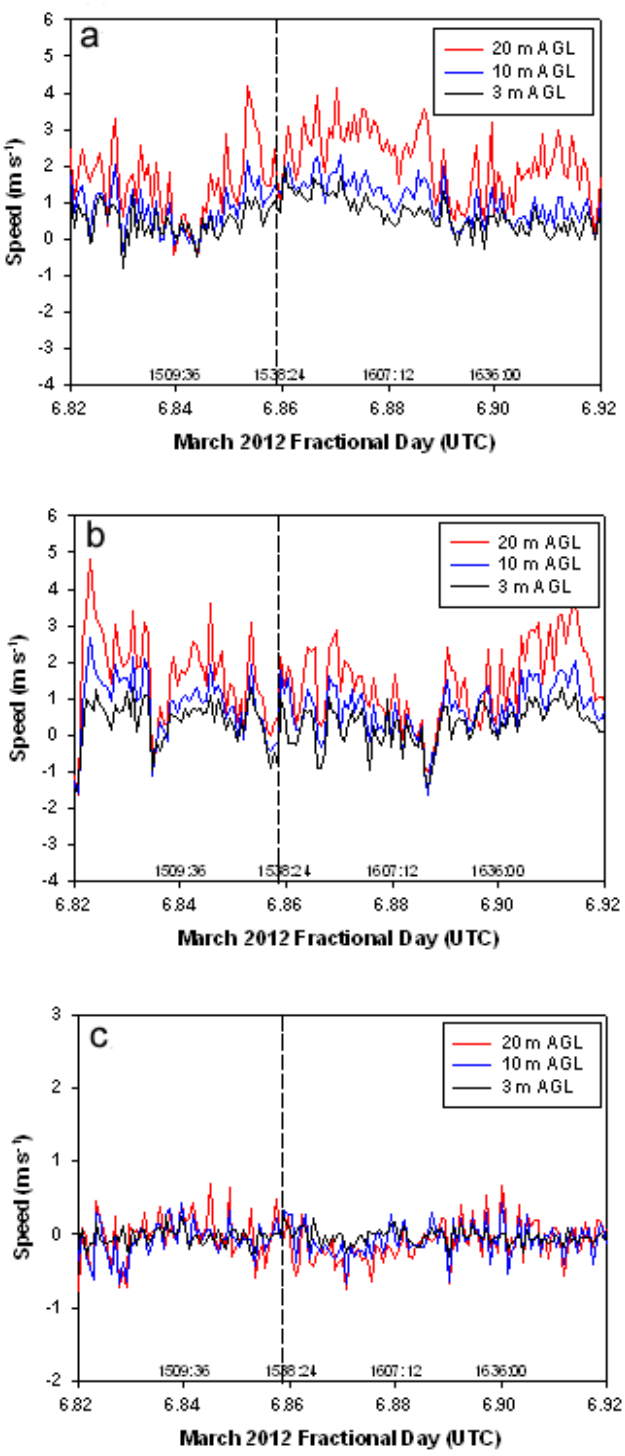

Fig. 18. Observed (a) east-west (U), (b) north-south (V), and (c) vertical (W) wind speeds at 3, 10, and 20 m AGL on the 20 m tower (see Fig. 2) before, during, and after one of the E2 fire lines passed the tower. The vertical dashed lines indicate time of fire front passage (1537 EST). Time stamps in EST (hhmm:ss) are shown above the lower axes.

Fig. 19. Typical smoke plume observed within the E2 burn block during the 6 March 2012 prescribed fire experiment (photo taken at 1351 EST).

4) Turbulence

The atmospheric turbulence levels at the 20 m tower location for the E2 experiment were higher at 20 m AGL than at the 10 m and 3 m levels, which was consistent with the pattern observed for the E1 fire (Fig. 20). Several occurrences of one-minute averaged TKE values at the 20 m level exceeding 5 m^2 s^{-2} characterized the TKE time series for the duration of the experiment. However, the TKE variations with height for the E2 experiment were less than the variations for the E1 experiment. The passage of the fire front through the 20 m tower location did not produce significant increases in TKE at any level. One-minute averaged TKE values during the period of fire front passage were less than 3 m^2 s^{-2} at all levels, indicating essentially non-turbulent conditions in the vicinity of the fire line and limited turbulent

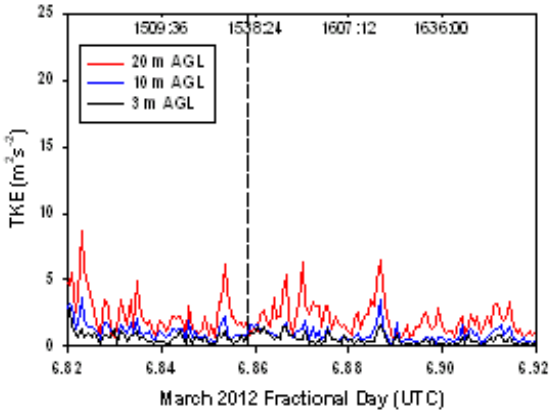

Fig. 20. Observed TKE at 3, 10, and 20 m AGL on the 20 m tower (see Fig. 2) before, during, and after one of the E2 fire lines passed the tower. The vertical dashed line indicates time of fire front passage (1537 EST). Time stamps in EST (hhmm:ss) are shown below the upper axis.

mixing of heat, moisture, momentum, and smoke from the surface to the top of the vegetation layer. The relatively low intensity of the fire lines for the E2 experiment coupled with the presence of overstory vegetation resulted in the limited buoyant production of TKE and enhanced non-buoyant dissipation of TKE within the vegetation layer. It was only after smoke plumes from the E2 fire lines penetrated the canopy-atmosphere interface that they experienced significant turbulent mixing and entrainment of ambient air, mainly through wind-shear generated turbulence above the canopy tops.

Like the E1 burn experiment, computed TKE_h and TKE_w values (see the Turbulence subsection for the E1 burn experiment results for a description of these variables) at the 20 m tower during the E2 burn suggest that anisotropic turbulence was present at all levels within the vegetation layer before, during, and after fire front passage. The horizontal component of TKE usually comprised more than 80% of the total TKE on average, and turbulence anisotropy was stronger at the 3 m and 20 m levels than at the 10 m level. Although the E2 fire lines were generally lower in intensity and led to lower overall TKE values in their vicinity than for the E1 fire line, the vertical component of the total TKE (i.e. w'^2), which is generated through buoyancy, comprised larger average proportions of the total TKE at all levels on the 20 m tower during the period of E2 fire front passage than the proportions observed during the E1 fire front passage. Average TKE_w values at the 20 m, 10 m, and 3 m levels during the 10 minute period (1532-1542 EST) when the E2 fire front passage occurred were 0.174, 0.216, and 0.129, respectively. The corresponding 20 m, 10 m, and 3 m TKE_w values during the E1 fire front passage period (1515-1525 EST) were 0.153, 0.188, and 0.078. These observed turbulence anisotropy characteristics are counterintuitive to the assumed enhanced relative importance of the vertical component of TKE (w'^2) compared to the horizontal components (u'^2 and v'^2) in the vicinity of more intense fires. The extent to which forest overstory vegetation might contribute to this counterintuitive observation has yet to be resolved, and will likely require additional sensitivity analyses with modeling systems like ARPS-CANOPY or RAFLES.

4) Air Quality

Maximum and average near-surface $PM_{2.5}$ concentrations measured by the four Dataram monitors located at various points downwind (east) of the E2 burn block (see Fig. 2) were higher than the maximum and average concentrations observed during the E1 burn experiment. Figure 21 shows the individual $PM_{2.5}$ concentration time series for the E2 Dataram monitors. The highest concentrations were observed at the PM3 Dataram monitor, which was located along the eastern boundary of the E2 burn block. A maximum concentration of 711 μg m^{-3} was measured there at 1000 EST, about 30 minutes after the initial fire line along the eastern boundary of the burn block was ignited. Following the initial peak in $PM_{2.5}$ concentrations, subsequent

concentrations at the PM3 monitor dropped rapidly and fluctuated between 30 and 130 μg m^{-3} from 1050 to 1435 EST, when the monitor stopped functioning. The next highest near-surface $PM_{2.5}$ concentrations were observed at the PM2 and PM4 monitor sites, both about 300 m east of the E2 burn block. Maximum observed concentrations were 114 μg m^{-3} (1553 EST) and 122 μg m^{-3} (1603 EST) at the PM2 and PM4 monitors, respectively. Concentrations at the PM2 and PM4 monitors also dropped rapidly to values less than 50 μg m^{-3} after the times of peak concentrations. The lowest overall $PM_{2.5}$ concentrations were observed at the PM1 Dataram monitor, about 600 m east of the E2 burn block. There was no prominent peak in concentrations observed there; concentrations generally fluctuated between 3 and 25 μg m^{-3} throughout the duration of the burn.

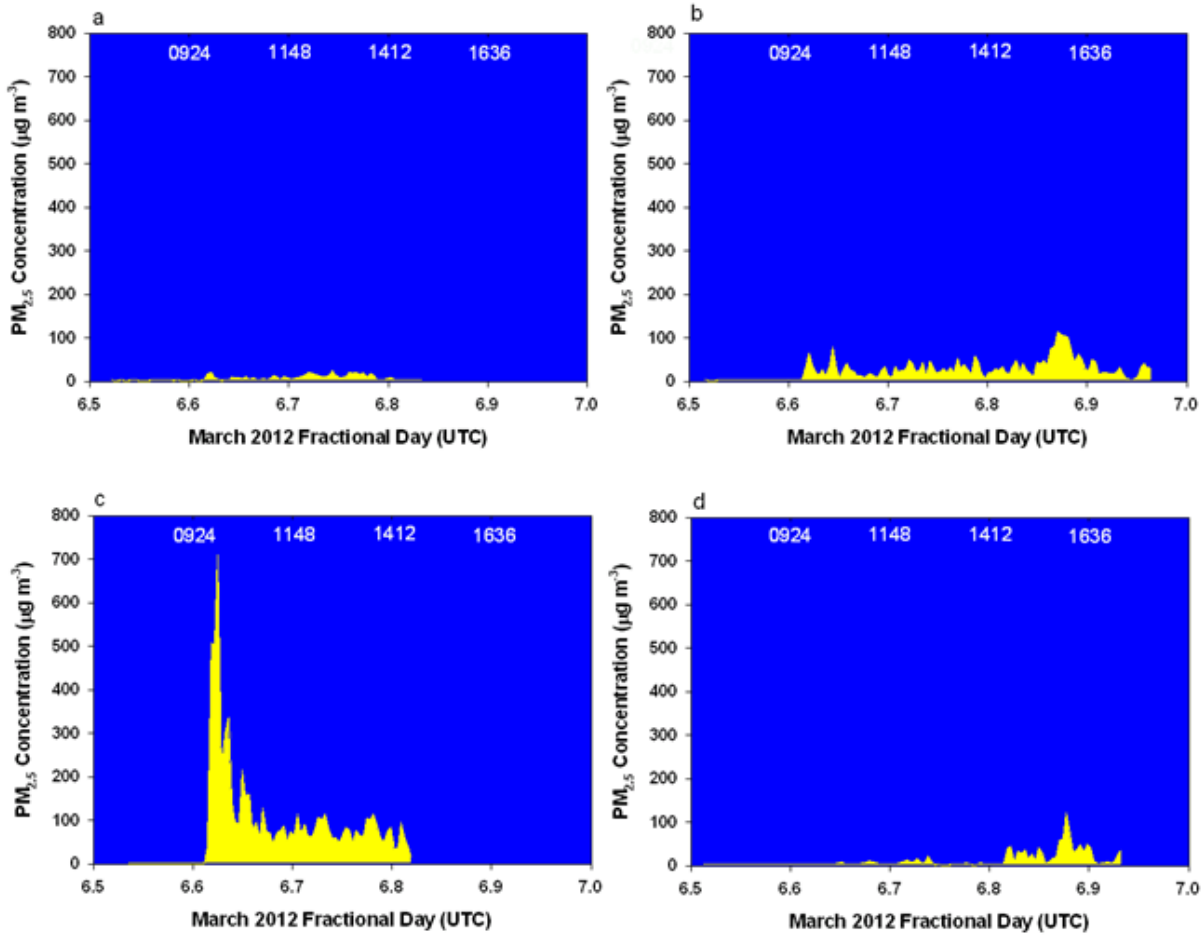

Fig. 21. Observed time series of near-surface $PM_{2.5}$ concentrations at the (a) PM1, (b) PM2, (c) PM3, and (d) PM4 Dataram monitors located downwind of the E2 burn block (see Fig. 2) for the 21 burn experiment. Time stamps in EST (hhmm) are shown below the upper axis. Measurements after 1501, 1808, 1440, and 1723 EST for the PM1, PM2, PM3, and PM4 monitors, respectively, were not available.

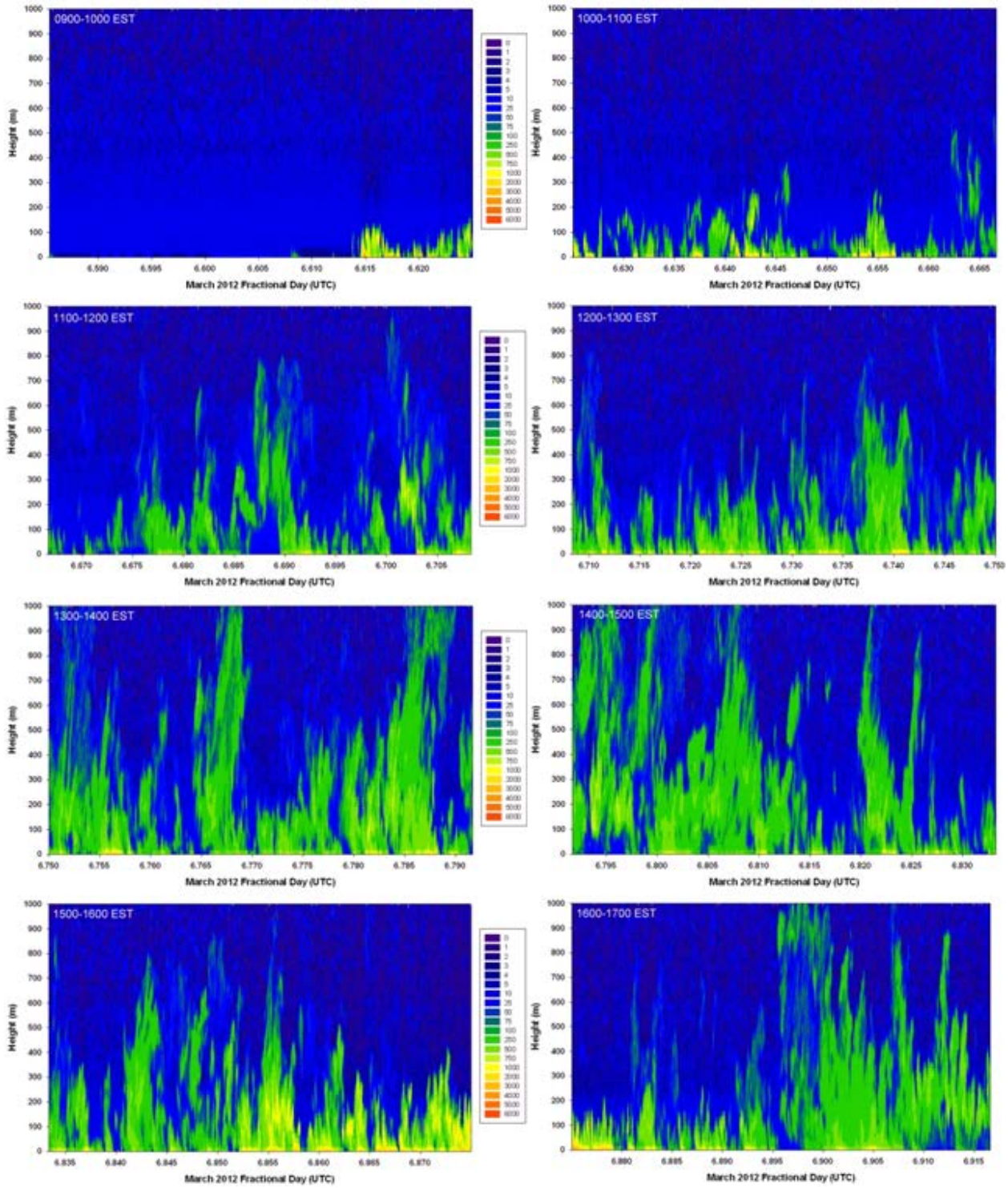

Fig. 22. Time-height cross-sections of derived $PM_{2.5}$ concentrations (μg m^{-3}) from ceilometer measurements (see Fig. 2) during the E2 burn experiment for eight one-hour periods beginning at 0900 EST and ending at 1700 EST.

For the E2 burn experiment, plume heights and $PM_{2.5}$ vertical profile concentrations were measured and derived via a ceilometer located about 100 m east (downwind) of the burn block

(see Fig. 2). Figure 22 shows time-height cross-sections of derived $PM_{2.5}$ concentrations from the surface up to 1000 m AGL for eight one-hour-long periods starting at 0900 EST and ending at 1700 EST on 6 March 2012. The $PM_{2.5}$ concentrations and implied plume heights at this location showed considerable temporal variability over the duration of the burn experiment. Elevated $PM_{2.5}$ concentrations above ambient conditions at the ceilometer site were confined to lower levels in the boundary layer during the morning hours of the E2 burn experiment, due to the proximity of the ceilometer to the initial fire line established in the morning along the eastern boundary of the E2 burn block as well as the low-level capping inversion that existed during the morning hours. As the atmospheric mixed layer height increased during the day, elevated $PM_{2.5}$ concentrations were observed at higher levels above the ceilometer site. Beginning with the 1300-1400 EST time period, elevated $PM_{2.5}$ concentrations reached 1 km AGL at the ceilometer site. By this time, north-south oriented fire lines had been established throughout the E2 burn block, allowing transported emissions from the western portions of the burn block to rise to higher levels in the boundary layer by the time they were directly over the ceilometer site. Plume heights at the ceilometer site were highly variable during the afternoon hours, ranging from ~100 m to higher than 1000 m. However, throughout the burn experiment, maximum $PM_{2.5}$ concentrations above the ceilometer site were usually found between the surface and 100 m AGL. The low-intensity E2 surface fire lines underneath the forest overstory vegetation in the E2 burn block contributed to the poor near-surface air-quality conditions immediately downwind (east) burn block; vertical transport and turbulent mixing of the fire emissions was inhibited by the relatively low buoyancy induced by the E2 fire lines and the effect of the overstory vegetation on reducing the vertical component of turbulent energy (and thus vertical turbulent mixing) within and immediately above the vegetation layer.

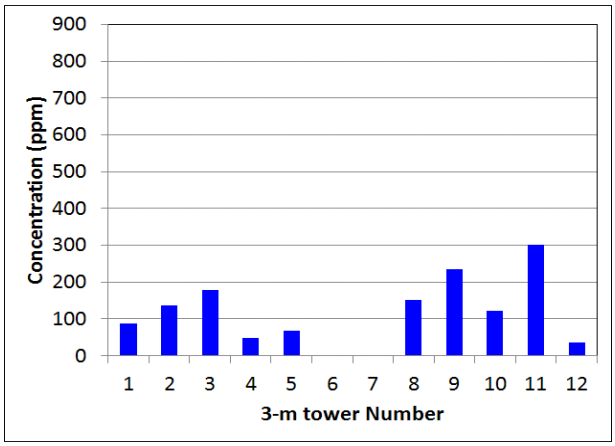

Fig. 23. Observed maximum CO concentrations at the twelve 3-m towers located within the E2 burn block (see Fig. 2) during the E2 burn experiment.

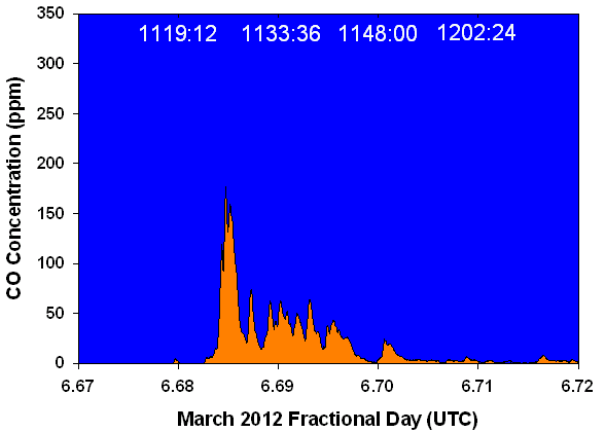

Fig. 24. Observed CO concentrations at tower #3 (see Fig. 2) located within the E2 burn block (see Fig. 2) during the E2 burn experiment. Time stamps in EST (hhmm:ss) are shown below the upper axis.

In contrast to the observed higher near-surface $PM_{2.5}$ concentrations during the E2 burn compared to the E1 burn, observed near-surface CO concentrations were generally lower during the E2 burn than during the E1 burn (Fig. 23). Maximum CO concentrations measured at the 3-m tower locations within the E2 burn block ranged from 36 ppm (tower 12, Fig. 2) to 302 ppm (tower 11, Fig. 2). Similar to the E1 burn experiment, periods of elevated near-surface CO

concentrations were relatively short (~30 minutes). Concentrations increased rapidly as the individual fire lines approached each tower, and then they decreased to negligible levels more gradually following fire front passage when smoldering was prevalent (see Fig. 24). There were no episodes of one-hour averaged CO concentrations exceeding the 35 ppm one-hour average NAAQS.

Application of ARPS-CANOPY/FLEXPART to the 20 March 2011 NJ Pine Barrens Prescribed Fire Experiment: Following the development of the ARPS-CANOPY model and its evaluation with observational data from the non-fire environment CHATS field experiment (see Pages 13-14), the coupled ARPS-CANOPY/FLEXPART system was evaluated using observational data from the 20 March 2011 prescribed fire experiment in the NJ Pine Barrens (experiment E1). A series of one-way nested simulations were performed with ARPS-CANOPY using domains with horizontal grid spacing ranging from 8.1 km in the outer domain to 100 m in the innermost domain (Fig. 25). The outermost domain (domain 1) covered the northeastern U.S., while the innermost domain (domain 5) covered only the area within several kilometers of the E1 burn block (see star in Fig. 25b). Initial and lateral boundary conditions were supplied to the outermost domain from the North American Regional Reanalysis (NARR) dataset (Mesinger et al. 2006), while the imposed upper boundary condition for all simulations was a sponge layer in the upper 2 km of the domain. Terrain data for domains 1-3 were generated from 30-arc-second resolution U.S. Geological Survey (USGS) datasets and for domains 4-5 from 3-arc-second resolution USGS datasets. Land-use data for the outer four domains were generated from 1-km resolution USGS land-use data, while for the innermost domain, the land-use was specified as heterogeneous forest and defined at each grid point with a vertical profile of plant area density

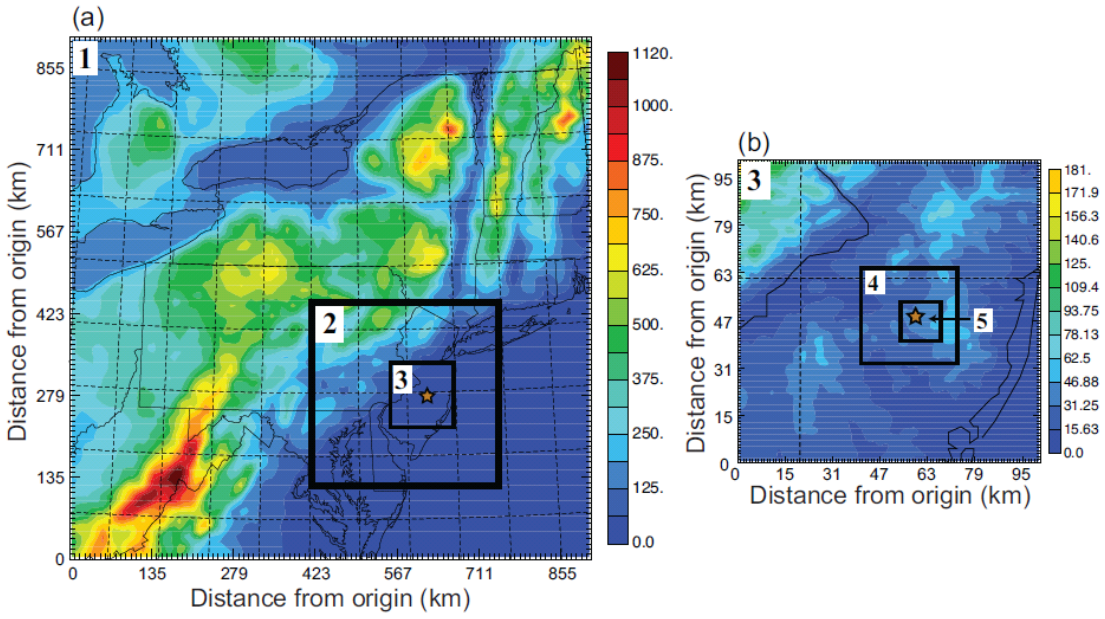

Fig. 25. Maps of surface elevation (m) from (a) domain 1, with outlines of domains 2 and 3 overlaid, and (b) domain 3 with outlines of domains 4 and 5 overlaid for the ARPS-CANOPY/FLEXPART simulations of the E1 burn experiment. Star indicates approximate location of the E1 burn block.

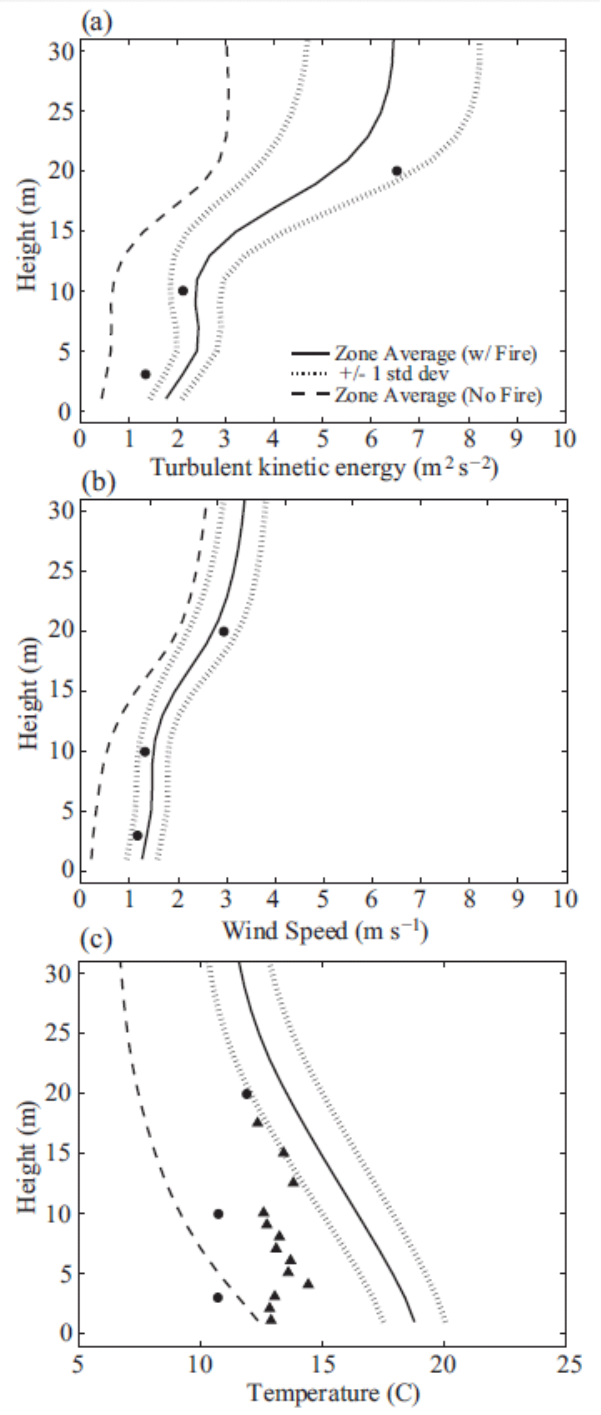

Fig. 26. Vertical profiles of (a) TKE, (b) wind speed, and (c) temperature, averaged in time from 1510-1610 EDT on 20 March 2011. ARPS-CANOPY simulated fields are averaged around all grid points within the parameterized burn zone. Solid line indicates the mean and dotted lines indicate the mean ± one standard deviation (perturbations computed with respect to burn zone mean). Long dashed line indicates mean from simulation with no fire. Symbols represent 20 m tower observations.

derived from LiDAR observations using the methodology of Skowronski et al. (2011). For domains 1-4, all simulations were initialized at 2000 EDT 18 March 2011 and run for 60 hours; for domain 5 containing the E1 burn block, two 12-hour simulations were run, the first initialized at 0800 EDT 19 March 2011 (pre-burn day) and the second at 0800 EDT 20 March 2012 (burn day). The presence of the spreading surface fire line through the E1 burn block was parameterized in ARPS-CANOPY via an imposed surface turbulent heat flux value (15 kW m^{-2}) at surface grid point locations corresponding to the actual observed E1 fire line locations over time periods consistent with the estimated observed spread rate of the E1 fire line (1.5 m min^{-1}). A complete discussion of the ARPS-CANOPY set-up and parameterizations for the E1 simulation can be found in Kiefer et al. (2013b).

Despite some discrepancies between the ARPS-CANOPY model predictions and the E1 observations, ARPS-CANOPY was shown to be capable of simulating the atmosphere at the synoptic scale and mesoscale, as well as the salient aspects of the planetary boundary layer before and during the burn experiment. At micrometeorological scales, the ARPS-CANOPY profile simulations of mean TKE, wind speed, wind direction, and temperature during the E1 burn were found to largely agree with the 20-m tower observations within the E1 burn block (Fig. 26). The observed fire-induced increases in TKE values within and above the E1 burn block forest vegetation layer were captured very well by ARPS-CANOPY (Fig. 26a), especially the substantial increase in TKE just above the canopy top, a factor critically important for the dispersion of smoke as it exits the top of the vegetation layer. Predicted average wind speed profiles in the vicinity of the parameterized E1 fire line by ARPS-CANOPY closely matched the average wind speed profiles computed from *in situ* tower observations (Fig. 26b), suggesting that the

parameterized canopy-drag effects incorporated into ARPS-CANOPY generated the proper air-flow reduction within the E1 vegetation layer. The largest errors in the ARPS-CANOPY simulations were associated with average temperatures within the E1 vegetation layer in the vicinity of the E1 fire line. Predicted average temperatures in the vicinity of the E1 fire line were ~2° warmer than the observations in the upper portions of and immediately above the E1 vegetation layer, and ~3-5°C warmer than the observations in the lower portions of the E1 vegetation layer (Fig. 26c). Some of the discrepancy is associated with the vegetation clearing under the *in situ* towers that inhibited burning directly underneath the towers. Although there was a warm bias in the simulated temperatures near the E1 fire line within the vegetation layer, the simulated lapse rates within the vegetation layer were quite similar to the observed lapse rates, which suggests that ARPS-CANOPY was able to capture the overall near-surface stability conditions that governed the near-surface buoyancy generation of turbulence near the fire line.

The ARPS-CANOPY simulations also revealed significant horizontal spatial variability in the wind and turbulence regimes within and immediately above the vegetation layer in the E1 burn block as the E1 fire line progressed through the burn block. Figure 27 (top panels) shows horizontal cross-sections (3 m, 10 m, and 20 m AGL) of simulated mean (1-h averages) TKE and wind in and around the E1 burn block when the E1 fire line was near the 20 m tower (1510-1610 EDT) (see Fig. 2 for location of 20 m tower). Corresponding horizontal cross-sections from a "no-fire" simulation for the same 1510-1610 EDT time period are included for reference (bottom panels). The horizontal cross-sections from the simulation with fire (Fig. 27a-c) depict a broad

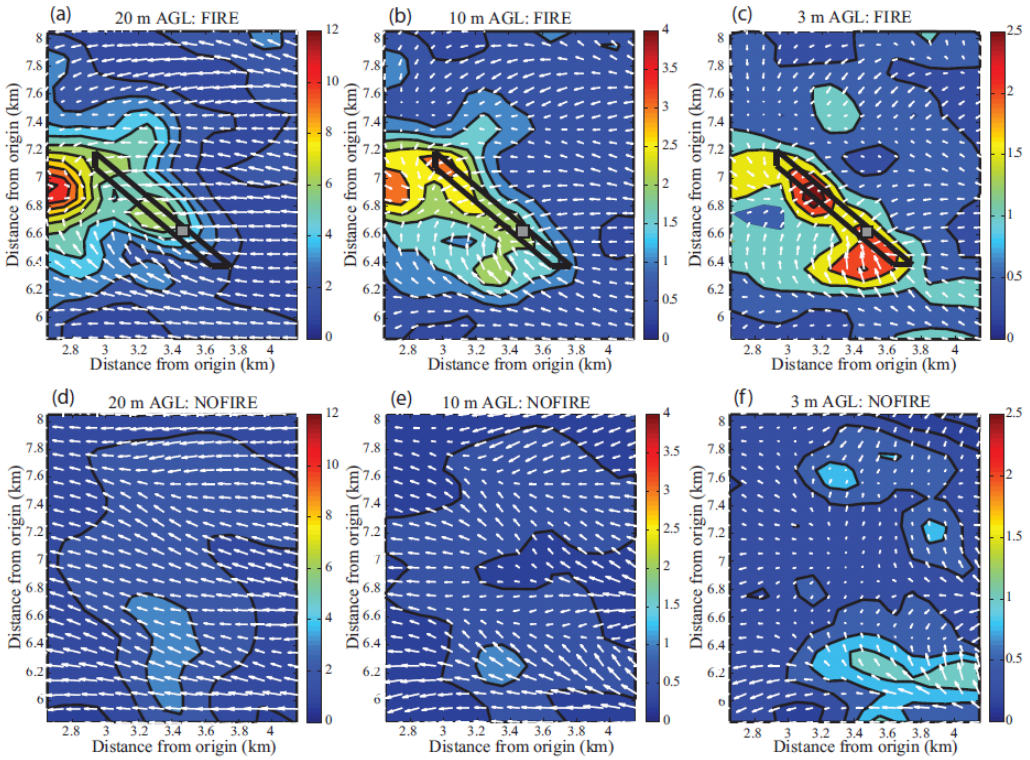

Fig. 27. TKE at (a,d) 20 m AGL, (b,e) 10 m AGL, and (c,f) 3 m AGL averaged from 1510-1610 EDT on 20 March 2011 from ARPS-CANOPY simulations with fire (upper panels) and without fire (lower panels). Horizontal wind vectors are overlaid along with the perimeter of the parameterized burn zone (black quadrilateral) containing the 20 m tower (gray square) over which averages were computed to produce Fig. 26. Contour interval in (a,d) is 1 m^2 s^{-2}; in all other panels interval is 0.5 m^2 s^{-2}.

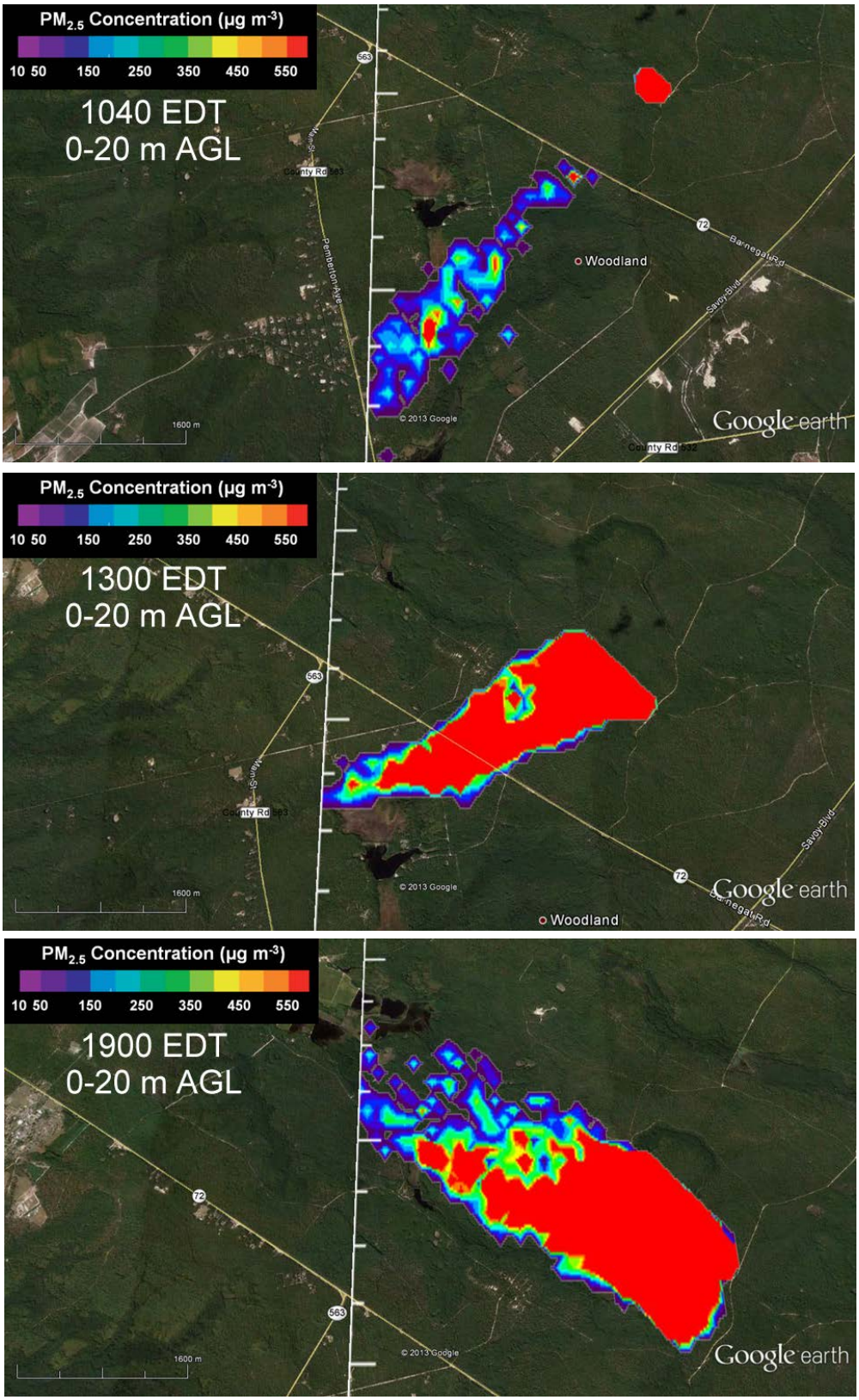

Fig. 28. Integrated $PM_{2.5}$ concentrations (µg m^{-3}) for the 0-20 m AGL layer at three different times during the E1 prescribed fire experiment on 20 March 2011 as simulated by ARPS-CANOPY/FLEXPART. Sharp boundary of plume concentrations downwind of the burn block coincides with the FLEXPART lateral domain boundary used in the simulations.

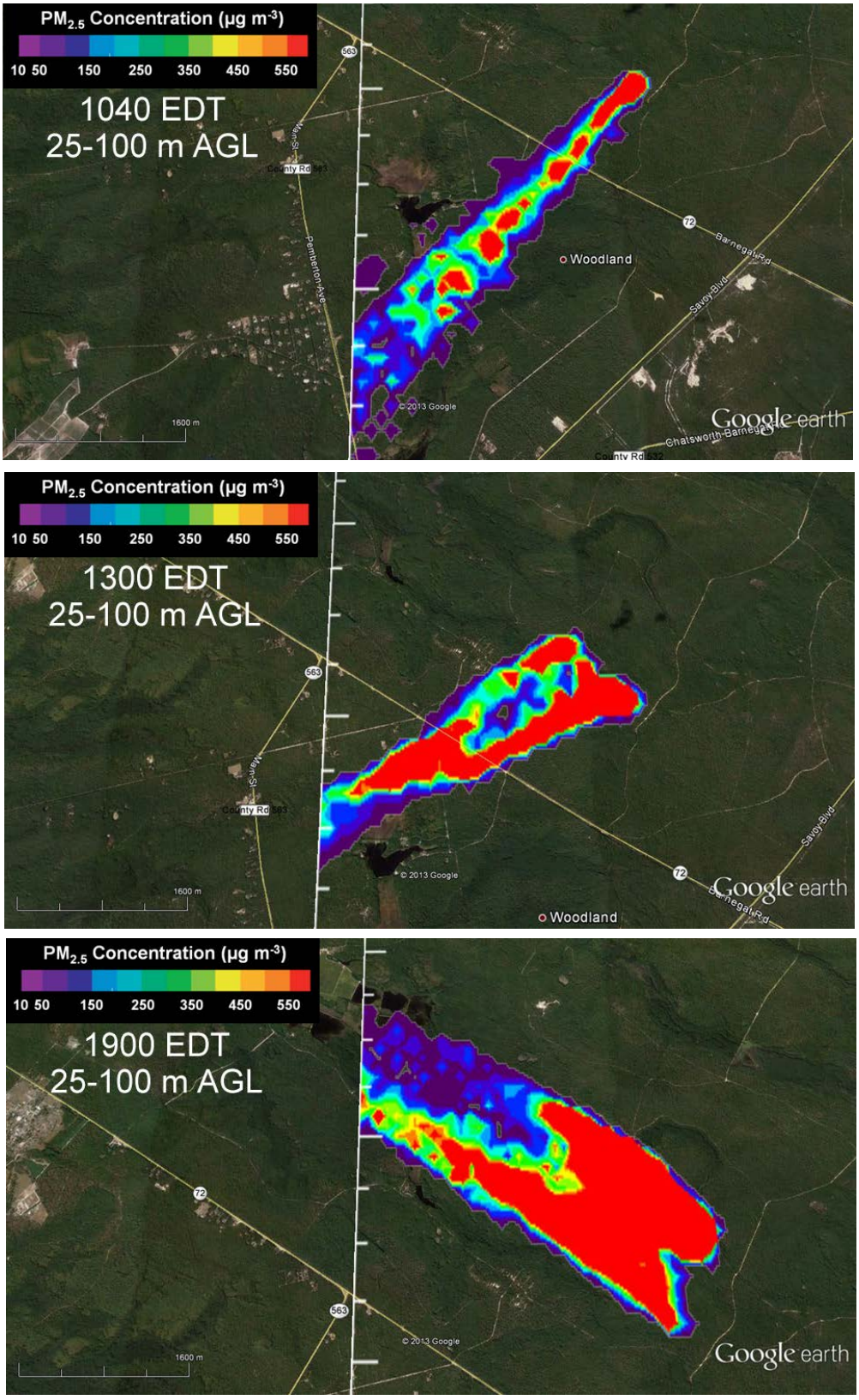

Fig. 29. Integrated $PM_{2.5}$ concentrations (µg m^{-3}) for the 25-100 m AGL layer at three different times during the E1 prescribed fire experiment on 20 March 2011 as simulated by ARPS-CANOPY/FLEXPART. Sharp boundary of plume concentrations downwind of the burn block coincides with the FLEXPART lateral domain boundary used in the simulations.

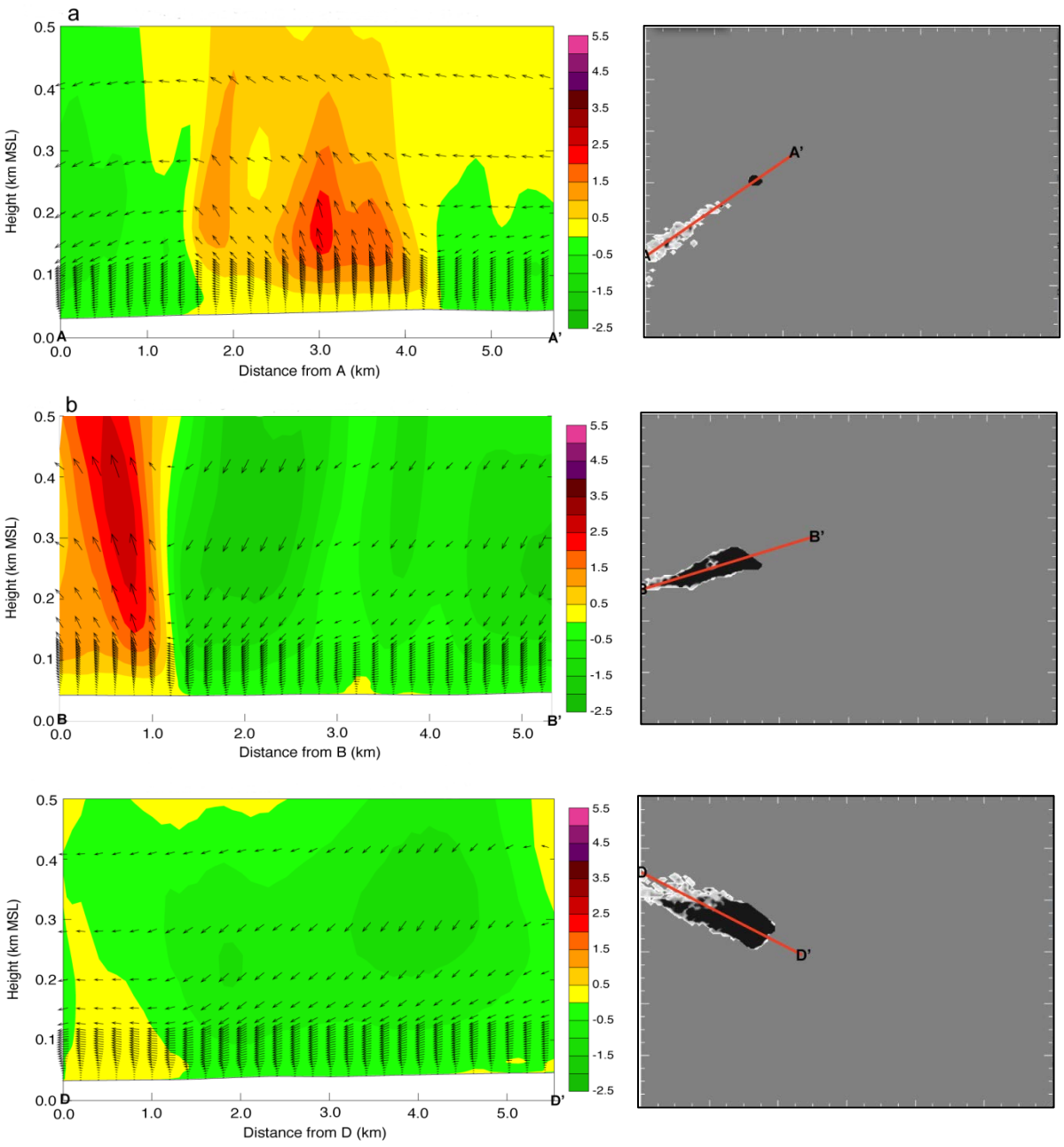

Fig. 30. Vertical cross-sections of ARPS-CANOPY simulated vertical wind speed (m s^{-1}) (color contours) and wind speed/direction (vectors) in the vertical plane at (a) 1040 EDT, (b) 1300 EDT, and (c) 1900 EDT on 20 March 2011 during the E1 burn experiment. The cross-section orientation along the general smoke plume axis is shown to the right of each cross- section. The lower boundary in each cross-section reflects terrain variations.

area of mean TKE in the fire simulation that is not present when the fire is omitted (Fig. 27d-f). Interestingly, this fire-induced TKE is found not only along the axis of the parameterized burn zone in ARPS-CANOPY (denoted by the black quadrilateral) but well away from the fire line itself. In fact, the largest TKE value at 20 m AGL is located several hundred meters west of the fire, at the western edge of the analysis area. Furthermore, the impact of the fire on the horizontal wind field is manifested as a broad zone of convergent winds in an otherwise east to southeast flow. While alternating bands of confluent and diffluent winds can be seen in the no-fire simulation (Fig. 27d-f), evidence of convective structures in the planetary boundary layer, the convergent wind field in the vicinity of the fire line is an unmistakable outcome of the strong heat source and buoyant updraft above it.

Using the meteorological output from ARPS-CANOPY (5 min time intervals) and estimated fire emissions computed from the Fire Emissions Production Simulator (FEPS) (Anderson et al. 2004) to drive the FLEXPART particle dispersion model, predictions of the local $PM_{2.5}$ and CO concentrations resulting from the 20 March 2011 burn experiment were carried out. The coupled ARPS-CANOPY/FLEXPART system provided a four-dimensional (space and time) picture of the spatial and temporal evolution of the $PM_{2.5}$ and CO plumes resulting from the fire, including plume characteristics within and immediately above the forest vegetation layer that characterized the burn site. Figures 28 and 29 show example integrated $PM_{2.5}$ concentration predictions for the 0-20 m and 25-100 m AGL layers, respectively, from the coupled ARPS-CANOPY/FLEXPART system at different times during the E1 burn experiment. The integrated concentration figures reveal rather complex local plume behavior, including plume dispersion within the vegetation layer and lofting of plumes above the vegetation layer followed by downward transport of $PM_{2.5}$ back into the vegetation layer downwind of the fire. Vertical cross-sections of wind speeds/directions (Fig. 30) along the axes of the plumes shown in Figs. 28 and 29 reveal the critical role that local circulation variability over and downwind of the fire played in dispersing the smoke in the lower boundary layer.

Application of ARPS-CANOPY/FLEXPART to the 6 March 2012 NJ Pine Barrens Prescribed Fire Experiment: Following the application of ARPS-CANOPY/FLEXPART to the E1 prescribed fire experiment, the modeling system was further evaluated using observational data from the E2 experiment carried out on 6 March 2012. For simulation of the E2 burn event, a model configuration similar to the E1 case study was utilized, with three exceptions. First, the outermost domain (domain 1; Fig. 25) was initialized with Global Forecast System (GFS) (http://www.emc.ncep.noaa.gov/GFS/doc.php) 0.5-degree resolution analysis data, rather than NARR. Unphysical NARR surface winds on 6 March 2012 necessitated the use of an alternate initialization option. Second, the outermost domain was doubled in size, compared to the E1 case study, in order to better capture a frontal system over the Mid-Atlantic on 5 March 2012, and the innermost domain was shifted westward in order to center the domain on the E2 burn unit; all other domains were identical to what was used for the E1 case study. Third, a fire configuration was chosen to represent the E2 burn, with surface turbulent heat flux values of 0.855 kW m^{-2} representing the heat flux from the relatively narrow fire in each 100-m x 100-m grid cell. For other details of the model configuration and parameterization, see the details of the E1 case study setup in Kiefer et al. (2013b).

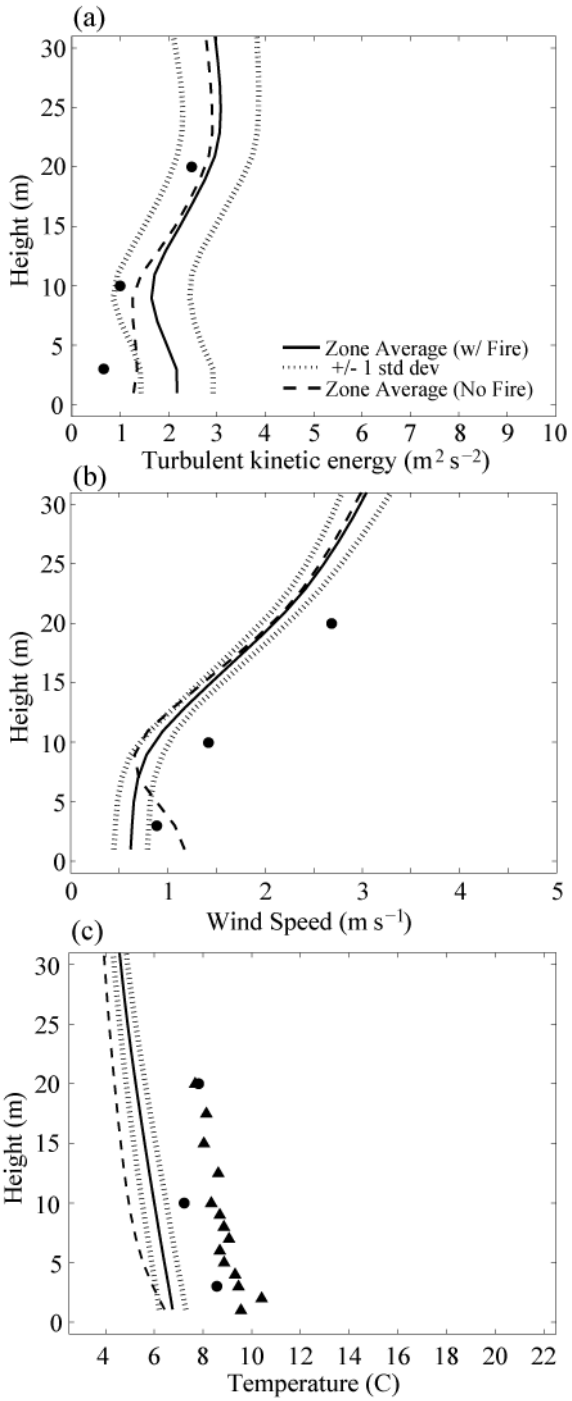

Fig. 31. Vertical profiles of (a) TKE, (b) wind speed, and (c) temperature, averaged in time from 1520-1620 EST on 6 March 2012. ARPS-CANOPY simulated fields are averaged around all grid points within the parameterized burn zone. Solid line indicates the mean and dotted lines indicate the mean ± one standard deviation (perturbations computed with respect to burn zone mean). Long dashed line indicates mean from simulation with no fire. Symbols represent 20 m tower observations.

Profiles of mean TKE, wind speed, and temperature reveal that in general the magnitude of ARPS-CANOPY error was comparable for the E2 (Fig. 31) and E1 cases (Fig. 26). Profiles of mean TKE (Fig. 31a) show that the atmosphere simulated above the fire line that passed through the 20 m tower location was more turbulent than what was observed, although the zone-average-minus-one-standard deviation does indicate that there were areas along the simulated fire line where TKE values were in better agreement with the 20-m tower observations. The TKE profile from a no-fire simulation (also shown in Fig. 31a) suggests that the simulated background atmosphere was probably too turbulent, as the no-fire profile agrees best with observations, despite the lack of heat from the fire. Simulated wind speeds throughout the canopy were generally too weak, although the model correctly captured the weaker wind flow in the lower portion of the canopy (Fig. 31b). The largest errors in the ARPS-CANOPY simulation were associated with mean temperatures, with a ~3°C cold bias evident throughout the profile (Fig. 31c). This bias was not restricted to the innermost domain simulation; it can be traced back to the outermost domain simulation. Efforts to reduce or eliminate this cold bias are ongoing. Despite the notable cold bias in the simulated temperatures, the simulated lapse rates within and above the vegetation layer were found to generally correspond with the observed lapse rates. As in the E1 case study, this result suggests that ARPS-CANOPY is able to generally represent the near-surface stability conditions near the fire line.

The ARPS-CANOPY simulations of the E2 case study exhibited pronounced horizontal variability of wind and turbulence across the burn block and surrounding regions (Fig. 32), generally consistent with simulations of the E1 case study (Fig. 27). Comparing the fire simulation (Figs. 32a-c) with the no-fire simulation (Figs. 32d-f), one finds enhancement of the background mean TKE by the parameterized fire, with strong indication that the background pattern of mean TKE is present despite the fire (cf. Figs. 32a,d). Note that in contrast to the

E1 burn experiment, multiple fire lines were ignited near-simultaneously during the E2 burn experiment, necessitating the ARPS-CANOPY fire configuration displayed in Fig. 32a-c (black rectangles indicate the locations of the fire heat sources at 1620 EDT). Comparing the region of enhanced TKE in Fig. 32a-c to the locations of the fire heat sources, we found that the largest mean TKE was generally over and downstream of the parameterized fire. In further contrast to the E1 case (Figs. 27a-c), the simulated winds in the E2 case (Figs. 32a-c) showed no distinguishable fire-induced convergence zone. The absence of an E2 convergence zone is consistent with the smaller parameterized surface turbulent heat flux used for the E2 simulation (0.854 kW m^{-2}) compared to the E1 simulation (15.5 kW m^{-2}).

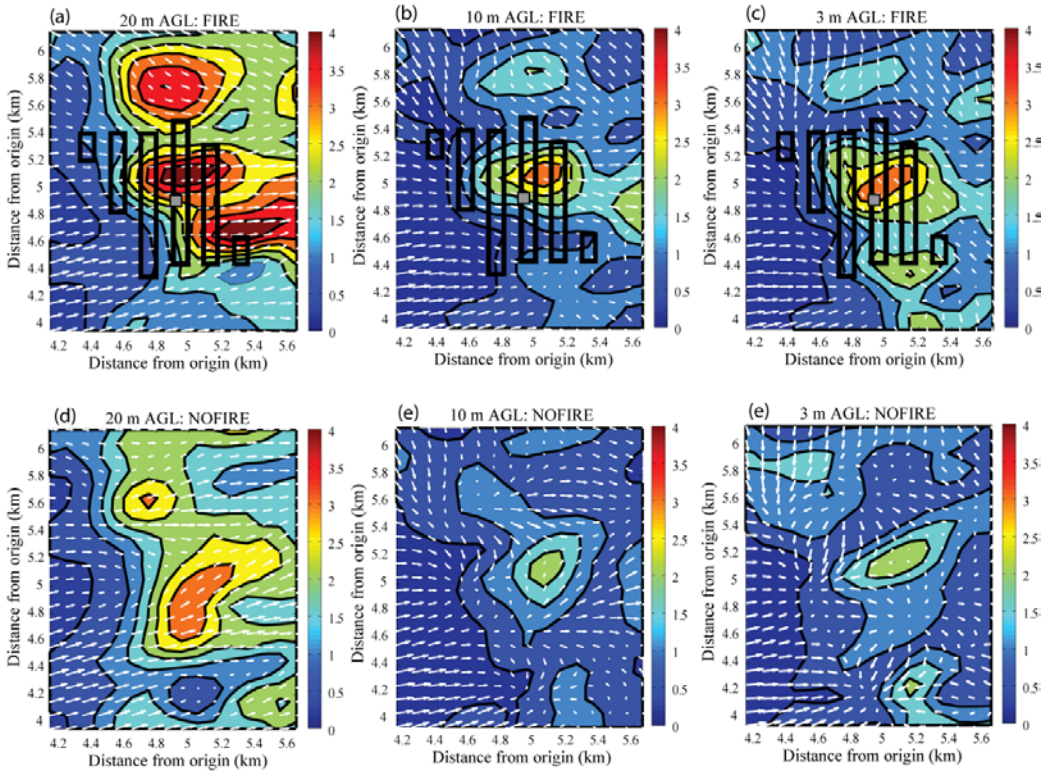

Fig. 32. TKE at (a,d) 20 m AGL, (b,e) 10 m AGL, and (c,f) 3 m AGL averaged from 1520-1620 EST on 6 March 2012 from ARPS-CANOPY simulations with fire (upper panels) and without fire (lower panels). Horizontal wind vectors are overlaid along with the groups of grid cells where the heat source was applied at 1620 EDT (black rectangles). The rectangle with the gray square (20 m tower location), denotes the area averaged to produce Fig. 31. Contour interval in (a,d) is 0.5 m^2 s^{-2} and 0.25 m^2 s^{-2} in all other panels.

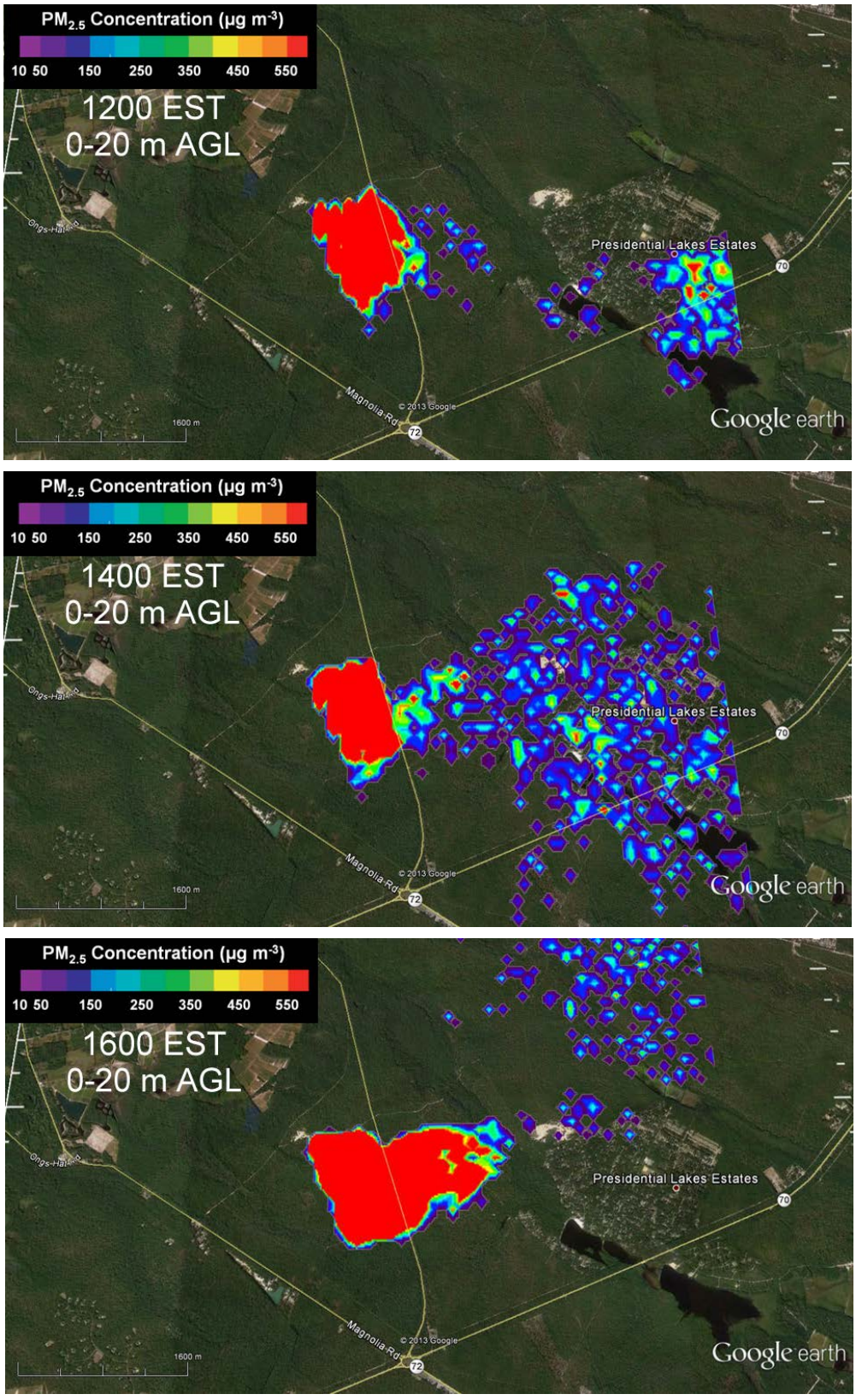

Fig. 33. Integrated $PM_{2.5}$ concentrations (µg m^{-3}) for the 0-20 m AGL layer at three different times during the E2 prescribed fire experiment on 6 March 2012 as simulated by ARPS-CANOPY/FLEXPART. Sharp boundary of plume concentrations downwind of the burn block coincides with the FLEXPART lateral domain boundary used in the simulations.

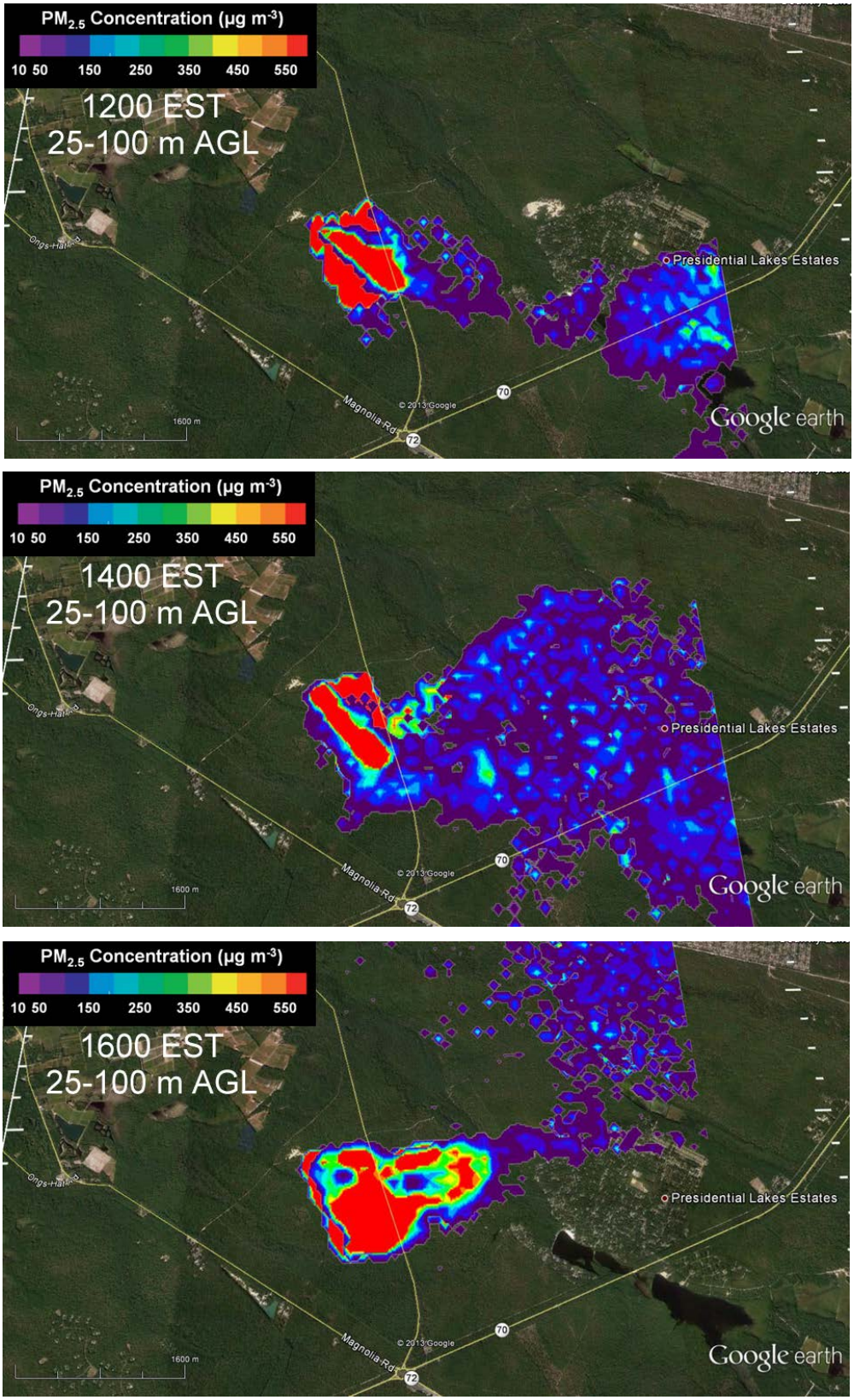

Fig. 34. Integrated $PM_{2.5}$ concentrations (µg m^{-3}) for the 25-100 m AGL layer at three different times during the E2 prescribed fire experiment on 6 March 2012 as simulated by ARPS-CANOPY/FLEXPART. Sharp boundary of plume concentrations downwind of the burn block coincides with the FLEXPART lateral domain boundary used in the simulations.

Like the 20 March 2011 case study, meteorological output from the ARPS-CANOPY simulation of the 6 March 2012 case study along with FEPS-computed fire emissions were used to drive the FLEXPART particle dispersion model for predictions of local $PM_{2.5}$ and CO concentrations due to the prescribed fire event. Figures 33 and 34 show the ARPS-CANOPY/FLEXPART simulation of integrated $PM_{2.5}$ concentrations for the 0-20 m and 25-100 m AGL layers, respectively, at 1200, 1400, and 1600 EST during the E2 burn experiment. The simulation suggests that $PM_{2.5}$ concentrations within the forest vegetation layers were substantial over and immediately downwind of the burn block during much of the burn experiment (Fig. 33). The simulation indicated an overall eastward transport of smoke below and above the forest canopy, resulting in 0-20 m AGL integrated $PM_{2.5}$ concentrations exceeding 550 $\mu g\ m^{-3}$ over broad areas within the burn block and sometimes up to 800 m downwind of the burn block. Isolated pockets of 550+ $\mu g\ m^{-3}$ occasionally occurred around 2 km downwind of the burn block, including locations in the Presidential Lakes Estates residential area. For much of the duration of the E2 burn experiment, the ARPS-CANOPY/FLEXPART simulations indicated 4 Mile Road along the eastern perimeter of the burn block experienced relatively high $PM_{2.5}$ concentrations, a result consistent with observed near-surface concentrations at the PM3 monitor site just east of 4 Mile Road (see Fig. 2 and Fig. 21c). In the 25-100 m AGL layer (above the forest canopy), the simulated plume patterns differed from the below-canopy patterns (Fig. 34). Whereas the areas of simulated high $PM_{2.5}$ concentrations within the vegetation layer were quite broad over the burn block, the above-canopy high-concentration areas over the burn block were more limited in extent. Transport of $PM_{2.5}$ from above the canopy back into the vegetation layer in areas downwind of the burn block was evident in the simulations, similar to what was found in the E1 experiment.

The differences in simulated plume structures between the within-vegetation layer and the above-vegetation layer for both the E1 and E2 burn experiments point to the inherent complexity of the ambient and fire-induced turbulent circulations that can occur in forested environments. The ARPS-CANOPY/FLEXPART simulations in this study support the hypothesis that predicting local plume behavior during low-intensity fires in forested environments requires modeling tools that can adequately resolve and account for these complex turbulent circulations both within and above the forest vegetation layer.

Sensitivity Analyses of the Effects of Canopy and Fire Properties on Wind and Temperatures in the Lower Atmosphere Using ARPS-CANOPY: Having established reasonable confidence in the ability of ARPS-CANOPY to simulate the atmospheric environments observed during the 20 March 2011 and 6 March 2012 low-intensity prescribed fires in the New Jersey Pine Barrens, additional sensitivity analyses were carried out with the ARPS-CANOPY modeling system to assess the effects of canopy and surface fire properties on wind and temperatures in the lower atmosphere. The interplay between low-intensity fires, forest vegetation, and background atmospheric properties is complex, and the impact of fire processes on nearby turbulent and mean flow, which is central to smoke transport and diffusion during wildland fire events, is poorly understood. The ARPS-CANOPY modeling system was used to explore these complex relationships. A set of 14 (4-hour long; initialized at 1200 LT) idealized three-dimensional ARPS-CANOPY simulations (10 km x 7.5 km x 3 km spatial domain; horizontal grid spacing: $\Delta x = \Delta y = 50$ m; vertical grid spacing: $\Delta z = 2$ m up to 84 m AGL and stretched above 84 m to model top at 3 km AGL) were set up to examine how different

combinations of ambient wind speed, plant-area density profiles (canopy height = 18 m), and ambient atmospheric stability affect the atmospheric response to a low-intensity surface fire line (surface heat flux = 5 kW m-2) located in the interior of the model domain and oriented perpendicular to the ambient wind direction (see Table 2 and Figs. 35 and 36).

Table 2. Idealized simulation experiments carried out with ARPS-CANOPY to assess the sensitivity of atmospheric responses to a low-intensity fire line under different ambient wind speeds, plant area density profiles, and ambient stability conditions (U0 = Ambient wind speed (m s^{-1}); PAI = Plant Area Index; Qo = Ground/canopy heat source outside of fire).

Experiment	U0	PAI	Qo (Y/N)?
U0P2N	0	2	N (neutral)
U0P2C	0	2	Y (convective)
U5P0N	5	0	N (neutral)
U5P0C	5	0	Y (convective)
U5P2N	5	2	N (neutral)
U5P2C	5	2	Y (convective)
U5P4N	5	4	N (neutral)
U5P4C	5	4	Y (convective)
U5P6N	5	6	N (neutral)
U5P6C	5	6	Y (convective)
U5P8N	5	8	N (neutral)
U5P8C	5	8	Y (convective)
U10P2N	10	2	N (neutral)
U10P2C	10	2	Y (convective)

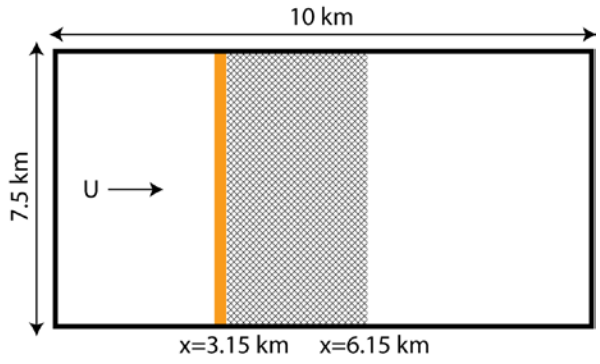

Fig. 35. Horizontal domain used for the ARPS-CANOPY idealized simulations. Orange shading indicates fire line position, gray shading denotes averaging zone for analyses, and arrow indicates a westerly direction for the ambient wind.

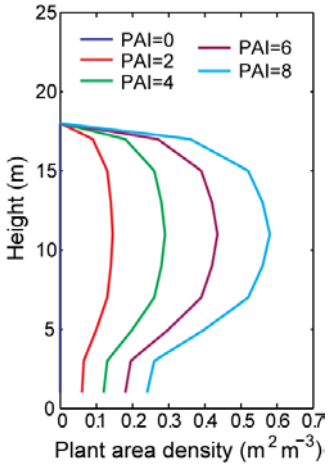

Fig. 36. Plant area density profiles and corresponding plant area index (PAI) values used for the ARPS-CANOPY idealized simulations.

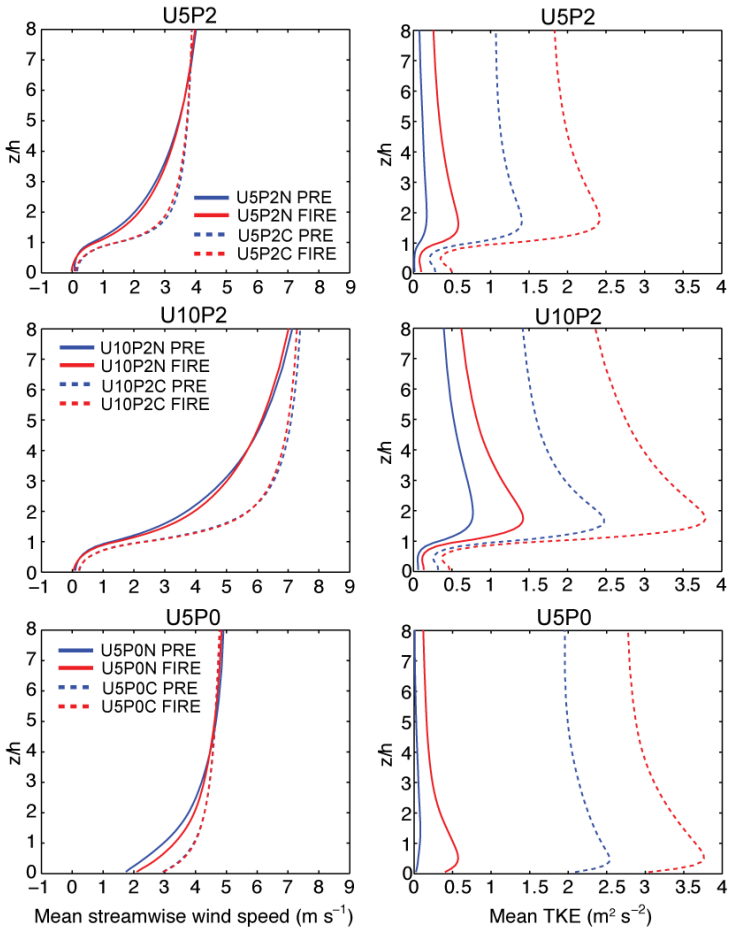

Fig. 37. ARPS-CANOPY simulated vertical profiles of (left) streamwise component of wind mean and (right) turbulent kinetic energy (TKE), averaged temporally over a 20-min period and spatially over an area downstream of fire (see shaded area in Fig. 35). PRE refers to 20 min period before fire begins; FIRE refers to 20 min period after fire begins.

The sensitivity simulations revealed that in all cases, downwind lower atmospheric boundary layer turbulence increases with the presence of a surface fire (Fig. 37). When overstory vegetation is present, the largest increases in atmospheric turbulence tend to occur at heights equal to 1.5 to 1.7 times the canopy height where vertical wind shear is enhanced. When no overstory vegetation is present, the largest increases tend to occur about 9 m AGL. The simulations also suggested that the largest changes to streamwise winds and TKE in response to a low-intensity surface fire tend to occur under unstable background stability conditions, but changes are muted inside vegetation layers. A more dense vegetation layer tends to reduce the atmospheric response to a surface fire, especially within the vegetation layer and at heights above twice the canopy height (not shown). The non-buoyant dissipation of turbulence within dense vegetation layers due to canopy drag effects tends to overwhelm the buoyant production of turbulence there.

The sensitivity simulation results provide insight into potential smoke transport and diffusion behavior during low-intensity wildland fires in forested environments. An increase in TKE downstream of a fire may serve to enhance horizontal and vertical dispersion of smoke downwind of the fire. Smoke from low intensity fires has the potential to be transported by fire-generated convection through the atmospheric boundary layer and exchanged with the free atmosphere. The greatest potential for smoke to enter the free atmosphere occurs when ambient winds are weak and upright convection columns develop. The presence of forest overstory vegetation reduces overall turbulence within the vegetation layer, which is conducive to smoke from low-intensity fires lingering inside the vegetation layers relatively close to the emissions sources.

Idealized RAFLES Simulations of Overstory Vegetation Variability Impacts on Fire-Induced Circulations, Temperature Fields, and Smoke Dispersion: Simple test simulations were carried out with RAFLES to examine the effects of a heterogeneous vs. homogeneous forest vegetation layer on circulations, temperatures, and smoke dispersion resulting from a

surface fire line. An idealized fire line, parameterized as near-surface grid points having elevated turbulent heat flux values, was introduced into a model domain and allowed to move through the domain in the direction of an imposed ambient wind. Simulations with homogeneous and heterogeneous forest vegetation layers were completed. Figure 38 shows some of the resulting circulations and temperatures from those simulations. The simulations revealed that forest overstory vegetation variability can result in local fire-induced circulations and temperature fields that may be quite different than the induced circulations and temperature fields under homogeneous overstory conditions. This finding is relevant for the application of research or operational models for simulating/predicting actual local meteorological and air quality impacts of wildland fires in forested environments. Parameterizing heterogeneous forest overstory vegetation layers as homogeneous vegetation layers in modeling systems used for local meteorological and air quality predictions can be problematic.

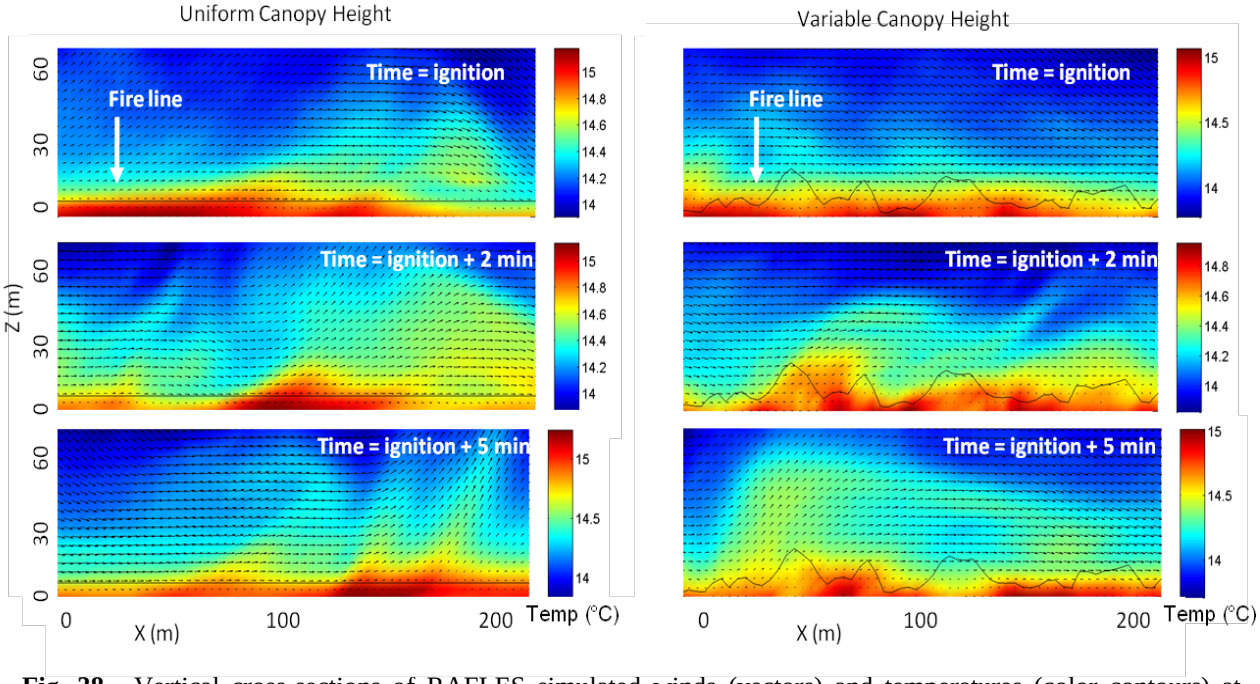

Fig. 38. Vertical cross-sections of RAFLES simulated winds (vectors) and temperatures (color contours) at different times resulting from an imposed fire line parameterized as an elevated surface heat flux that moves through the domain in the direction of the ambient wind (increasing x) under a homogeneous vegetation layer (left column) and a heterogeneous vegetation layer (right column). Canopy height is shown as a solid black line or curve in each figure.

Initial test simulations were also performed with RAFLES to examine the dispersion of smoke from a very low-intensity "smoldering" fire line beneath a heterogeneous forest canopy. Figure 39 shows an example vertical cross-section of RAFLES-simulated particle concentrations after 30 minutes of continuous particle emissions into a vegetation layer (1 particle per square meter per second) under light ambient winds from a 93 m long "smoldering" fire line oriented perpendicular to the cross-section along the right boundary of the figure. The simulation results show that local plume transport through forest vegetation layers and through the forest-canopy interface is highly variable and dependent on the forest vegetation architecture. Additional RAFLES simulations of particle dispersion within and above heterogeneous forest vegetation layers resulting from more intense surface fires are needed to fully assess the sensitivity of small-

scale plume transport processes in forested environments to different surface fire intensities (see Section VII.).

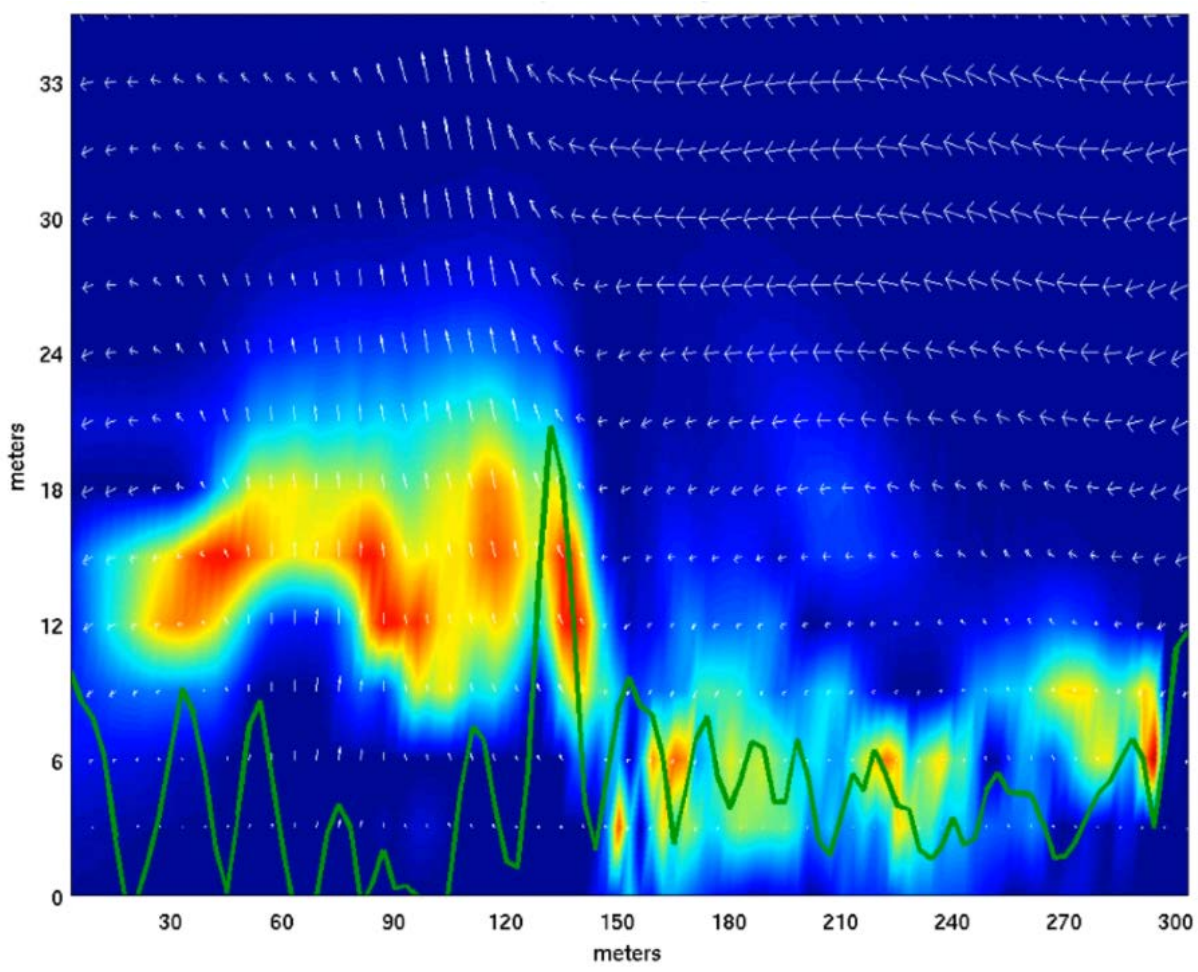

Fig. 39. Example vertical cross-section of RAFLES-simulated particle concentrations after 30 minutes of continuous particle emissions into a vegetation layer (1 particle per square meter per second) under light ambient winds from a 93 m long "smoldering" fire line oriented perpendicular to the cross-section along the right boundary of the figure. Vectors represent relative wind speed and direction in the cross-section; color contours indicate relative particle concentrations (blue – low, red – high). Canopy height is shown as a solid green line.

V. Management Implications

The monitoring and modeling results from this project have extended our scientific understanding of fire-atmosphere interactions that occur during low-intensity wildland fires in forested environments. The results also have important implications for the planning and management of low-intensity fires in forested environments and the smoke they generate. This section provides a summary of a few key management implications of our findings.

Forest Overstory Vegetation Affects Local Plume Behavior During Low-Intensity Fires: The presence of forest overstory vegetation and its typical heterogeneous qualities can alter the atmospheric turbulence environment near the surface and throughout the vegetation layer, which

in turn, affects how smoke plumes behave as they are transported away from low-intensity surface fires and through the canopy-atmosphere interface. Forest overstory vegetation tends to enhance atmospheric turbulence and the mixing/diffusion of smoke plumes immediately above the canopy top. Most of the turbulent mixing of these smoke plumes within and immediately above forest vegetation layers occurs in the horizontal direction. This enhances the local horizontal spread of smoke plumes and the potential for air quality in areas surrounding low-intensity fires beneath forest canopies to be reduced, an important factor for fire managers in planning for prescribed burn activities.

Local Plume Heights Associated with Low-Intensity Fire Emissions in Forested Environments Can Be Highly Variable: When low intensity prescribed fires are carried out beneath forest canopies, local plume heights can be highly variable. While smoke-plume concentrations of $PM_{2.5}$ during the low-intensity fires conducted in this project tended to be highest at heights below 50 m AGL, above-ambient $PM_{2.5}$ concentrations were observed as high as 1000 m AGL for brief and sporadic periods, especially during the afternoon hours when mixing heights were at their maximum. The observed variability in local plume heights during the low-intensity fires for this project suggest that corresponding plume heights further downwind of the low-intensity fires could be highly variable as well. Highly variable downwind plume heights associated with low-intensity wildland fires in forested environments is another factor for fire and air-quality managers to consider in assessing the extent to which these fires can impact the lower regions of the atmosphere and create potential health and transportation safety concerns.

ARPS-CANOPY/FLEXPART is a Potential Predictive Tool Option for Fire Managers: With the development and initial testing of ARPS-CANOPY/FLEXPART in this project, it will be made available for further feasibility testing to fire and air quality mangers who are interested in identifying possible local air-quality effects of planned low-intensity prescribed fires in forested environments. A prototype version of ARPS-CANOPY/FLEXPART is planned as part of the suite of fire and air quality products available from the Eastern Area Modeling Consortium web site (http://www.nrs.fs.fed.us/eamc/products), where users will have the opportunity to test its usefulness as a predictive tool for select domains in the eastern U.S. Future implementation of ARPS-CANOPY/FLEXPART as a pathway in the BlueSky smoke prediction framework (Larkin et al. 2009) is also planned following prototype testing, which would bring the ARPS-CANOPY/FLEXPART system completely into the operational fire and air-quality management realm.

VI. Relationship to Other Recent Findings and Ongoing Work on This Topic

The goals, objectives, experimental design, and tasks developed for this project are consistent with the overall goals and strategies outlined in a similar project funded by the JFSP (Project #09-1-04-2; PI - Dr. Tara Strand; *Sub-Canopy Transport and Dispersion of Smoke: A Unique Observation Dataset and Model Evaluation*). Both projects involved the development of high temporal resolution observational datasets of atmospheric and air-quality conditions during and in the vicinity of low-intensity prescribed fires in forested environments. Numerous consultations took place between the PIs and Co-PIs from both projects to design similar monitoring strategies for the prescribed fire experiments carried out in each project.

Comparisons of atmospheric turbulence data collected during the prescribed fire experiments of both projects are underway to assess how different forest overstory conditions can affect turbulence regimes (and resulting smoke dispersion) before, during, and after the passage of low-intensity fire fronts. Drawing upon the results of both projects, the PIs from both projects have developed collaborative research plans to develop improved methods/formulations for predicting plume rise and plume heights associated with fire emissions beneath forest canopies.

This JFSP project contributed to the Core Fire Science and the Ecological and Environmental Fire Science portfolios under the USDA Forest Service's Wildland Fire and Fuels Research and Development Strategic Plan. It also addressed key elements of the JFSP Smoke Science Plan (Riebau and Fox 2010), the USDA Forest Service – Northern Research Station's Fire Research Strategic Plan, the USDA Forest Service – Northern Research Station's Forest Disturbance Processes Theme, and the research mission of the Eastern Area Modeling Consortium (EAMC) under Research Work Unit NRS-06 in the Northern Research Station. Specifically within the EAMC, the monitoring results from this JFSP project are being compared to the monitoring results from an EAMC-funded study carried out by Dr. Craig Clements at San Jose State University (07-JV-11242300-073: Experimental Studies of Fire-Atmosphere Interactions and Turbulence During Grass Fires of Different Scales).

This JFPS project is also viewed as a complementary effort to the past and ongoing FireFlux experiments in Texas, New Jersey, and California (Clements et al. 2007, Clements 2010, Seto and Clements 2011, Seto et al. 2013, Clark et al. 2011) and RxCADRE experiments in Florida (Hiers et al. 2009, JFSP Project #11-2-1-11). All of these projects involved similar *in situ* monitoring techniques to examine and better understand fire-fuel-atmosphere interactions that govern fire behavior and smoke transport processes and to develop new observational data sets for evaluating current and future fire behavior and smoke dispersion predictive systems. Preliminary comparisons of atmospheric data collected during all these experiments indicate some common features in the turbulence regimes observed in the vicinity of the fire environments.

Finally, the monitoring techniques and ARPS-CANOPY/FLEXPART modeling approaches used in this study will be applied to a new EPA-funded study of fire emissions and transport associated with a prescribed fire event at the Lehigh Gap Super Fund site in Pennsylvania. The monitoring and modeling efforts will focus on determining the heavy metal content of smoke plumes resulting from prescribed burning of the prairie grass on site and determining the local transport of those plumes to off-site locations.

VII. Future Work Needed

With the completion of this project, there are a number of follow-up research, model development, and program delivery tasks that will be addressed over the next 3-5 years as part of the USDA Forest Service – Northern Research Station's Core Fire Science research portfolio.

In the area of fire-fuel-atmosphere monitoring research, additional prescribed fire experiments incorporating *in situ* instrumentation are needed to further expand our understanding of how forest vegetation architecture, terrain heterogeneities, fire intensity, and ambient atmospheric

conditions affect fire-fuel-atmosphere interactions and resulting smoke dispersion within and in the vicinity of the fire environment. The observational data sets generated in this study and other similar-type studies (e.g. JFSP Project #09-1-04-2, RxCADRE, FireFlux) are unique and provide critical evaluation/validation data for current and yet-to-be-developed fire behavior and local smoke transport prediction systems used for research or operational purposes. Additional analyses of the data sets generated in this study and in the Fireflux study (Clements et al. 2007) are also underway to assess how the presence or absence of forest vegetation affects post fire-front-passage turbulence regimes and the dispersion of smoke in smoldering areas. Recent advances in the application of LIDAR technology for characterizing forest vegetation structure/architecture need to be incorporated into future fire-fuel-atmosphere interaction monitoring studies in order to develop improved parameterizations of canopy effects on atmospheric circulations in coupled fire-atmosphere and smoke prediction models.

Further refinements of the ARPS-CANOPY modeling system should be explored to enhance its versatility in simulating the interactions between low-intensity fires, forest vegetation, and the atmosphere. For example, one weakness of the current version of ARPS-CANOPY is the lack of consideration of the canopy moisture source, which can have an effect on the thermodynamics within and above forest vegetation layers. Follow-up research to this project is planned in order to develop an appropriate moisture parameterization for inclusion in ARPS-CANOPY to account for the direct effect of forest overstory vegetation on moisture distributions within forest vegetation layers. Observational data from the CHATS experiment and the E1 and E2 experiments conducted for this project will provide critical validation data for testing the parameterizations incorporated into ARPS-CANOPY. Future research is also planned to assess the current and relatively simple turbulent length-scale and canopy temperature parameterizations used in ARPS-CANOPY, which affect the computations of turbulence dissipation and atmospheric temperatures within forest vegetation layers. The follow-up research to address some of these refinements to the ARPS-CANOPY modeling system has been incorporated into a new collaborative research study between the Forest Service – Northern Research Station and Michigan State University (Research Joint Venture Agreement # 11-JV-11242306-058) using funding from the National Fire Plan.

The unique observational data sets generated in this project (see Section X) are available for uploading to the Smoke Emissions Model Intercomparison Project (SEMIP) data warehouse. As a follow-up effort to this project, appropriate metadata files will be developed to accompany the observational data sets, and the full suite of metadata/observational data sets will then be uploaded to the SEMIP data warehouse.

An ARPS-CANOPY/FLEXPART prototype system will be made available for initial "operational-type testing" via the Eastern Area Modeling Consortium (EAMC) web site (http://www.nrs.fs.fed.us/eamc/products/) shortly after the completion of this project (~1-3 months). The prototype system will allow fire and air quality managers to see example real-time daily predictions of local smoke transport from user-specified or "default" fire locations, sizes, and times. This initial prototype system will provide users with an opportunity to further assess the feasibility of applying ARPS-CANOPY/FLEXPART to prescribed fire activities and to provide feedback to EAMC scientists on needed improvements to the system. Future collaborations with the USDA Forest Service – Pacific Northwest Research Station (PNWRS) are needed to

incorporate an ARPS-CANOPY/FLEXPART pathway into the BlueSky framework so that users who are interested in the local air-quality impacts of low-intensity prescribed fires can choose that pathway in the framework. As a follow-up to this project, discussions will be initiated with scientists in the AirFire group in the PNWRS to plan for and potentially incorporate ARPS-CANOPY/FLEXPART into the BlueSky framework.

Additional development and evaluation of the RAFLES modeling system as a research tool for examining fundamental fire-atmosphere-vegetation interactions will continue after the completion of this project using funding from the National Fire Plan. RAFLES simulations of the 2011 and 2012 New Jersey Pine Barrens prescribed fire experiments will be completed over the next four months to further our understanding of how three-dimensional atmospheric turbulent processes at scales on the order of a few meters affected the fluxes of momentum, heat, moisture, and particulates during the low-intensity fires. More sensitivity simulations using RAFLES will be carried out to examine the impacts of canopy heterogeneity, forest gaps, and fire intensity on the local atmospheric environment, local smoke dispersion, and plume rise during surface fire events.

VIII. Deliverables Crosswalk Table

Deliverable	Delivered	Status
Web Site	http://www.geo.msu.edu/firesmoke/index.html	Updated as needed
Conference/ Symposium/ Workshop	Project description and results presented at numerous conferences, workshops, and meetings, and briefings (See Section X. for citations): • 4th International Fire Congress • 29th Conference on Agricultural & Forest Meteorology • 3rd Fire Behavior and Fuels Conference • 4th Fire Behavior and Fuels Conference • IUFRO Research Conference: Wind & Trees • 9th Symposium on Fire and Forest Meteorology • 20th Symposium on Boundary Layers and Turbulence • Briefing for Forest Service Chief • Stewardship Network Conference • Lakes States Fire Science Consortium Webinar Series	Completed – Presentations and citations posted on JFSP web site.
Non-refereed Publications	User's Guide for coupled ARPS-CANOPY modeling system. User's Guide for converting ARPS-CANOPY output data files into a format useable by the FLEXPART modeling system	Completed - Documents posted on JFSP web site.
Training Sessions	Results from project incorporated into curriculum for upper undergraduate/graduate class on environmental modeling (GEO 890: Advanced Geography Reading; GEO 892: Advanced Geography Research – Weather and Climate Modeling) at Michigan State University. Overview and application of smoke modeling tools	Completed

	presented to land and fire/forest managers during special session of 2012 Stewardship Network Conference.	
Refereed Publications	See Section X. for citations.	Completed - Documents posted on JFSP web site.
Computer Model/ Software/Algorithm	Coupled ARPS-CANOPY/FLEXPART prototype system included as part of the suite of predictive tools on the FCAMMS – Eastern Area Modeling Consortium (EAMC) web site: http://www.nrs.fs.fed.us/eamc/products/.	Under development; Available July-September 2013

IX. Literature Cited

Achtemeier, G. L. 2005. Planned burn – Piedmont. A local operational numerical meteorological model for tracking smoke on the ground at night: model development and sensitivity tests. *International Journal of Wildland Fire* 14:85-98.

Achtemeier, G. L., S. A. Goodrick, Y. Liu, F. Garcia-Menendez, Y. Hu, and M. T. Odman. 2011. Modeling smoke plume-rise and dispersion from southern United States prescribed burns with Daysmoke. *Atmosphere* 2:358-388.

Alexander, M. E., B. J. Stocks, B. M. Wotton, M. D. Flannigan, J. B. Todd, B. W. Butler, and R. A. Lanoville. 1998. The International Crown Fire Modeling Experiment: An overview and progress report. Preprints, Second Symposium on Fire and Forest Meteorology, Phoenix, AZ, American Meteorological Society, 20-23.

Anderson, G., D. Sandberg and R. Norheim. 2004. Fire emission production simulator (FEPS) user's guide. U.S. Forest Service. Available at http://www.fs.fed.us/pnw/fera/feps.

Bohrer, G. 2007. Large eddy simulations of forest canopies for determination of biological dispersal by wind. Ph.D. Dissertation, Department of Civil and Environmental Engineering, Duke University, Durham, NC.

Bohrer, G., G. G. Katul, R. Nathan, R. L. Walko, and R. Avissar. 2008. Effects of canopy heterogeneity, seed abscission and inertia on wind-driven dispersal kernels of tree seeds. *Journal of Ecology* 96:569-580.

Bohrer, G., G. G. Katul, R. L. Walko, and R. Avissar. 2009. Exploring the effects of microscale structural heterogeneity of forest canopies using large-eddy simulations. *Boundary-Layer Meteorology* 132:351-382.

Bohrer, G., S. R. Garrity, E. K. Chatziefstratiou, and W. E. Heilman. 2011. Large eddy simulation of canopy-structure effects on smoke dispersion from low-burning prescribed fires. *9th Symposium on Fire and Forest Meteorology*. American Meteorological Society, Palm Springs, CA.

Byun, D. W., and J. Ching. 1999. Science algorithms of the EPA Model-3 Community Multiscale Air Quality (CMAQ) modeling system. EPA/600/R-99/030, U.S. Environmental Protection Agency, National Exposure Research Laboratory, Research Triangle Park, NC.

Charney, J. J., A. L. Acheson, and A. Stacy. 2006. Top ten smoke management questions for fire in eastern oak forests. In: Dickinson, M. B., ed., Fire in eastern oak forests: delivering science to land managers, proceedings of a conference; 2005 November 15-17; Columbus, OH. Gen. Tech. Rep. NRS-P-1. Newtown Square, PA: U.S. Department of Agriculture, Forest Service, Northern Research Station: 199-209.

Chen, Q. 2007. Airborne LiDAR data processing and information extraction. *Photogrammetric Engineering and Remote Sensing* 73:109-112.

Cheng, S., D. Chen, J. Li, H. Wang, and X. Guo. 2007. The assessment of emission-source contributions to air quality by using a coupled MM5-ARPS-CMAQ modeling system: A case study in the Beijing metropolitan region, China. *Environmental Modeling and Software* 22:1601-1616.

Clark, K. L., N. Skowronski, J. Hom, M. Duveneck, Y. Pan, S. Van Tuyl, J. Cole, M. Patterson, and S. Maurer. 2009. Decision support tools to improve the effectiveness of hazardous fuel reduction treatments in the New Jersey Pine Barrens. *International Journal of Wildland Fire* 18:268-277.

Clark, K. L., N. Skowronski, M. Gallagher, W. Heilman, and J. Hom. 2010. Fuel consumption and particulate emissions during fires in the New Jersey Pinelands. *Proceedings 3rd Fire Behavior and Fuels Conference*, October 25-29, 2010, Spokane, WA, International Association of Wildland Fire.

Clark, K. L., N. Skowronski, M. Gallagher, W. E. Heilman, J. L. Hom, M. Patterson, and X. Bian. 2011. Turbulence and energy fluxes during prescribed fires in the New Jersey Pine Barrens. *9th Symposium on Fire and Forest Meteorology*, October 18-20, 2011, Palm Springs, CA, American Meteorological Society.

Clements, C. B. 2010. Thermodynamic structure of a grass fire plume. *International Journal of Wildland Fire* 19:895–902.

Clements, C. B., S. Zhong, S. Goodrick, J. Li, B. E. Potter, X. Bian, W. E. Heilman, J. J. Charney, R. Perna, M. Jang, D. Lee, M. Patel, S. Street, and G. Aumann. 2007. Observing the dynamics of wildland grass fires: FireFlux – a field validation experiment. *Bulletin of the American Meteorological Society* 88:1369-1382.

Collischonn, W., R. Haas, I. Andreolli, and C. E. M. Tucci. 2005. Forecasting River Uruguay flow using rainfall forecasts from a regional weather-prediction model. *Journal of Hydrology* 305:87-98.

Cotton,W. R., R. A. Pielke Sr., R. L. Walko, G. E. Liston, C. J. Tremback, H. Jiang, R. L. McAnelly, J. Y. Harrington, M. E. Nicholls, G. G. Carrio, and J. P. McFadden. 2003. RAMS 2001: Current status and future directions. *Meteorology and Atmospheric Physics* 82:5-29.

de Foy, B., M. Zavala, N. Bei, and L. T. Molina. 2009. Evaluation of WRF mesoscale simulations and particle trajectory analysis for the MILAGRO field campaign. *Atmospheric Chemistry and Physics* 9:4419–4438.

Dupont, S., and Y. Brunet. 2008. Influence of foliar density profile on canopy flow: A large-eddy simulation study. *Agricultural and Forest Meteorology* 148:976-990.

Doran, J. C., J. D. Fast, J. C. Barnard, A. Laskin, Y. Desyaterik, and M. K. Gilles. 2008. Applications of Lagrangian dispersion modeling to the analysis of changes in the specific absorption of elemental carbon. *Atmospheric Chemistry and Physics* 8:1377–1389.

Draxler, R. R., and G. D. Rolph. 2003. HYSPLIT (HYbrid Single-Particle Lagrangian Integrated Trajectory) Model access via NOAA ARL READY, NOAA Air Resources Laboratory, Silver Spring, MD. Available at http://www.arl.noaa.gov/ready/hysplit4.html [Verified 25 January 2013]

Fast, J. D., and R. C. Easter. 2006. A Lagrangian particle dispersion model compatible with WRF. 7th Annual WRF User's Workshop, 19-22 June 2006, Boulder, CO.

Ferguson, S. A., S. J. McKay, D. E. Nagel, T. Piepho, M. L. Rorig, C. Anderson, and L. Kellogg. 2003. Assessing values of air quality and visibility at risk from wildland fires. Res. Pap. PNW-RP-550, U.S. Department of Agriculture, Forest Service, Pacific Northwest Research Station, Portland, OR.

Goodrick, S. L., G. L. Achtemeier, N. K. Larkin, Y. Liu, and T. M. Strand. 2012. Modelling smoke transport from wildland fires: a review. *International Journal of Wildland Fire,* http://dx.doi.org/10.1071/WF11116.

Hardiman, B. S., G. Bohrer, C. M. Gough, C. S. Vogel, and P. S. Curtis. 2011. The role of canopy structural complexity in wood net primary production of a maturing northern deciduous forest. *Ecology* 92:1818–1827.

Hays, M. D., P. M. Fine, C. D. Geron, M. J. Kleeman, and B. K. Gullett. 2005. Open burning of agricultural biomass: Physical and chemical properties of particle-phase emissions. *Atmospheric Environment* 39:6747-6764.

Heilman, W. E., J. L. Hom, K. L. Clark, N. S. Skowronski, X. Bian, S. Zhong, J. J. Charney, M. Gallagher, M. Patterson, M. T. Kiefer, and R. Kremens. 2013. Observations of fire-atmosphere interactions during low-intensity prescribed fires in the New Jersey Pine Barrens. *International Journal of Wildland Fire.* (In review)

Hiers, J. K., R. Ottmar, B. W. Butler, C. Clements, R. Vihnanek, M. B. Dickinson, and J. O'Brien. 2009. An overview of the prescribed fire combustion and atmospheric dynamics research experiment (Rx-CADRE). In '4th International Fire Ecology & Management Congress: Fire as a Global Process'. (Ed. S Rideout-Hanzak).

Hom, J., K. Clark, Y. Pan, S. Van Tuyl, N. Skowronski, and W. Heilman. 2013. Fire research in the New Jersey Pine Barrens. In Remote Sensing and Modeling Applications to Wildland Fires, (Eds.) J. J. Qu, W. Sommers, R. Yang, A. Riebau, and M. Kafatos. Springer and Tsinghua University Press.

Kenny, W. T., R. Frasson, G. Bohrer, E. Chatziefstratiou, L. Hadlocon, B. Wyslouzil, L. Zhao, and W. E. Eichinger. 2012. Measurements and large-eddy simulations of particulate matter dispersion over a vegetative wind-break. *30th Conference on Agricultural and Forest Meteorology*, Boston, MA, American Meteorological Society.

Kiefer, M. T., S. Zhong, W. E. Heilman, J. J. Charney, and X. Bian. 2013a. Evaluation of an ARPS-based canopy flow modeling system for use in future operational smoke prediction efforts. *Journal of Geophysical Research* doi: 10.1002/jgrd.50491.

Kiefer, M. T., W. E. Heilman, S. Zhong, J. J. Charney, X. Bian, N. S. Skowronski, J. L Hom, M. Patterson, K. L. Clark, and M. R. Gallagher. 2013b. Multiscale simulation of a prescribed burn event in the New Jersey Pine Barrens using ARPS-CANOPY. *Journal of Applied Meteorology and Climatology.* (In review)

Larkin, N. K., S. O'Neill, R. Solomon, S. Raffuse, T. Strand, D. C. Sullivan, C. Krull, M. Rorig, J. Peterson, and S. Ferguson. 2009. The BlueSky Smoke Modeling Framework. *International Journal of Wildland Fire* 18:906-920.

Lavdas, L. G. 1986. An atmospheric dispersion index for prescribed burning. Research Paper SE-256, USDA Forest Service, Southeastern Forest Experiment Station, Macon, GA.

Lavdas, L. G. 1996. Program VSMOKE – users manual. General Technical Report SRS-6, USDA Forest Service, Southeastern Forest Experiment Station, Macon, GA.

Lu, W., S. Zhong, J. J. Charney, X. Bian, and S. Liu. 2012. WRF simulation over complex terrain during a southern California wildfire event. *Journal of Geophysical Research* 117, D05125, doi:10.1029/2011JD017004.

Massoli, P., T. S. Bates, P. K. Quinn, D. A. Lack, T. Baynard, B. M. Lerner, S. C. Tucker, J. Brioude, A. Stohl, and E. J. Williams. 2009. Aerosol optical and hygroscopic properties during TexAQS-GoMACCS 2006 and their impact on aerosol direct radiative forcing. *Journal of Geophysical. Research* 114, D00F07, doi:10.1029/2008JD011604.

McCarty, J. L., C. O. Justice, and S. Korontzi. 2006. Agricultural burning in the southeastern United States detected by MODIS. *Remote Sensing of Environment* 108:151-162.

Mesinger, F., G. DiMego, E. Kalnay, K. Mitchell, P. C. Shafran, W. Ebisuzaki, D. Jovic, J. Woollen, E. Rogers, E. H. Berbery, M. B. Ek, Y. Fan, R. Grumbine, W. Higgins, H. Li, Y. Lin, G.Manikin, D. Parrish, and W. Shi. 2006. North American Regional Reanalysis. *Bulletin of the American Meteorological Society* 87:343–360.

Mott, R., and M. Lehning. 2010. Meteorological modeling of very high-resolution wind fields and snow deposition for mountains. *Journal of Hydrometeorology* 11:934-949.

National Interagency Fire Center. 2012. Prescribed fires and acres by agency. http://www.nifc.gov/fireInfo/fireInfo_stats_prescribed.html.

Patton, E. G., T. W. Horst, P. P. Sullivan, D. H. Lenschow, S. P. Oncley, W. O. J. Brown, S. P. Burns, A. B. Guenther, A. Held, T. Karl, S. D. Mayor, L. V. Rizzo, S. M. Spuler, J. Sun, A. A. Turnipseed, E. J. Allwine, S. L. Edburg, B. K. Lamb, R. Avissar, R. J. Calhoun, J. Kleissl, W. J. Massman, K. T. Paw U, and J. C. Weil. 2011. The canopy horizontal array turbulence study (CHATS). *Bulletin of the American Meteorological Society* 92:593–611.

Pielke, R. A., W. R. Cotton, R. L. Walko, C. J. Tremback, W. A. Lyons, L. D. Grasso, M. E. Nicholls, M. D. Moran, D. A. Wesley, T. J. Lee, and J. H. Copeland. 1992. A comprehensive mesoscale modeling system – RAMS. *Meteorology and Atmospheric Physics* 49:69-91.

Riebau, A. R., and D. G. Fox. 2010. Joint Fire Science Program smoke science plan. Joint Fire Science Program, Project 10-C-01-01. Available at: http://www.firescience.gov [Verified 20 March 2013]

Schlegel, F., J. Stiller, A. Bienert, H.-G. Maas, R. Queck, and C. Bernhofer. 2012. Large-eddy simulation of inhomogeneous canopy flows using high resolution terrestrial laser scanning data. *Boundary-Layer Meteorology* 142:223–243.

Scire, J. S. 2000. CALPUFF: Overview of capabilities. In 'Technical Highlights of EPA's 7th Conference on Air Pollution Modeling', 1 August 2000. (North Carolina State University) Available at http://www.epa.gov/scram001/7thconf/information/t029day1.pdf [Verified 25 January 2013]

Sestak, M. L., and A. R. Riebau. 1988. SASEM, Simple approach smoke estimation model. U.S. Bureau of Land Management, Technical Note 382.

Seto, D., and C. B. Clements. 2011. Fire whirl evolution observed during a valley wind-sea breeze reversal. *Journal of Combustion* 2011, doi:10.1155/2011/569475.

Seto, D., C. B. Clements, and W. E. Heilman. 2013. Turbulence spectra measured during fire front passage. *Agricultural and Forest Meteorology* 169:195-210.

Skamarock, W. C., J. B. Klemp, J. Dudhia, D. O. Gill, D. M. Barker, W. Wang, and J. G. Powers. 2005. A description of the advanced research WRF Version 2. NCAR Technical Note (NCAR/TN-468+STR).

Skowronski, N. S., K. L. Clark, M. Duveneck, and J. Hom. 2011. Three-dimensional canopy fuel loading predicted using upward and downward sensing LiDAR systems. *Remote Sensing. Environment* 115:703–714.

Spainhour, L. K., D. Hill, J. O. Sobanjo, J. Wekezer, and P. V. Mtenga. 2005. Evaluation of traffic accident causes and effects: A study of fatal traffic accidents in Florida 1998-2000 focusing on heave truck crashes. Florida Department of Transportation Final Report BD-050.

Stocks, B. J., M. E. Alexander, and R. A. Lanoville. 2004. Overview of the International Crown Fire Modelling Experiment (ICFME). *Canadian Journal of Forest Research* 34:1543-1547.

Stohl, A., C. Forster, A. Frank, P. Seibert, and G. Wotawa. 2005. Technical note: The Lagrangian particle dispersion model FLEXPART version 6.2. *Atmospheric Chemistry and Physics* 5:2461-2474.

Stull, R. B. 1988. An introduction to boundary layer meteorology. Kluwer Academic Publishers, Dordrecht, The Netherlands.

Sun, X. M, Z. L. Zhu, X. F. Wen, G. F. Yuan, and G. R. Yu. 2006. The impact of averaging period on eddy fluxes observed at ChinaFLUX sites. *Agricultural and Forest Meteorology* 137:188-193.

Taylor, S. W., B. M. Wotton, M. E. Alexander, and G. N. Dalrymple. 2004. Variation in wind and crown fire behaviour in a northern jack pine – black spruce forest. *Canadian Journal of Forest Research* 34:1561-1576.

Velissariou, V. and G. Bohrer. 2010. Resolving a forest-strip induced uplift region using the shaved-grid-cell method with large eddy simulations. *29th Conference on Agricultural and Forest Meteorology*, Keystone, CO, American Meteorological Society.

Vodacek, A., R. Kremens, A. Ononye, and J. Faulring. 2005. Remote image and field data collection for a dynamic fire modeling system. In: Remote Sensing for Field Users. *Proc. 10th Biennial USDA Forest Service Remote Sensing Applications Conference*. Salt Lake City, UT. CD-ROM. ISBN 1-57083-075-4. ASPRS.

Wang, J., S. A. Christopher, U. S. Nair, J. S. Reid, E, M. Prins, J. Szykman, and J. L. Hand. 2006. Mesoscale modeling of Central American smoke transport to the United States: 1. 'Top-down' assessment of emission strength and diurnal variation impacts. *Journal of Geophysical Research* 111(D05), D05S17. doi:10.1029/2005JD006416.

Wilczak, J. M. S. P. Oncley, and S. A. Stage. 2001. Sonic anemometer tilt correction algorithms. *Boundary-Layer Meteorology* 99:127-150.

Winter, G. J., C. Vogt, and J. S. Fried. 2002. Fuel treatments at the wildland-urban interface: Common concerns in diverse regions. *Journal of Forestry* 100:15-21.

Weverberg, K. V., K. D. Ridder, and A. V. Rompaey. 2008. Modeling the contribution of the Brussels heat island to a long temperature time series. *Journal of Applied Meteorology and Climatology* 47:976-990.

Xue, M., K. K. Droegemeier, and V. Wong. 2000. The Advanced Regional Prediction System (ARPS) – A multiscale nonhydrostatic atmospheric simulation and prediction model. Part I: Model dynamics and verification. *Meteorology and Atmospheric Physics* 75:463-485.

Xue, M., K. K. Droegemeier, V. Wong, A. Shapiro, K. Brewster, F. Carr, D. Weber, Y. Liu, and D. Wang. 2001. The Advanced Regional Prediction System (ARPS) – A multiscale nonhydrostatic atmospheric simulation and prediction tool. Part II: Model physics and applications. *Meteorology and Atmospheric Physics* 76:143-165.

Xue, M., D. Wang, J. Gao, K. Brewster, and K. K. Droegemeier. 2003. The Advanced Regional Prediction System (ARPS), storm-scale numerical weather prediction and data assimilation, *Meteorology and Atmospheric Physics* 82:139-170.

Yamada, T. 2004. Merging CFD and atmospheric modeling capabilities to simulate airflows and dispersion in urban areas. *Computational Fluid Dynamics* 13(2):14 329-341.

X. Project Publications, Presentations, Datasets, and Other Output

a. Refereed Publications

Garrity, S. R., K. Meyer, K. D. Maurer, B. S. Hardiman, and G. Bohrer. 2012. Estimating plot-level tree structure in a deciduous forest by combining allometric equations, spatial wavelet analysis, and airborne lidar. *Remote Sensing Letters* 3:443-451.

Garrity, S. R., G. Bohrer, K. D. Maurer, K. L. Mueller, C. S. Vogel, and P. S. Curtis. 2011. A comparison of multiple phenology data sources for estimating seasonal transitions in forest carbon exchange. *Agricultural and Forest Meteorology* 151:1741-1752.

Kiefer, M. T., S. Zhong, W. E. Heilman, J. J. Charney, and X. Bian. 2013. Evaluation of an ARPS-based canopy flow modeling system for use in future operational smoke prediction efforts. *Journal of Geophysical Research* doi: 10.1002/jgrd.50491.

b. Refereed Publications Under Review

Kiefer, M. T., W. E. Heilman, S. Zhong, J. J. Charney, X. Bian, N. S. Skowronski, J. L. Hom, K. L. Clark, M. Patterson, and M. R. Gallagher. 2013. Multiscale simulation of a prescribed fire event in the New Jersey Pine Barrens using ARPS-CANOPY. *Journal of Applied Meteorology and Climatology.*

Heilman, W. E., J. L. Hom, K. L. Clark, N. S. Skowronski, X. Bian, S. Zhong, J. J. Charney, M. Gallagher, M. Patterson, M. T. Kiefer, and R. Kremens. 2013. Observations of fire-atmosphere interactions during low-intensity prescribed fires in the New Jersey Pine Barrens. *International Journal of Wildland Fire.*

c. Conference and Symposium Presentations

Heilman, W. E., S. Zhong, J. J. Charney, J. Hom, K. Clark, G. Bohrer, N. Skowronski, X. Bian, M. T. Kiefer, and R. Shadbolt. 2009. *Development of modeling tools for predicting smoke dispersion from low-intensity fires.* 4th International Fire Congress, Savannah, GA (11/30-12/4/2009).

Kiefer, M. T., X. Bian, J. J. Charney, W. E. Heilman, R. Shadbolt, and S. Zhong. 2010. *Application of a vegetation canopy parameterization to wildland fire modeling.* 29th Conference on Agricultural and Forest Meteorology, Keystone, CO (8/2-6/2010).

Heilman, W. E., N. S. Skowronski, S. Garrity, A. Bova, and G. Bohrer. 2010. *Large eddy simulation of canopy structure effects on smoke dispersion from prescribed fire.* 3rd Fire Behavior and Fuels Conference, Spokane, WA (10/25-29/2010). Published Abstract.

Heilman, W. E., S. Zhong, J. Hom, K. Clark, N. Skowronski, M. Kiefer, R. Shadbolt, G. Bohrer, X. Bian, and J. J. Charney. 2010. *Development and validation of modeling tools for predicting smoke dispersion during low-intensity fires.* 3rd Fire Behavior and Fuels Conference, Spokane, WA (10/25-29/2010)

Hom, J., M. Gallagher, W. Heilman, C. Clements, D. Seto, N. Skowronski, S. Roberts, T. Strand, M. Patterson, K. Clark. 2010. *Smoke modeling validation and field design: CO, $PM_{2.5}$, CO_2, and smoke monitoring from low intensity fires.* 3rd Fire Behavior and Fuels Conference, Spokane, WA (10/25-29/2010)

Clark, K. L., N. Skowronski, M. Gallagher, W. E. Heilman, and J. Hom. 2010. *Fuel consumption and particulate emissions during fires in the New Jersey Pinelands.* 3rd Fire Behavior and Fuels Conference, Spokane, WA (10/25-29/2010).

Kiefer, M., S. Zhong, W. Heilman, J. Charney, X. Bian, and R. Shadbolt. 2011. *Development of a canopy atmospheric modeling system for use in simulating smoke dispersion from low-intensity fires.* 2011 IUFRO Research Conference: Wind & Trees, Athens, GA (7/31-8/4/2011).

Bian, X, M. Katurji, S. Zhong, W. E. Heilman, and J. J. Charney. 2011. *A numerical study of high frequency velocity and temperature perturbations induced by a low-intensity prescribed fire.* 9th Symposium on Fire and Forest Meteorology, Palm Springs, CA (10/18-20/2011).

Bian, X., W. E. Heilman, J. J. Charney, J. L. Hom, K. L. Clark, N. S. Skowronski, M. Gallagher, and M. Patterson, S. Zhong, M. T. Kiefer, and R. P. Shadbolt. 2011. *Observations of atmospheric canopy layer turbulence generated by low-intensity prescribed fire.* 9th Symposium on Fire and Forest Meteorology, Palm Springs, CA (10/18-20/2011).

Bohrer, G., S. R. Garrity, E. Chatziefstratiou, and W. E. Heilman. 2011. *Large eddy simulation of canopy-structure effects on smoke dispersion from low-burning prescribed fires.* 9th Symposium on Fire and Forest Meteorology, Palm Springs, CA (10/18-20/2011).

Clark, K. L., N. Skowronski, M. Gallahger, W. E. Heilman, J. L. Hom, M. Patterson, X. Bian, and R. P. Shadbolt. 2011. *Turbulence and energy fluxes during prescribed fires in the New Jersey Pine Barrens.* 9th Symposium on Fire and Forest Meteorology, Palm Springs, CA (10/18-20/2011)

Heilman, W. E., X. Bian, J. L. Hom, K. L. Clark, N. S. Skowronski, S. Zhong, J. J. Charney, M. R. Gallagher, M. Patterson, M. T. Kiefer, and R. Shadbolt. 2011. *Observed fire-atmosphere interactions during a low-intensity prescribed fire in a forested environment.* 9th Symposium on Fire and Forest Meteorology, Palm Springs, CA (10/18-20/2011)

Hom, J. L., W. E. Heilman, M. Patterson, K. L. Clark, N. Skowronski, X. Bian, N. Saliendra, M. Gallagher, T. Strand, R. Mickler, C. Clements, and D. Seto. 2011. *Monitoring CO, $PM_{2.5}$, and CO_2 from low-intensity fires for the development of modeling tools for predicting smoke dispersion.* 9th Symposium on Fire and Forest Meteorology, Palm Springs, CA (10/18-20/2011)

Kiefer, M. T., S. Zhong, W. E. Heilman, J. J. Charney, X. Bian, and R. P. Shadbolt. 2011. *Development of a fine scale smoke dispersion modeling system. Part I: Validation of the canopy model component.* 9th Symposium on Fire and Forest Meteorology, Palm Springs, CA (10/18-20/2011)

Kiefer, M. T., S. Zhong, W. E. Heilman, J. J. Charney, X. Bian, R. Shadbolt, J. L. Hom, K. L. Clark, N. S. Skowronski, M. Gallagher, and M. Patterson. 2011. *Development of a fine scale smoke dispersion modeling system: Part II - Case study of a prescribed burn in the New Jersey Pine Barrens.* 9th Symposium on Fire and Forest Meteorology, Palm Springs, CA (10/18-20/2011)

Shadbolt, R. P., M. T. Kiefer, S. Zhong, W. E. Heilman, J. J. Charney, X. Bian, J. L. Hom, K. L. Clark, N. S. Skowronski, M. Gallagher, and M. Patterson. 2011. *A comparison of two coupled smoke modeling systems used for prediction of smoke dispersion and emissions from low-intensity wildland fires.* 9th Symposium on Fire and Forest Meteorology, Palm Springs, CA (10/18-20/2011)

Heilman, W. E., X. Bian, J. L. Hom, K. L. Clark, N. S. Skowronski, M. Gallagher, M. Patterson, Y. Liu, K. Forbus, C. Stegall, J. J. Charney, S. Zhong, M. T. Kiefer, and B. Kremens. 2013. *Fire-atmosphere interactions during low-intensity prescribed fires in the*

New Jersey Pine Barrens. 4th Fire Behavior and Fuels Conference, Raleigh, NC (02/18-22/2013)

Bian, X., W. Heilman, J. Charney, J. Hom, K. Clark, N. Skowronski, M. Gallagher, M. Patterson, Y. Liu, S. Lai, S. Zhong, M. Kiefer, L. Pei, and X. Zhu. 2013. *Evaluation of the WRF-Fire model with observational data from a prescribed fire experiment.* 4th Fire Behavior and Fuels Conference, Raleigh, NC (02/18-22/2013)

Kiefer, M. T., W. E. Heilman, S. Zhong, J. J. Charney, and X. Bian. 2013. *An investigation of the sensitivity of wind and temperature in the lower atmosphere to canopy and fire properties.* 2013. 4th Fire Behavior and Fuels Conference, Raleigh, NC (02/18-22/2013)

Kiefer, M. T., W. E. Heilman, S. Zhong, J. J. Charney, X. Bian, N. S. Skowronski, J. L. Hom, K. L. Clark, M. R. Gallagher, and M. Patterson. 2013. *Simulating prescribed burn events in the New Jersey Pine Barrens using ARPS-CANOPY*. 4th Fire Behavior and Fuels Conference, Raleigh, NC (02/18-22/2013)

Liu, Y., N. Skowronski, M. Gallagher, M. Patterson, W. Heilman, X. Bian, J. Hom, and K. Clark. 2013. *Detection and simulation of smoke feedbacks to atmospheric boundary layer for a prescribed burn.* 4th Fire Behavior and Fuels Conference, Raleigh, NC (02/18-22/2013)

Clark, K., N. Skowronski, M. Gallagher, W. E. Heilman, J. L. Hom, M. Patterson, and X. Bian. 2013. *Turbulence and energy fluxes during prescribed fires in the New Jersey Pinelands*. 4th Fire Behavior and Fuels Conference, Raleigh, NC (02/18-22/2013)

d. Extended Abstracts

Kiefer, M. T., S. Zhong, R. P. Shadbolt, W. E. Heilman, J. J. Charney, and X. Bian. 2010. *Application of a vegetation canopy parameterization to wildland fire modeling.* Proceedings of the 29th Conference on Agricultural and Forest Meteorology, 2-6 August 2010, Keystone, CO, American Meteorological Society. [Online]. Available: http://ams.confex.com/ams/19Ag19BLT9Urban/techprogram/paper_172309.htm

Clark, K. L., N. Skowronski, M. Gallagher, W. E. Heilman, and J. Hom. 2010. *Fuel consumption and particulate emissions during fires in the New Jersey Pinelands.* Proceedings of the 3rd Fire Behavior and Fuels Conference, 25-29 October 2010, Spokane, WA, International Association of Wildland Fire. [CD-ROM].

Kiefer, M. T., S. Zhong, W. E. Heilman, J. J. Charney, X. Bian, and R. P. Shadbolt. 2011. *Development of a fine scale smoke dispersion modeling system. Part I: Validation of the canopy model component.* Proceedings of the 9th Symposium on Fire and Forest Meteorology, 17-20 October 2011, Palm Springs, CA, American Meteorological Society. [Online]. Available: https://ams.confex.com/ams/9FIRE/webprogram/Paper192192.html

Kiefer, M. T., W. E. Heilman, S. Zhong, J. J. Charney, X. Bian, R. P. Shadbolt, J. L Hom, K. L. Clark, N. Skowronski, M. Gallagher, and M. Patterson. 2011. *Development of a fine scale smoke dispersion modeling system. Part II: Case study of a prescribed burn in the New Jersey Pine Barrens.* Proceedings of the 9th Symposium on Fire and Forest Meteorology, 17-20 October 2011, Palm Springs, CA, American Meteorological Society. [Online]. Available: https://ams.confex.com/ams/9FIRE/webprogram/Paper192199.html

e. Briefings

Heilman, W. E., and K. Clark. 2010. *Research and application highlights from the Eastern Area Modeling Consortium.* Briefing for the Chief of the Forest Service, Washington, DC (8/13/2010).

f. Training

Heilman, W. E. 2012. *Getting a handle on local smoke transport during prescribed fires.* Stewardship Network Conference, East Lansing, MI (1/20/2012).

g. Webinars

Heilman, W. E. 2012. *New research on local smoke transport and diffusion.* Lake States Fire Science Consortium Webinar Series, Joint Fire Science Program (4/19/2012).

h. Websites

Development of modeling tools for predicting smoke dispersion from low-intensity fires. Research Project Website. http://www.geo.msu.edu/firesmoke/index.html

i. Research Highlights Publications/Reports

Clark, K. L., N. Skowronski, M. Gallagher, W. Heilman and J. Hom. 2010. *Fuel consumption and particulate emissions during fires in the New Jersey Pinelands.* Report for New Jersey Forest Fire Service and the Natural Resources Division at Fort Dix, November 2010.

Clark, K. L., N. Skowronski, M. Gallagher, W. E. Heilman, J. J. Charney, X. Bian, J. Hom, and M. Patterson. 2011. *FireFlux experiments improve safety of prescribed burns in the New Jersey Pine Barrens.* Highlights 2011, Northern Research Station, USDA Forest Service, NRS-INF-15-12. p. 4.

Clark, K. L., N. Skowronski, M. Gallagher, W. E. Heilman, J. J. Charney, X. Bian, J. Hom, and M. Patterson. 2011. *FireFlux experiments improve safety of prescribed burns in the New Jersey Pine Barrens.* Forest Disturbance Processes: 2011 Research Highlights, Northern Research Station, USDA Forest Service. [Online]. Available: http://nrs.fs.fed.us/disturbance/research_highlights/

Clark, K. L., N. Skowronski, W. Heilman, J. Hom, X. Bian, M. Patterson, and M. Gallagher. 2011. *FireFlux experiments in the New Jersey Pine Barrens.* Solicited article for the Experimental Forest and Ranges Quarterly Newsletter.

j. User's Guides

Kiefer, M. T. 2013. ARPS-CANOPY V1.0 user's guide. U.S. Joint Fire Science Program.

Kiefer, M. T. 2013. ARPS2PILT V1.0 user's guide. U.S. Joint Fire Science Program.

k. Data Sets Available for SEMIP Data Warehouse

Prescribed Fire Experiment #1:

- *10-m Control Tower: Observed sonic anemometer wind speeds, temperatures, and turbulence data (1 min averages) on 19-20 March 2011.* JFSP Prescribed Fire Experiment #1, New Jersey Pine Barrens. (Excel Format – 3.3 MB)

- *10-m Control Tower: Observed air temperatures, soil temperatures, relative humidity, mixing ratios, carbon monoxide and carbon dioxide concentrations, and atmospheric pressure (1 min averages) on 19-20 March 2011.* JFSP Prescribed Fire Experiment #1, New Jersey Pine Barrens. (Excel Format – 0.7 MB)

- *3-m Towers: Observed temperatures, relative humidity, and carbon monoxide concentrations (temporal resolution of 2 s) on 19-20 March 2011.* JFSP Prescribed Fire Experiment #1, New Jersey Pine Barrens. (Excel Format – 60.2 MB)

- *10-m Tower: Observed sonic anemometer wind speeds, temperatures, and turbulence data (1 min averages) on 19-20 March 2011.* JFSP Prescribed Fire Experiment #1, New Jersey Pine Barrens. (Excel Format – 2.7 MB)

- *10-m Tower: Observed air temperatures, litter and soil temperatures, relative humidity, mixing ratios, carbon monoxide concentrations, radiative heat flux, and atmospheric pressure (1 min averages) on 19-20 March 2011.* JFSP Prescribed Fire Experiment #1, New Jersey Pine Barrens. (Excel Format – 0.6 MB)

- *20-m Tower: Observed sonic anemometer wind speeds, temperatures, and turbulence data (1 min averages) on 19-20 March 2011.* JFSP Prescribed Fire Experiment #1, New Jersey Pine Barrens. (Excel Format – 4.3 MB)

- *20-m Tower: Observed air temperatures, litter and soil temperatures, relative humidity, mixing ratios, carbon monoxide concentrations, radiative heat flux, and atmospheric pressure (1 min averages) on 19-20 March 2011.* JFSP Prescribed Fire Experiment #1, New Jersey Pine Barrens. (Excel Format – 0.8 MB)

- *30-m Tower: Observed sonic anemometer wind speeds, temperatures, and turbulence data (1 min averages) on 19-20 March 2011.* JFSP Prescribed Fire Experiment #1, New Jersey Pine Barrens. (Excel Format – 4.8 MB)

- *30-m Tower: Observed air temperatures, soil temperatures, relative humidity, mixing ratios, carbon monoxide and carbon dioxide concentrations, net radiation, and atmospheric pressure (1 min averages) on 19-20 March 2011.* JFSP Prescribed Fire Experiment #1, New Jersey Pine Barrens. (Excel Format – 0.9 MB)

- *Surface $PM_{2.5}$ Monitors: Observed $PM_{2.5}$ concentrations, temperatures, and relative humidity (temporal resolution of 5 min) on 20 March 2011.* JFSP Prescribed Fire Experiment #1, New Jersey Pine Barrens. (Excel Format – 0.066 MB)

<u>*Prescribed Fire Experiment #2*</u>:

- *10-m Control Tower: Observed sonic anemometer wind speeds, temperatures, and turbulence data (1 min averages) on 6-7 March 2012.* JFSP Prescribed Fire Experiment #2, New Jersey Pine Barrens. (Excel Format – 1.9 MB)

- *10-m Control Tower: Observed air temperatures, soil temperatures, relative humidity, mixing ratios, carbon monoxide and carbon dioxide concentrations, net radiation, and atmospheric pressure (1 min averages) on 6-7 March 2012.* JFSP Prescribed Fire Experiment #2, New Jersey Pine Barrens. (Excel Format – 0.5 MB)

- *3-m Towers: Observed temperatures, relative humidity, carbon monoxide concentrations, wind speed, and wind directions (temporal resolution of 2 s) on 6-7 March 2012.* JFSP Prescribed Fire Experiment #2, New Jersey Pine Barrens. (Excel Format – 47.2 MB)

- *10-m Tower: Observed sonic anemometer wind speeds, temperatures, and turbulence data (1 min averages) on 6-7 March 2012.* JFSP Prescribed Fire Experiment #2, New Jersey Pine Barrens. (Excel Format – 2.5 MB)

- *10-m Tower: Observed air temperatures, litter and soil temperatures, relative humidity, mixing ratios, carbon monoxide and carbon dioxide concentrations, radiative heat flux,*

and atmospheric pressure (1 min averages) on 6-7 March 2012. JFSP Prescribed Fire Experiment #2, New Jersey Pine Barrens. (Excel Format – 0.6 MB)

- *20-m Tower: Observed sonic anemometer wind speeds, temperatures, and turbulence data (1 min averages) on 6-7 March 2012.* JFSP Prescribed Fire Experiment #2, New Jersey Pine Barrens. (Excel Format – 3.7 MB)

- *20-m Tower: Observed air temperatures, litter and soil temperatures, relative humidity, mixing ratios, carbon dioxide concentrations, radiative heat flux, and atmospheric pressure (1 min averages) on 6-7 March 2012.* JFSP Prescribed Fire Experiment #2, New Jersey Pine Barrens. (Excel Format – 0.7 MB)

- *30-m Tower: Observed sonic anemometer wind speeds, temperatures, and turbulence data (1 min averages) on 6-7 March 2012.* JFSP Prescribed Fire Experiment #2, New Jersey Pine Barrens. (Excel Format – 3.7 MB)

- *30-m Tower: Observed air temperatures, soil temperatures, relative humidity, mixing ratios, carbon monoxide and carbon dioxide concentrations, net radiation, and atmospheric pressure (1 min averages) on 6-7 March 2012.* JFSP Prescribed Fire Experiment #2, New Jersey Pine Barrens. (Excel Format – 0.7 MB)

- *Surface $PM_{2.5}$ Monitors: Observed $PM_{2.5}$ concentrations, temperatures, and relative humidity (temporal resolution of 5 min) on 6 March 2011.* JFSP Prescribed Fire Experiment #1, New Jersey Pine Barrens. (Excel Format – 0.11 MB)